

Synthetic-Aperture Radar Images of California Coastal Waters under Upwelling Conditions

David L. Johnson

Committee:

Pierre Flament, chairman

Mark Merrifield

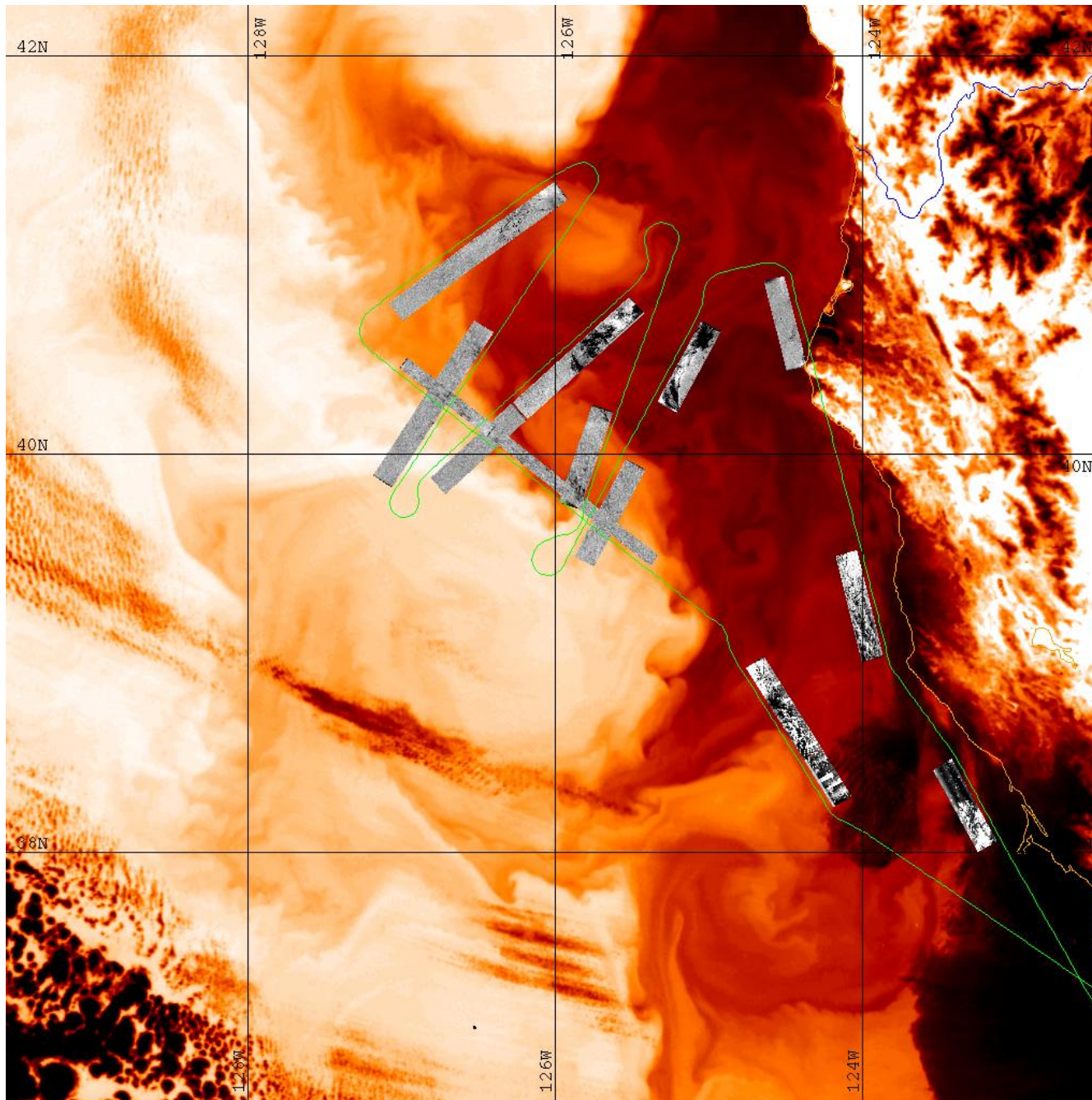
Eric Firing

Outline

- I Introduction to the Experiment
- II AVHRR Views of the California Current
- III ERS-1 SAR Views of the California Current
- IV Principles of SAR Imaging and an Estimate of Small Wave Coherence from AIRSAR C-band
- V AIRSAR Views of the California Current
- VI Comparison of Model Results to SAR Images of a Jet
- VII Conclusions

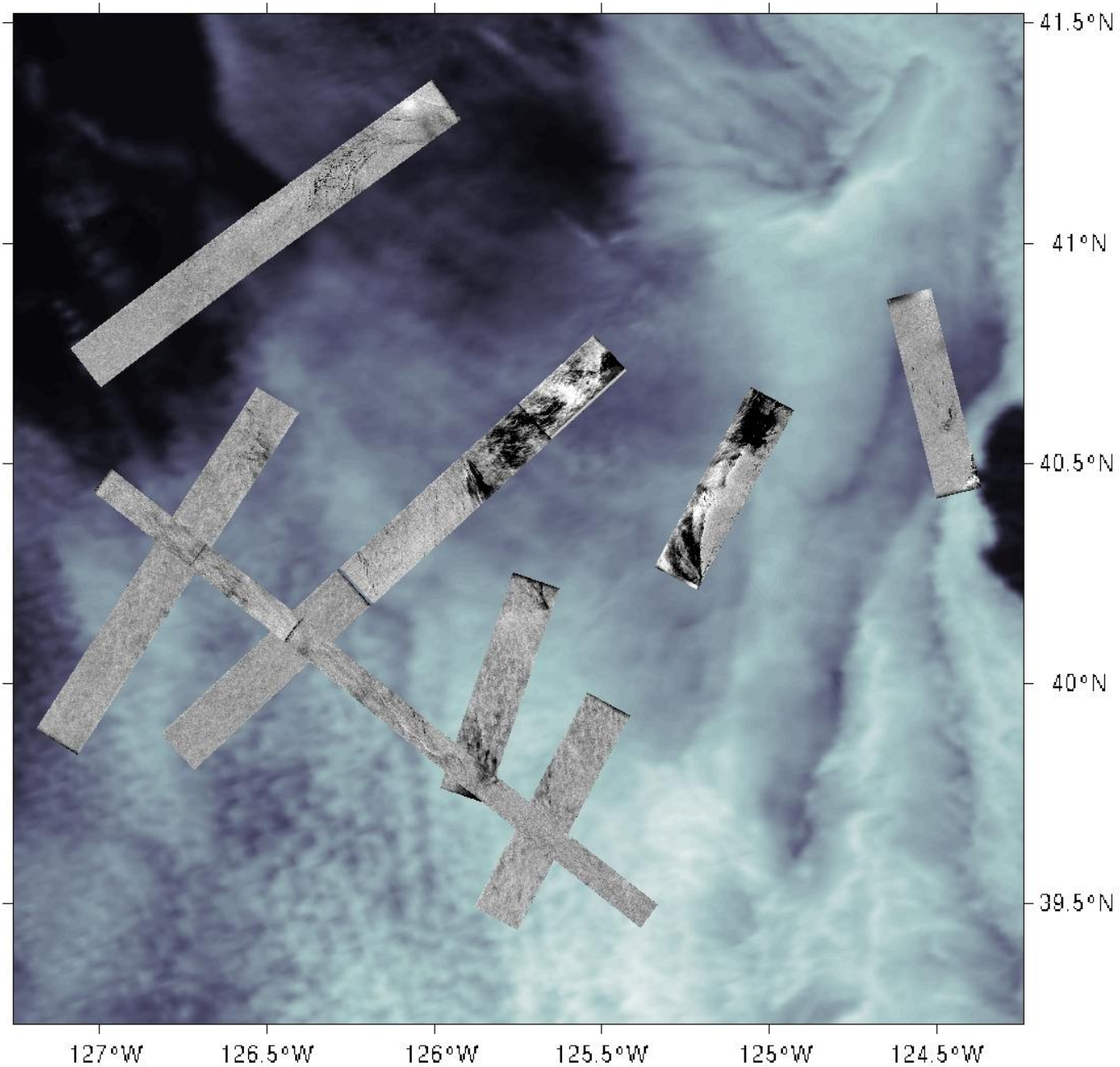
AVHRR ch_4 09/07/89 03:22 / SAR 09/08/89 16:47-19:08

ch_4:
10.3-11.5 μm
thermal IR

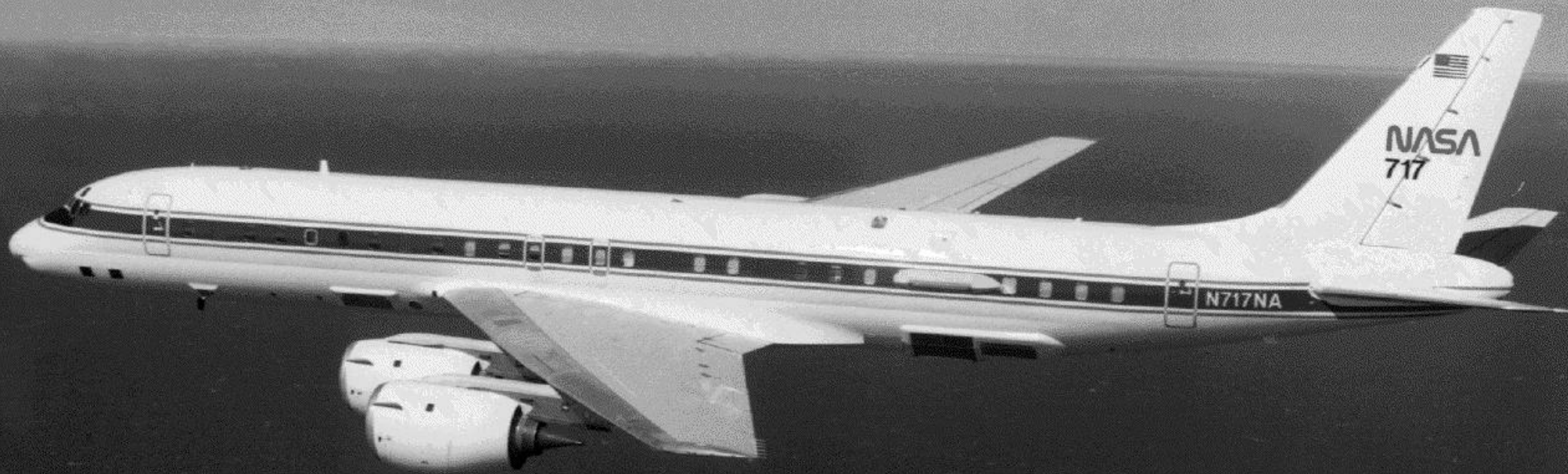


17
Approx. Temp. (°C)
6

09/08/89 21:07 AVHRR ch_1 (Optical) / SAR L-band

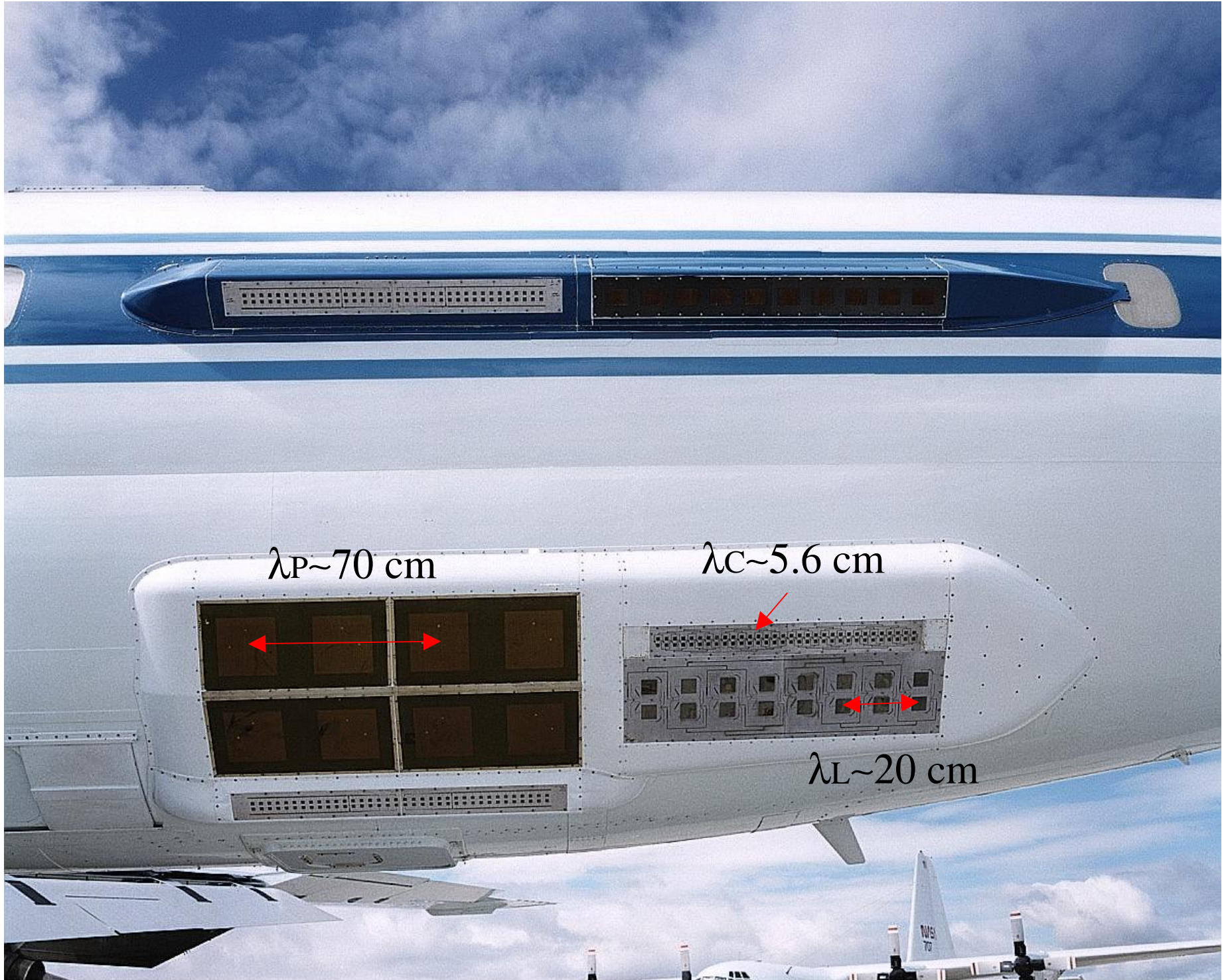


NASA AIRSAR DC-8



Ceiling~10000 meters

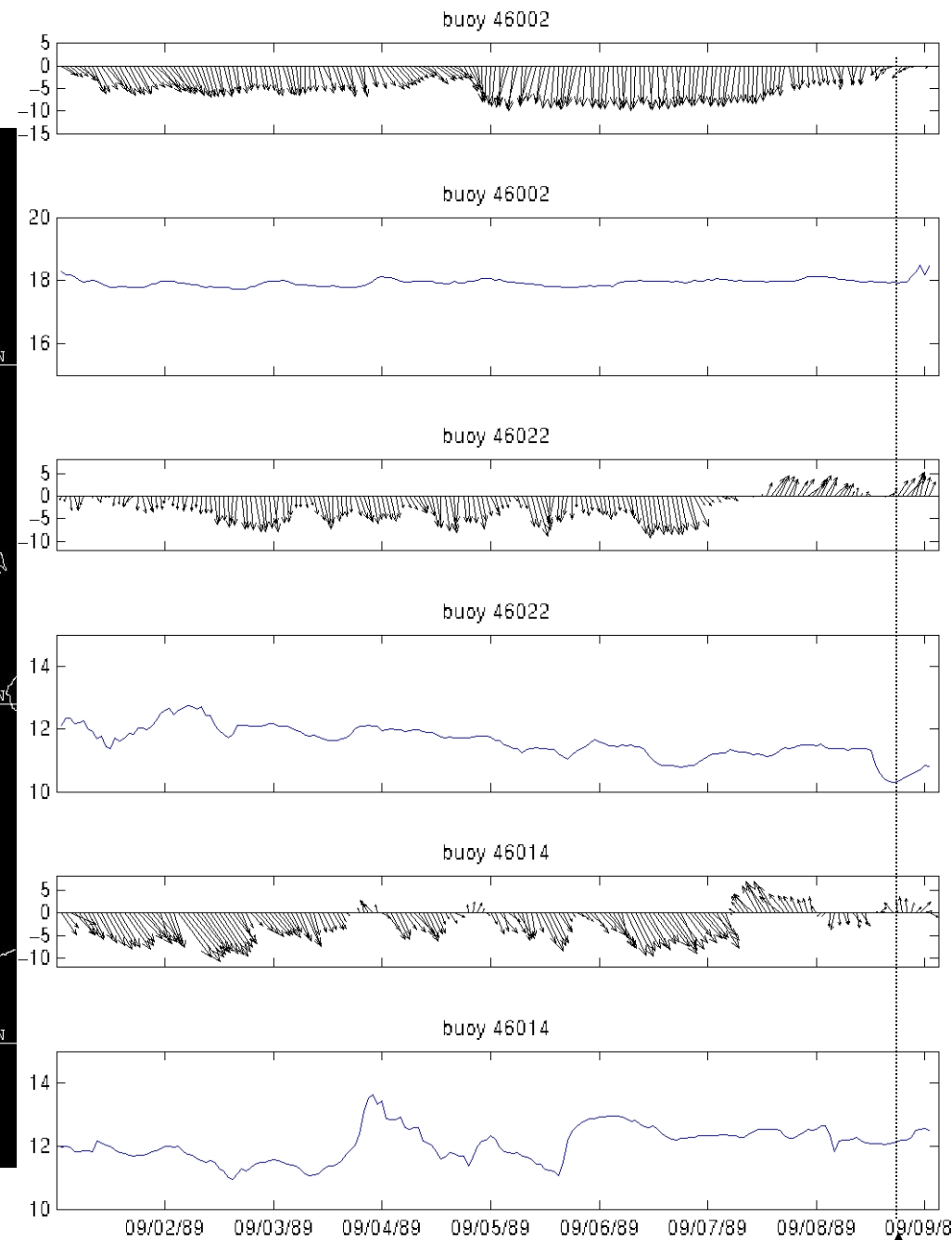
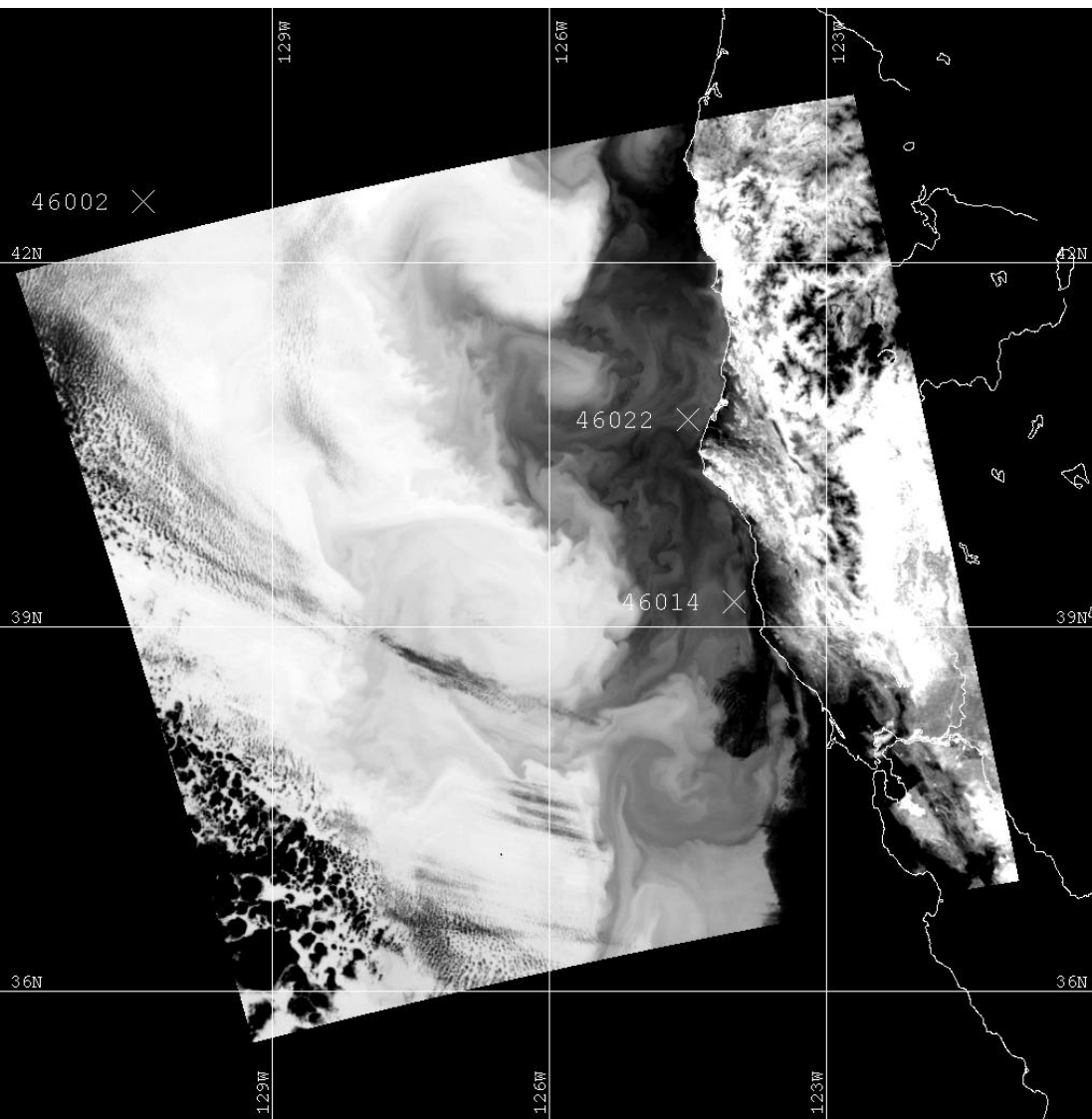
Speed~220 meters/second



Dryden Flight Research Center EC98-44485-1 Photographed 26MAR1998
Airborne Synthetic Aperture Radar (AIRSAR) on left rear fuselage of DC-8 (NASA/Wood)

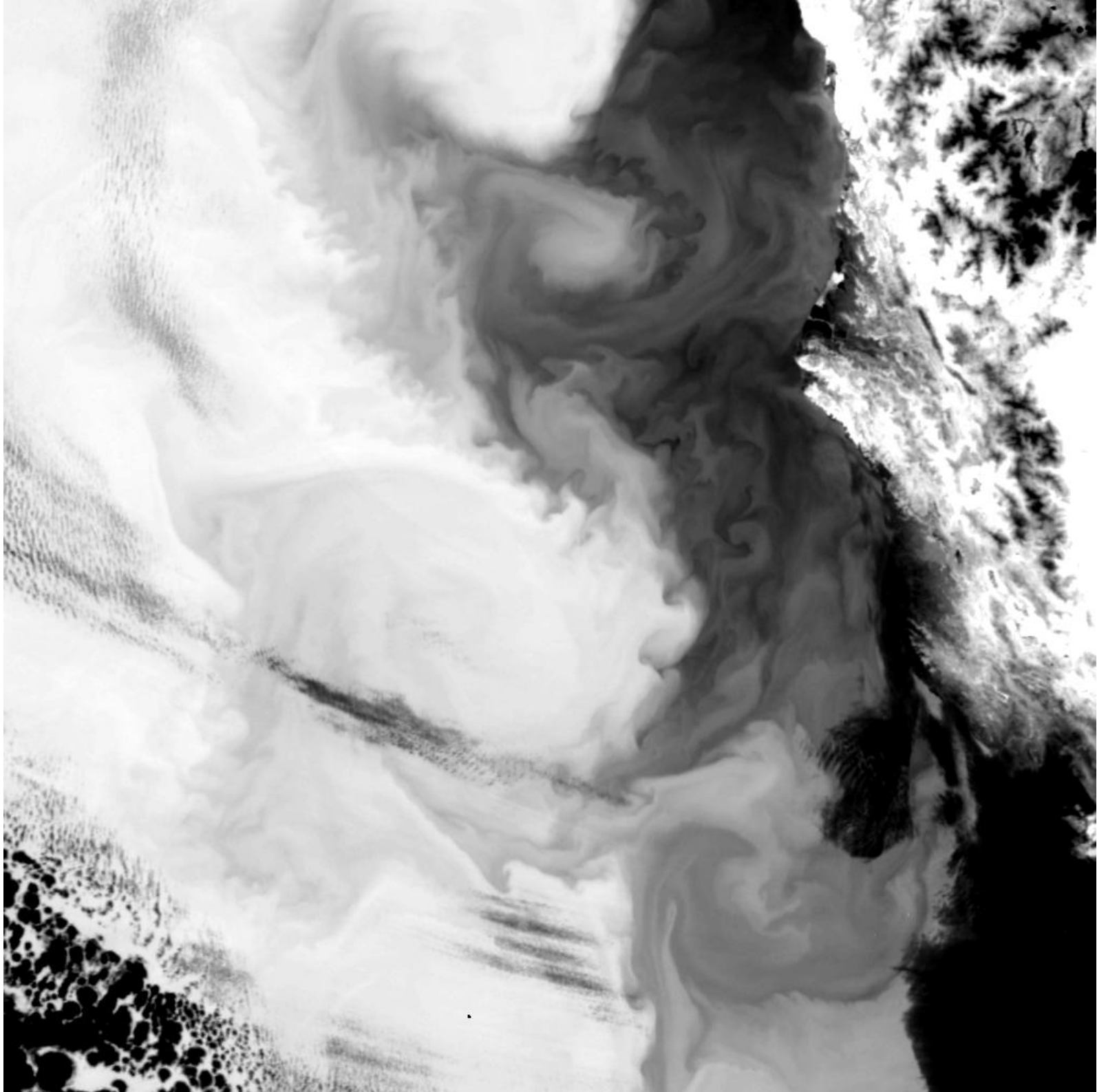
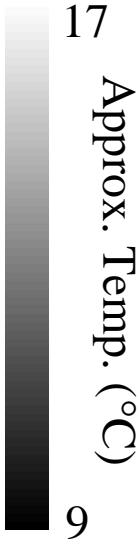


Wind and SST from NOAA Buoys

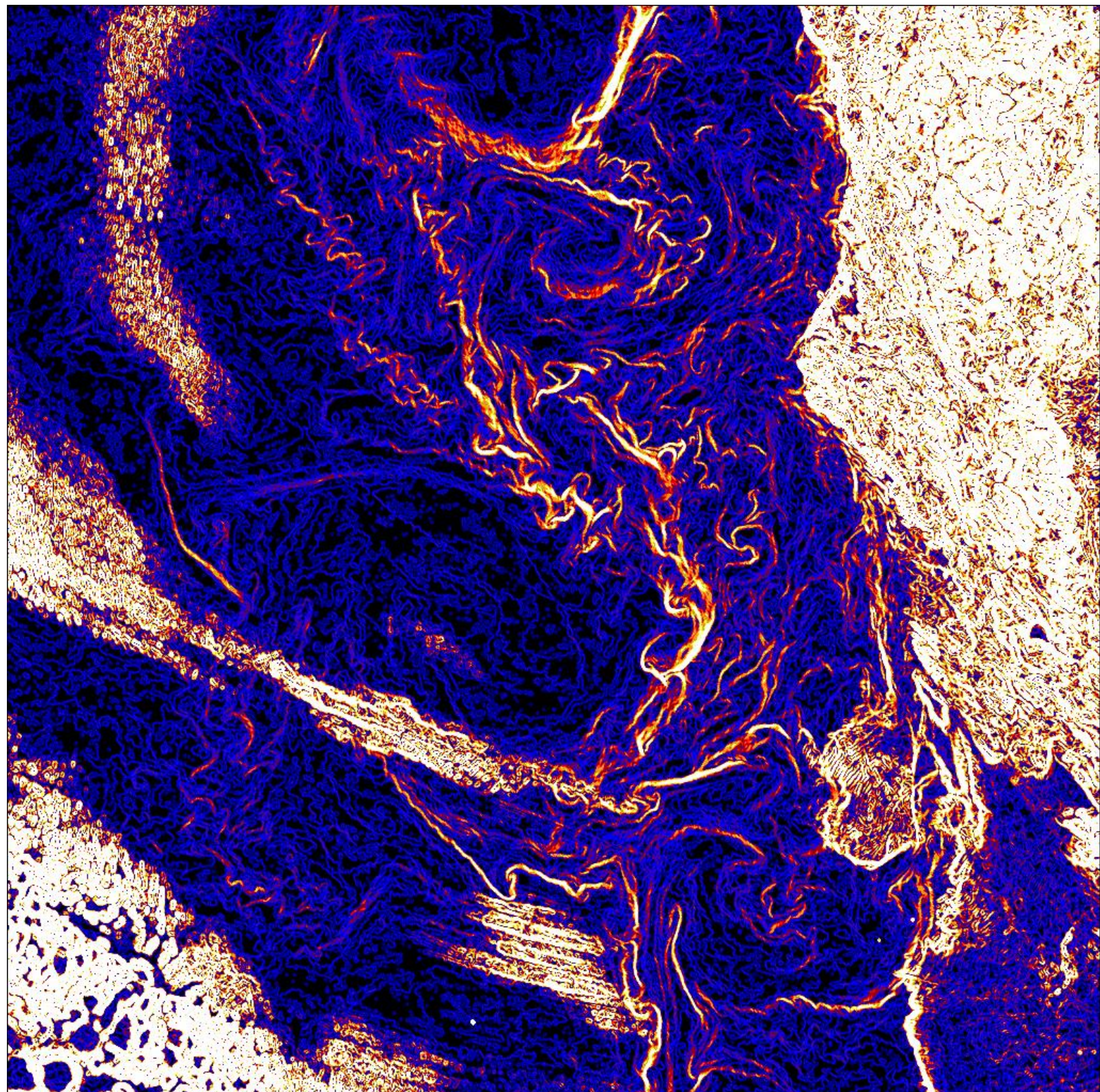


Time of AIRSAR Flight

AVHRR ch_4
09/07/89 03:22

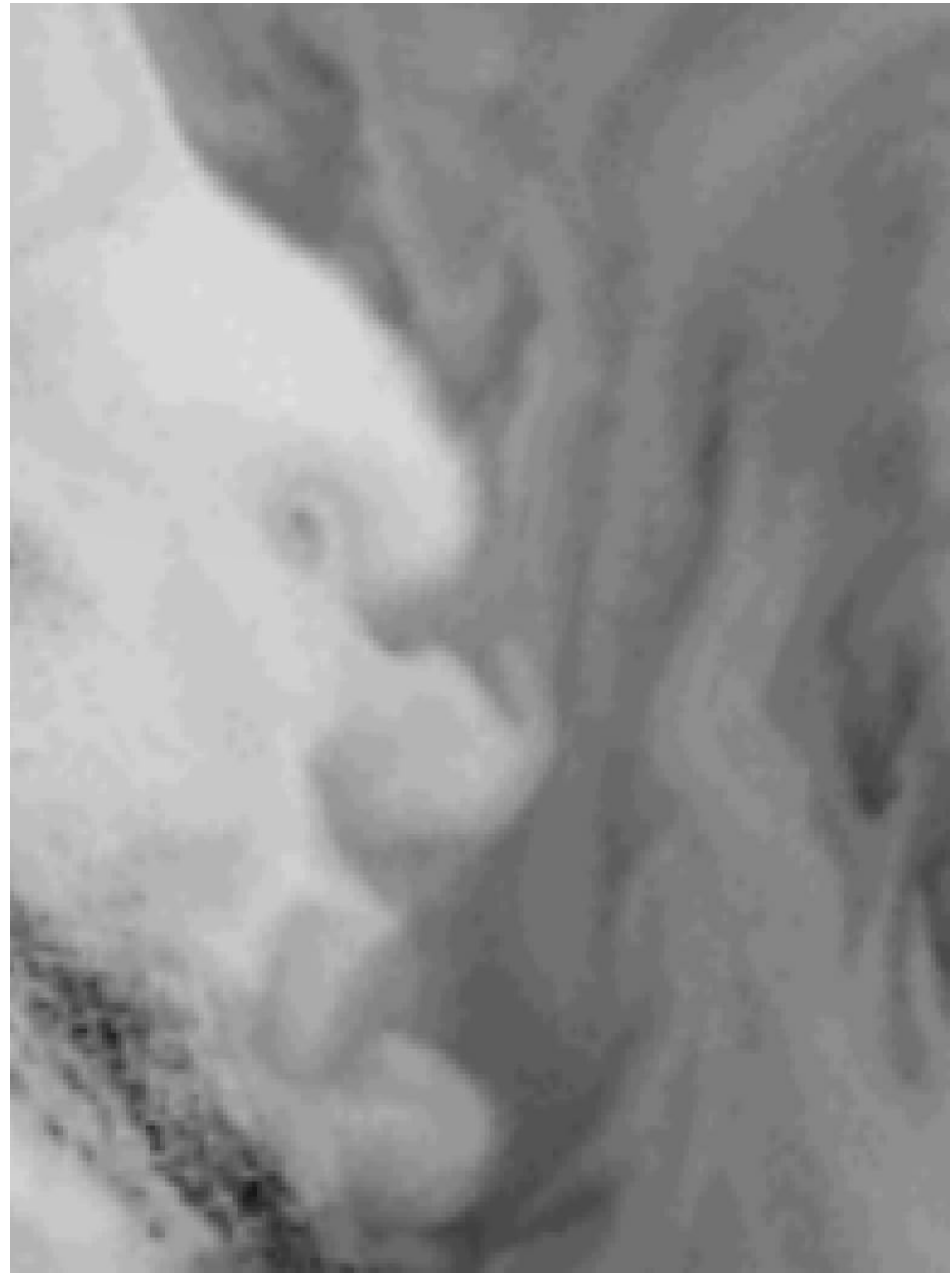


AVHRR ch_4 Gradient

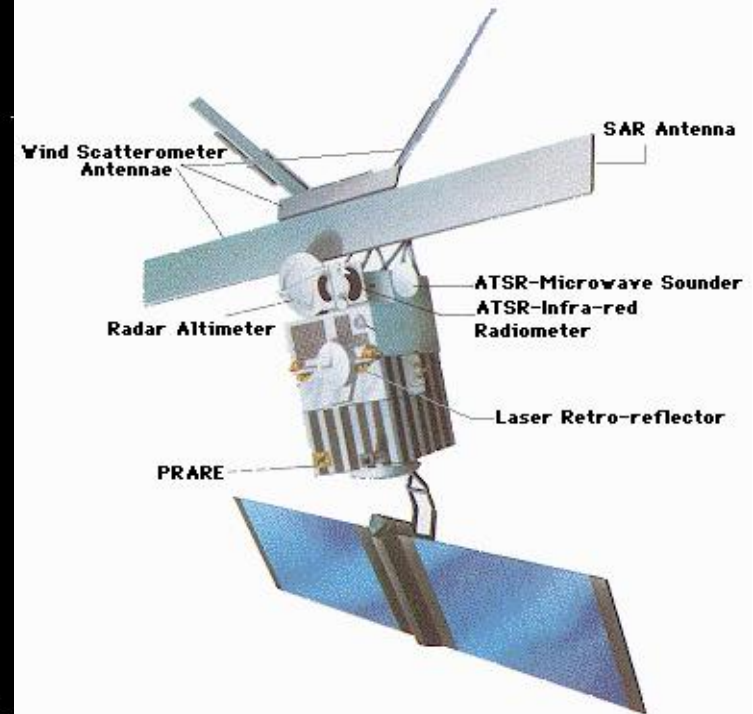
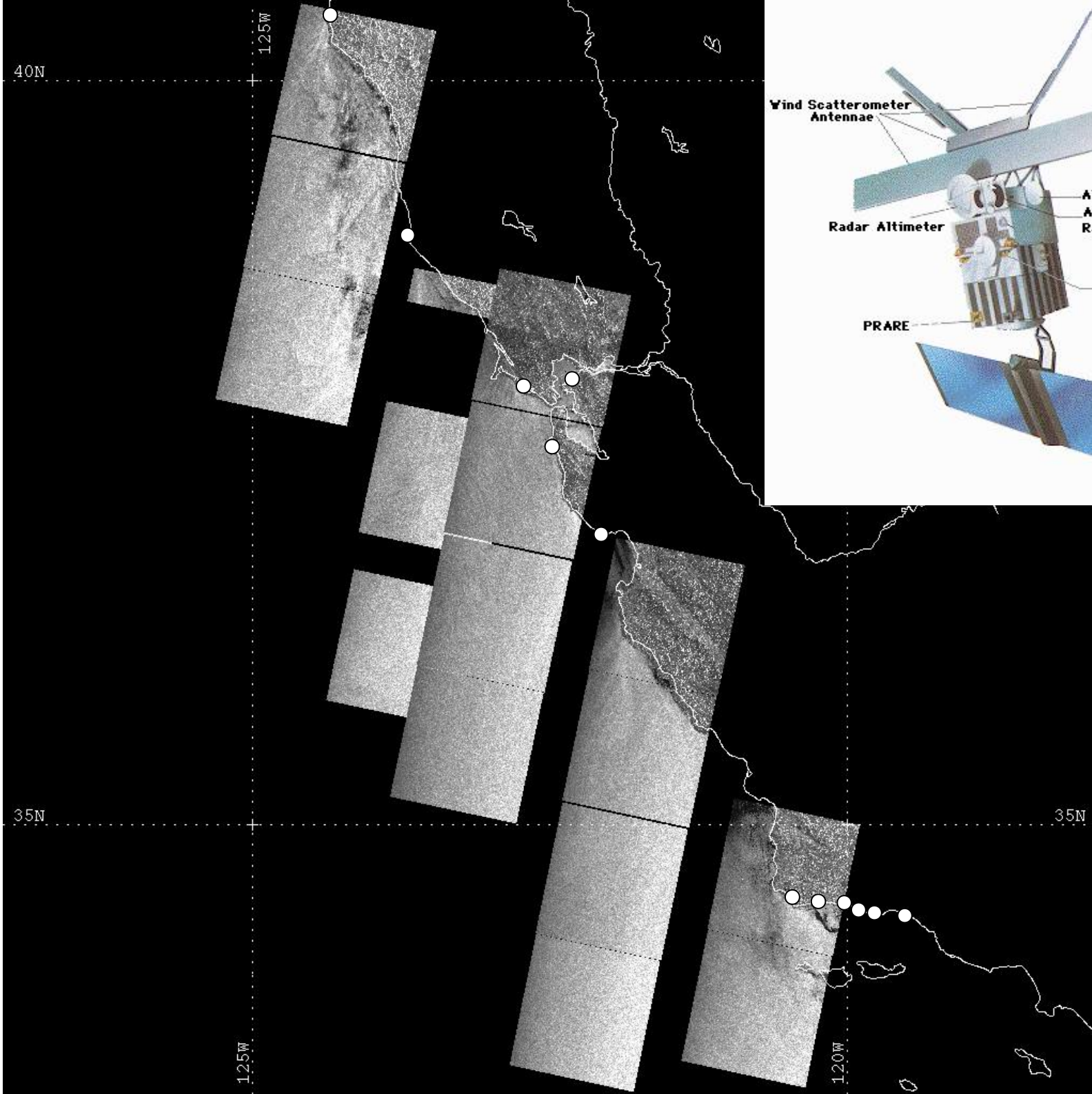


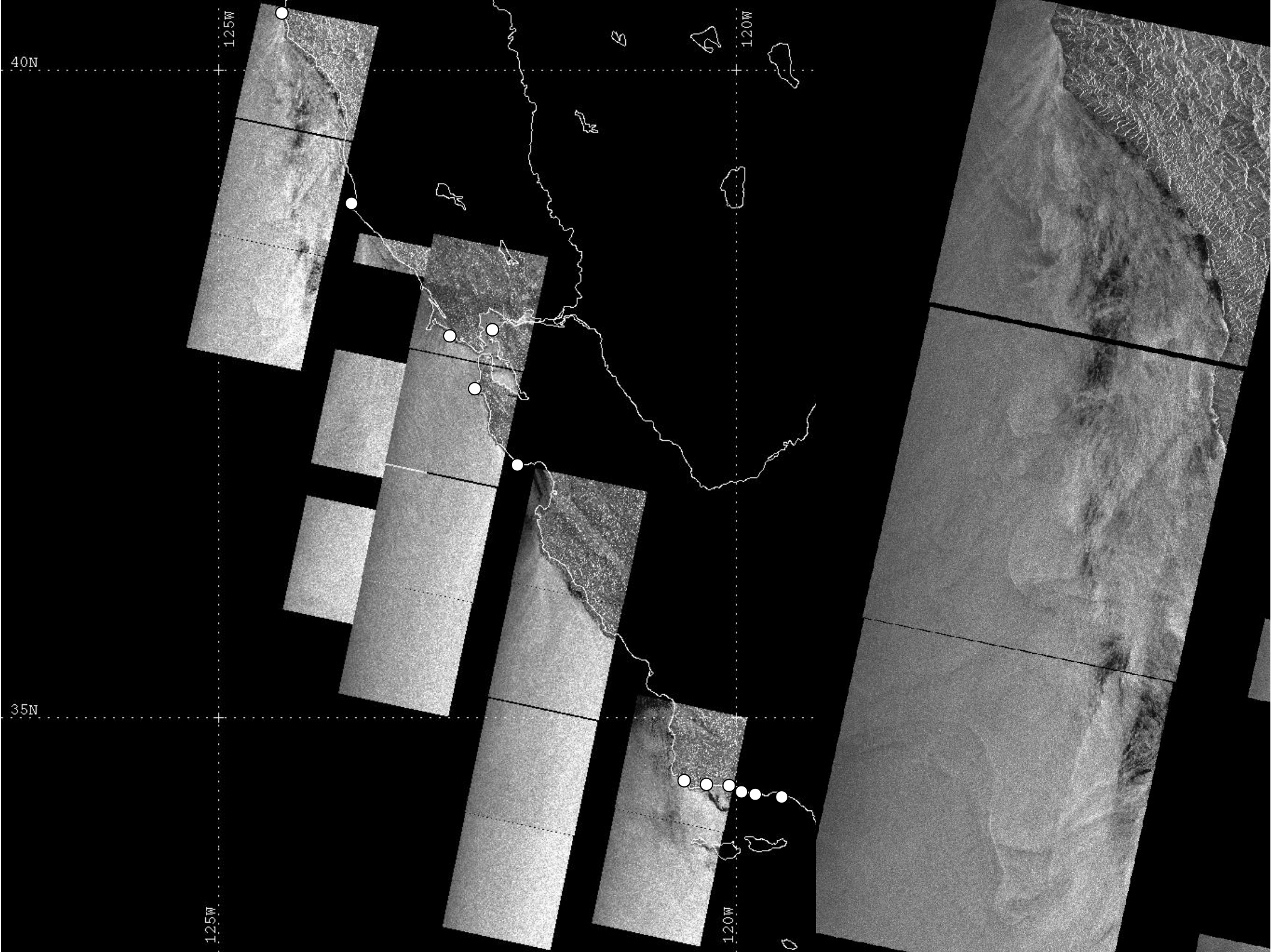
0.6
 \sim $^{\circ}\text{C} / \text{km}$
0

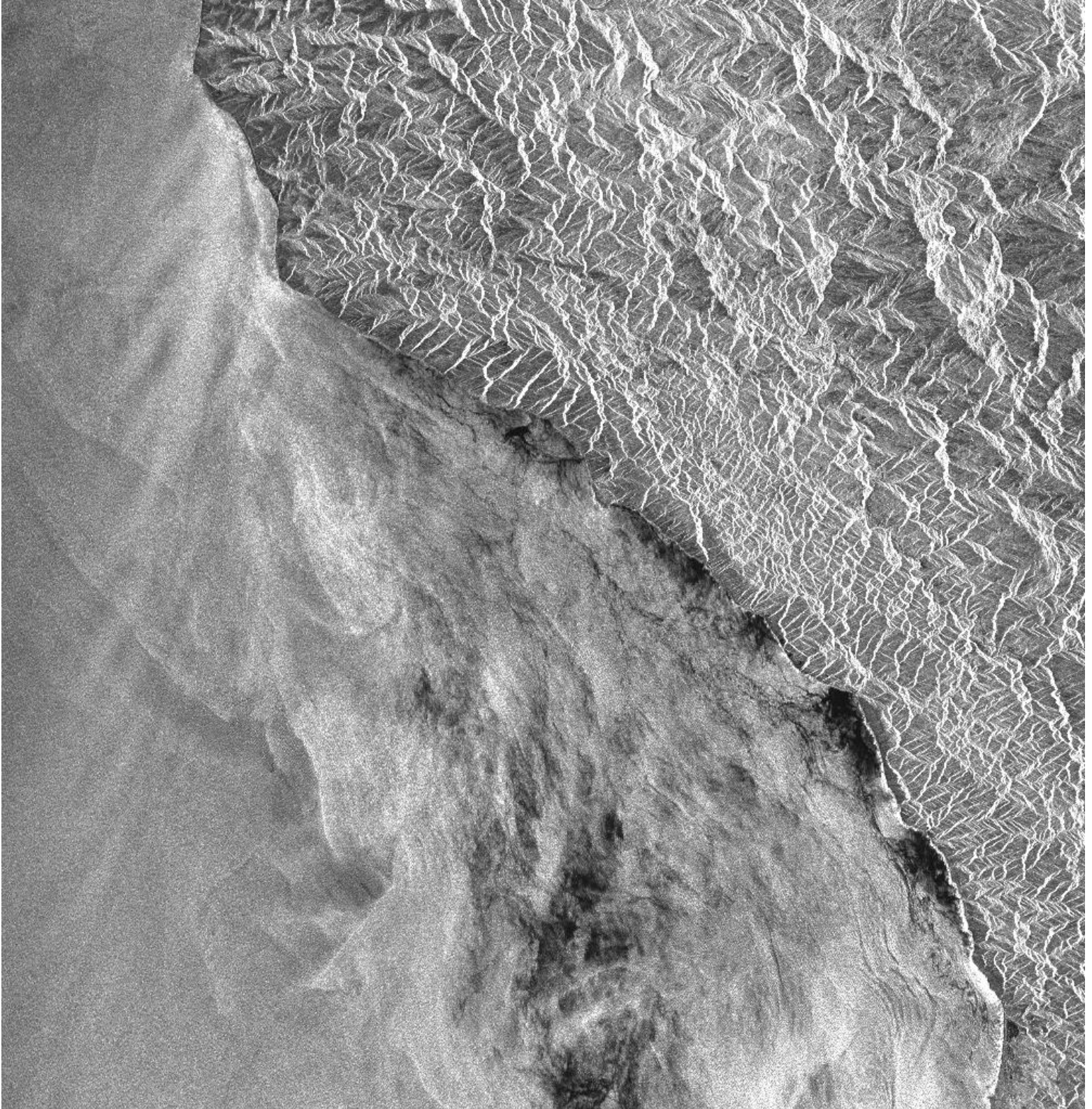
Unstable Shear Flow --> Vortex Generation

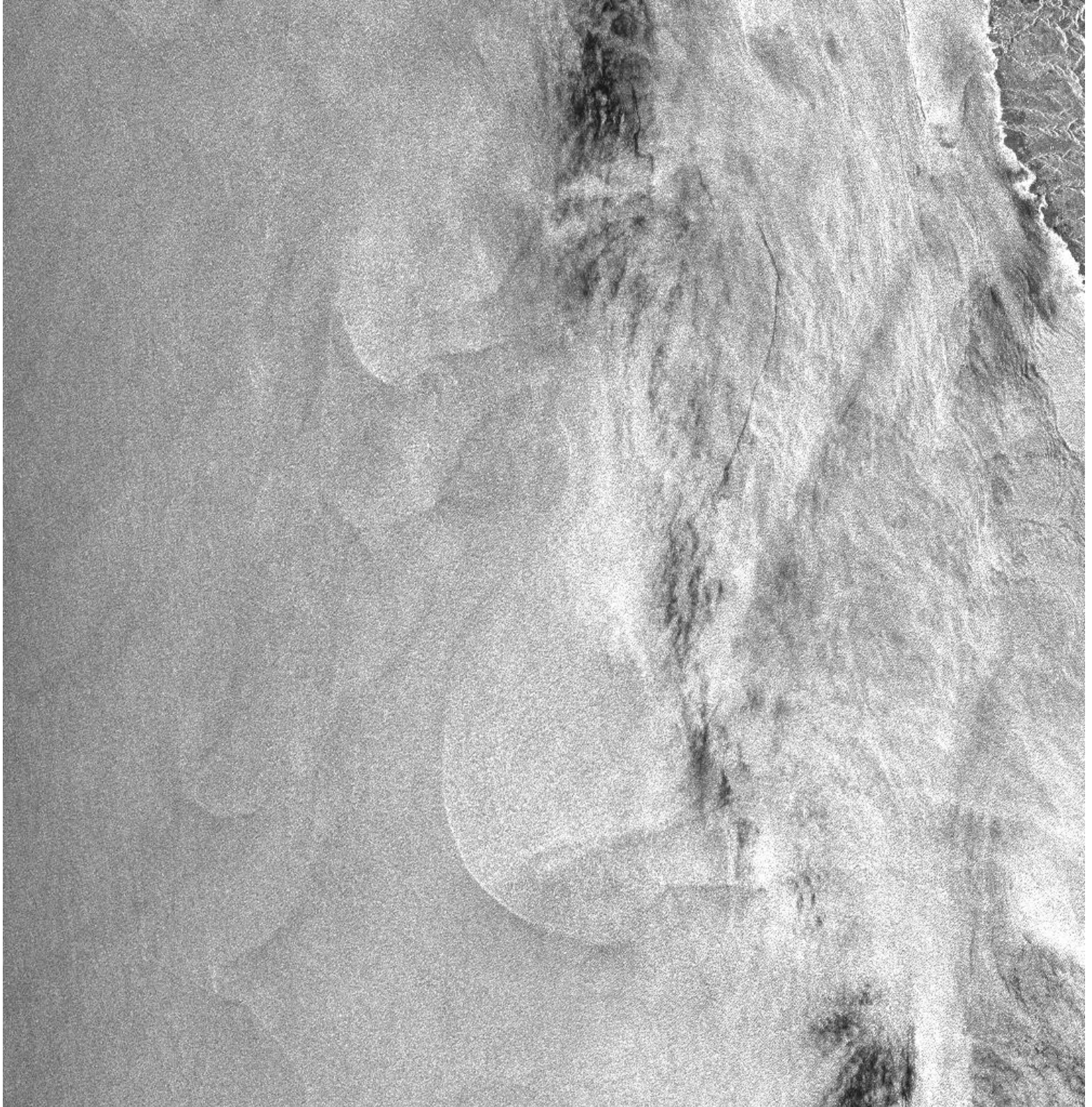


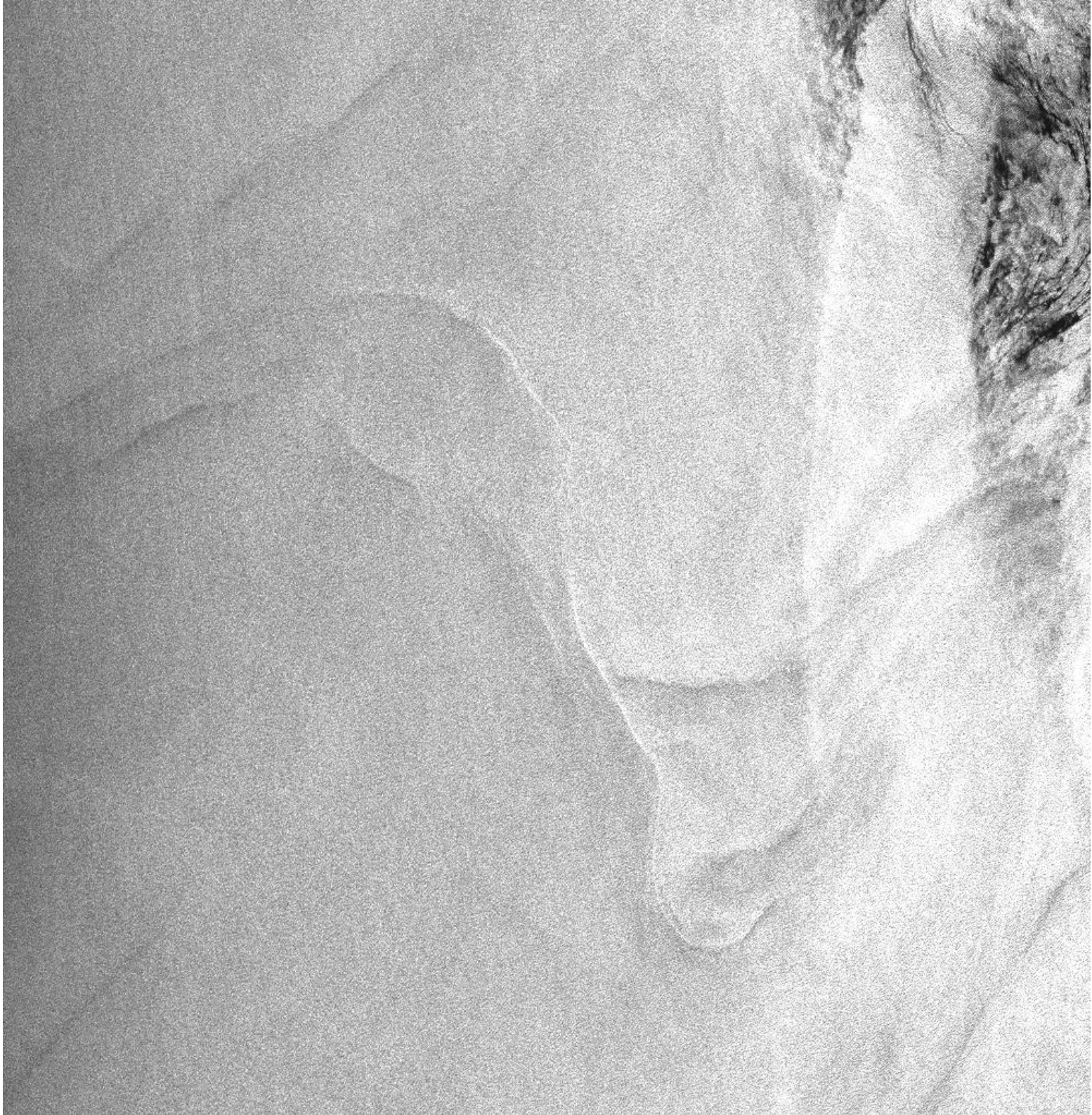
ERS-1 SAR Jul/Aug 1993

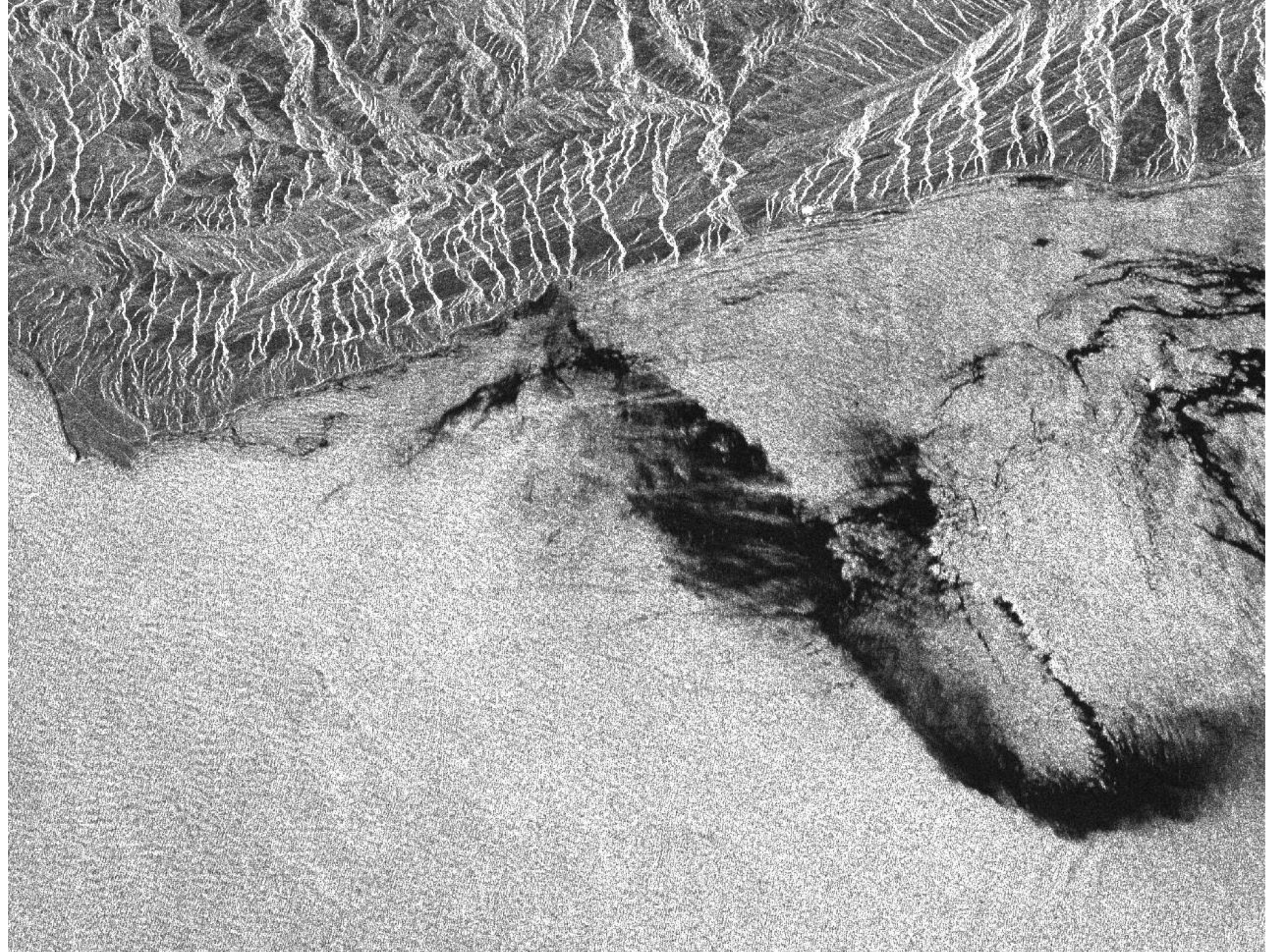








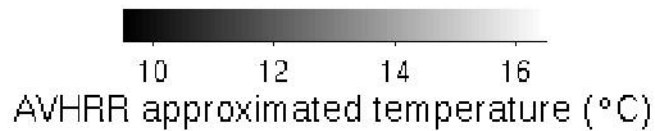
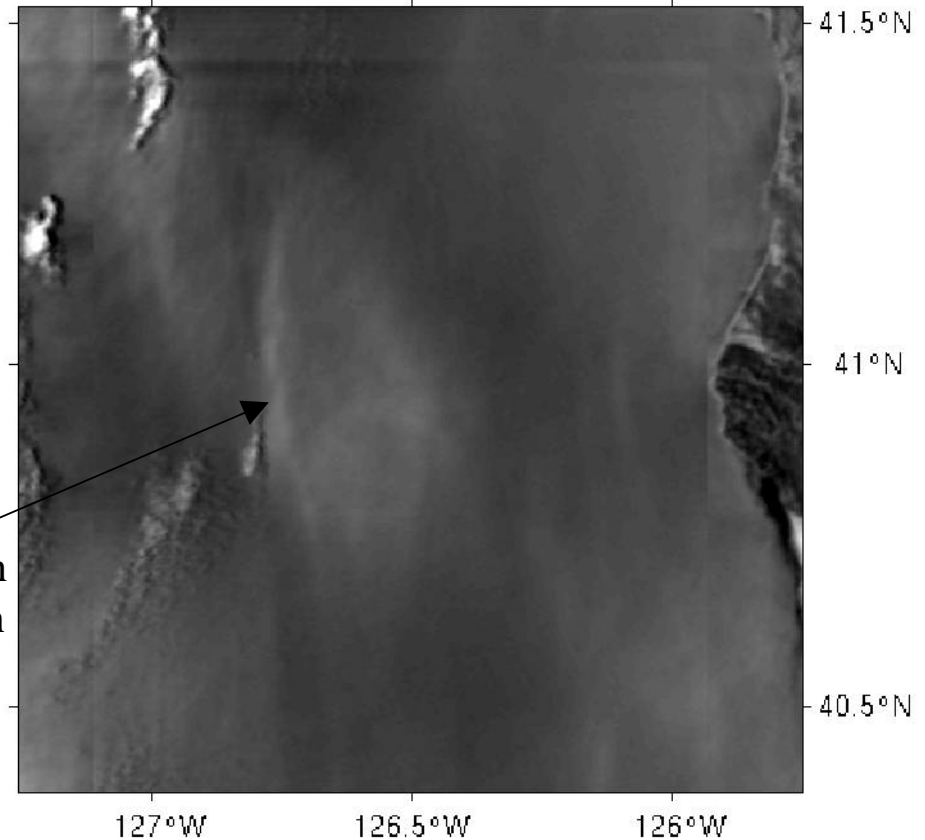
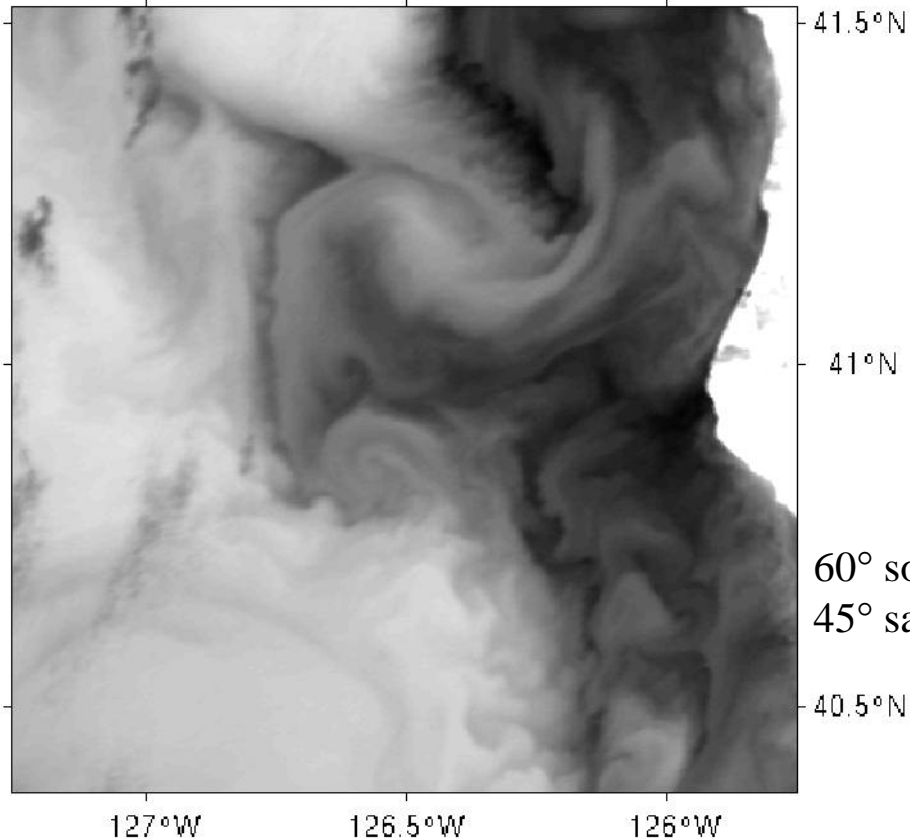




09/04/89 Optical Signal

09/04/89 AVHRR channel 4

09/04/89 AVHRR $[(ch_1 + ch_2)/2]$ (detrended)

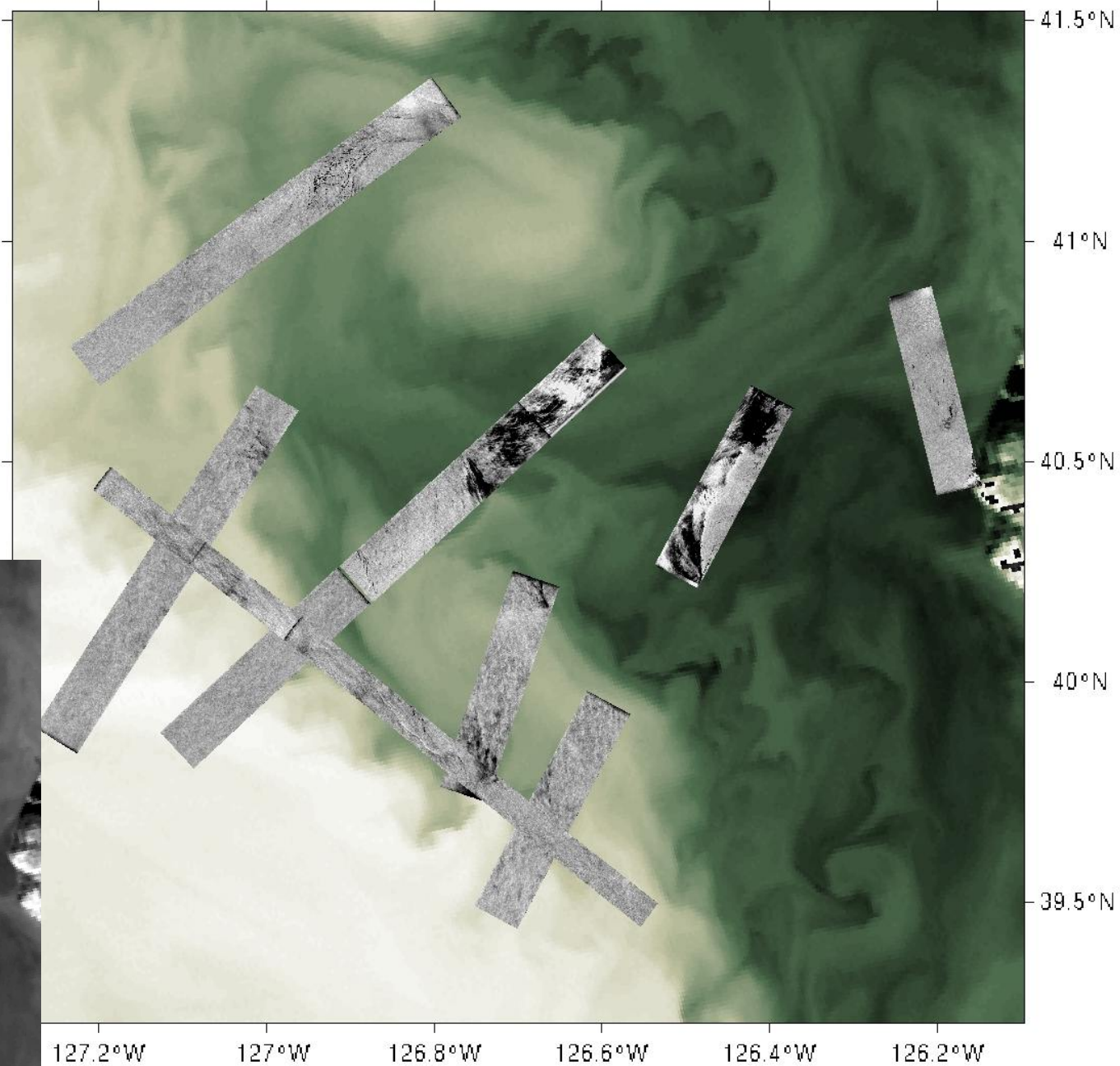
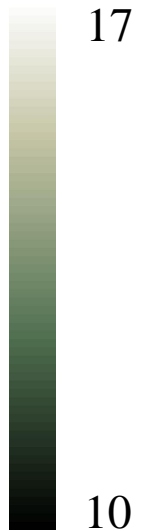


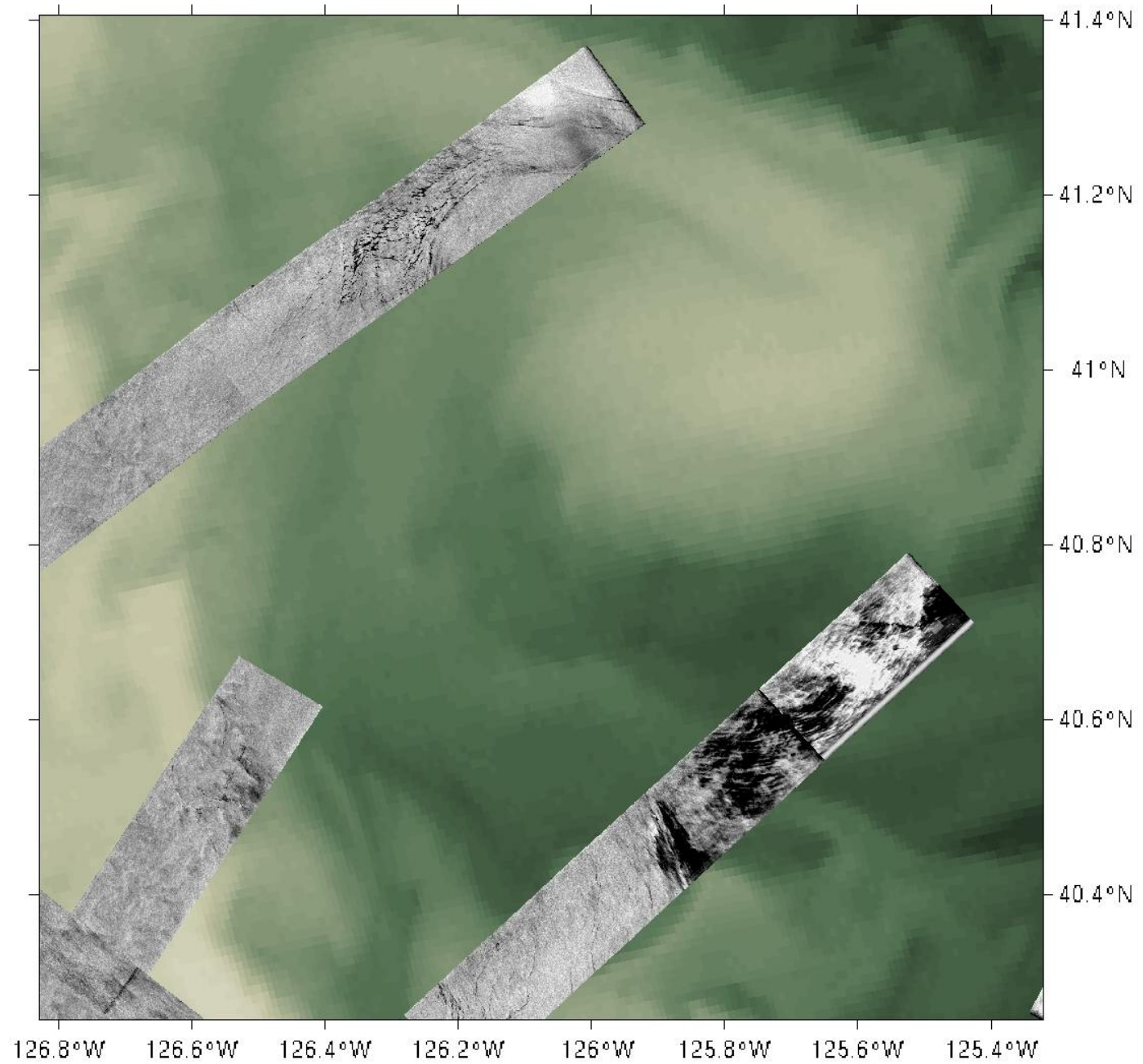
Increase in surface slope spectrum at 6°
(or marine stratus forming above fronts)

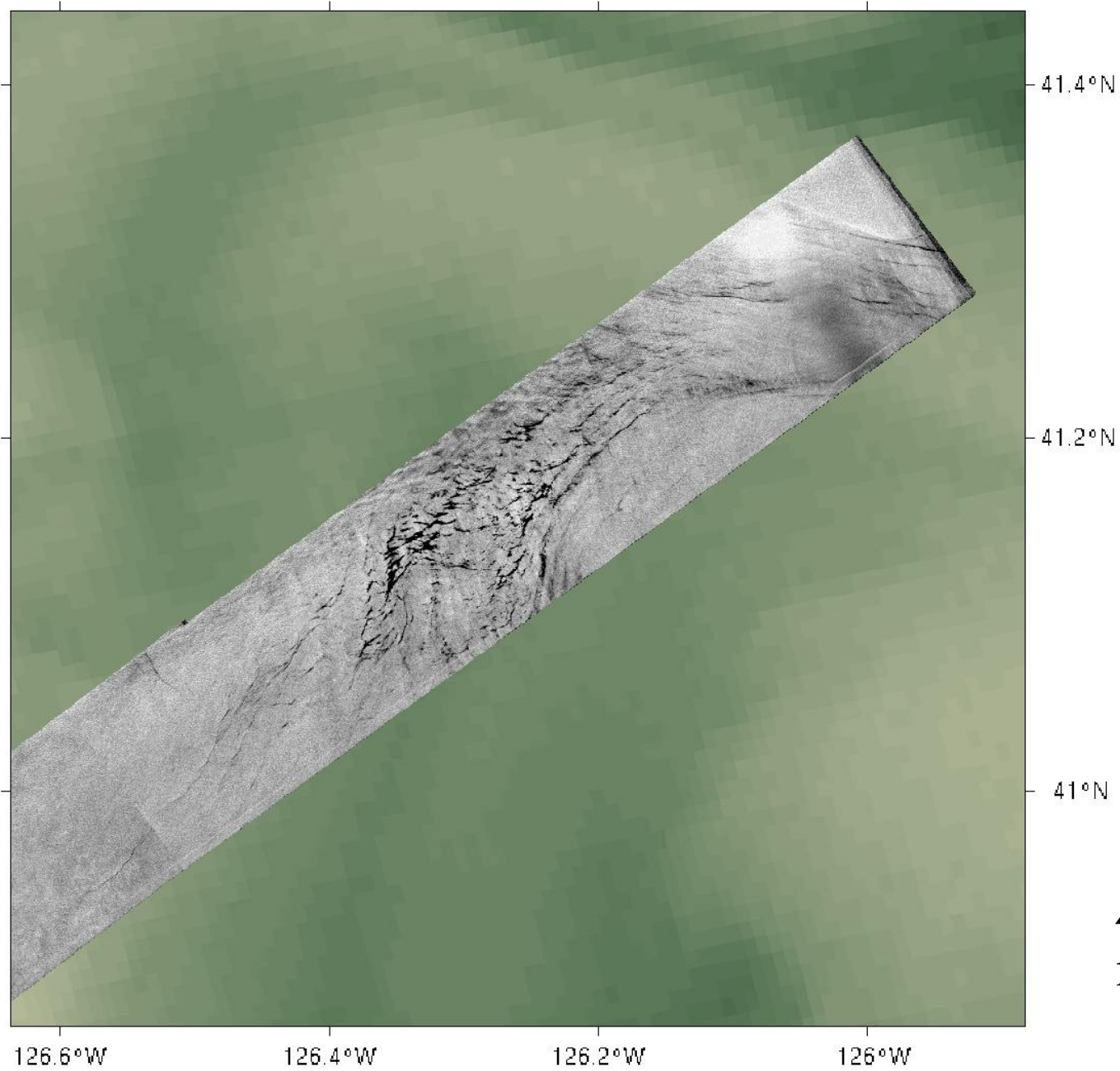
ch_1:	ch_2:
0.55-0.68 μm	0.72-1.10 μm
yellow-red	red-near IR

AVHRR ch_4 / SAR L-band

Approximate Temperature (°C)

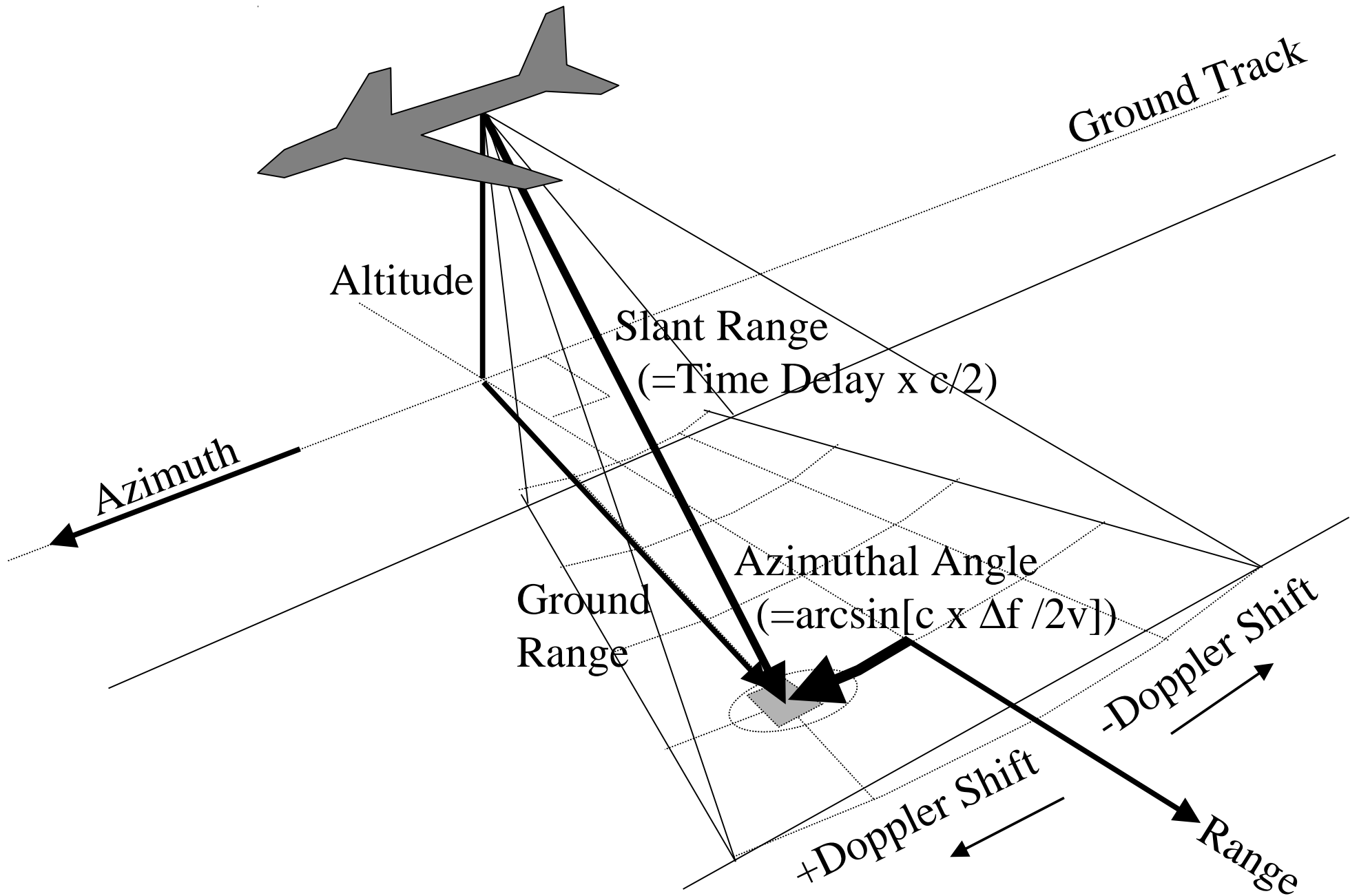




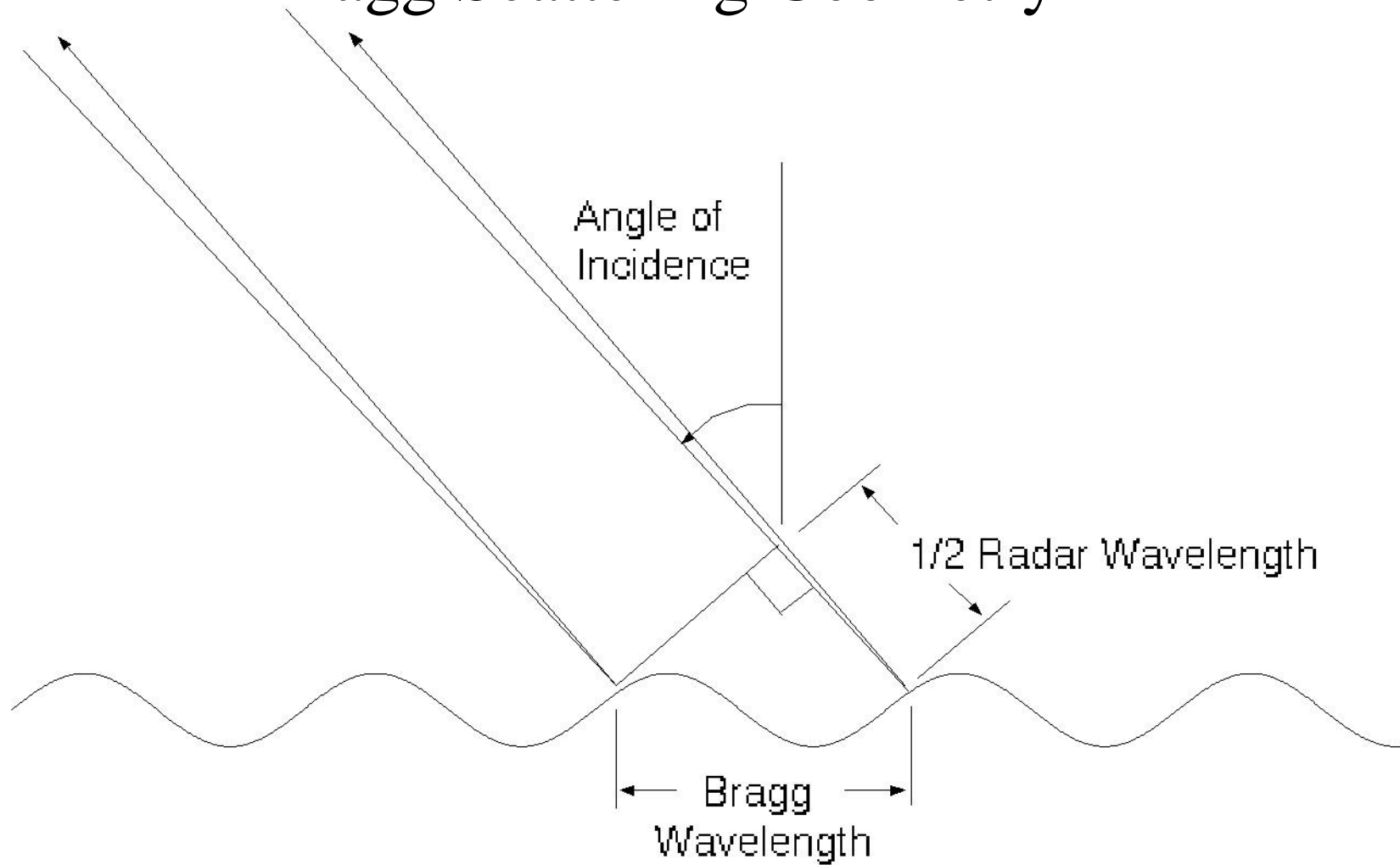


$\lambda \sim 1$ k
m

SAR IMAGING GEOMETRY



Bragg Scattering Geometry



$$\lambda_{\text{Bragg}} = \lambda_{\text{radar}} / 2 \sin \theta$$

AIRSAR Bragg Wavelengths

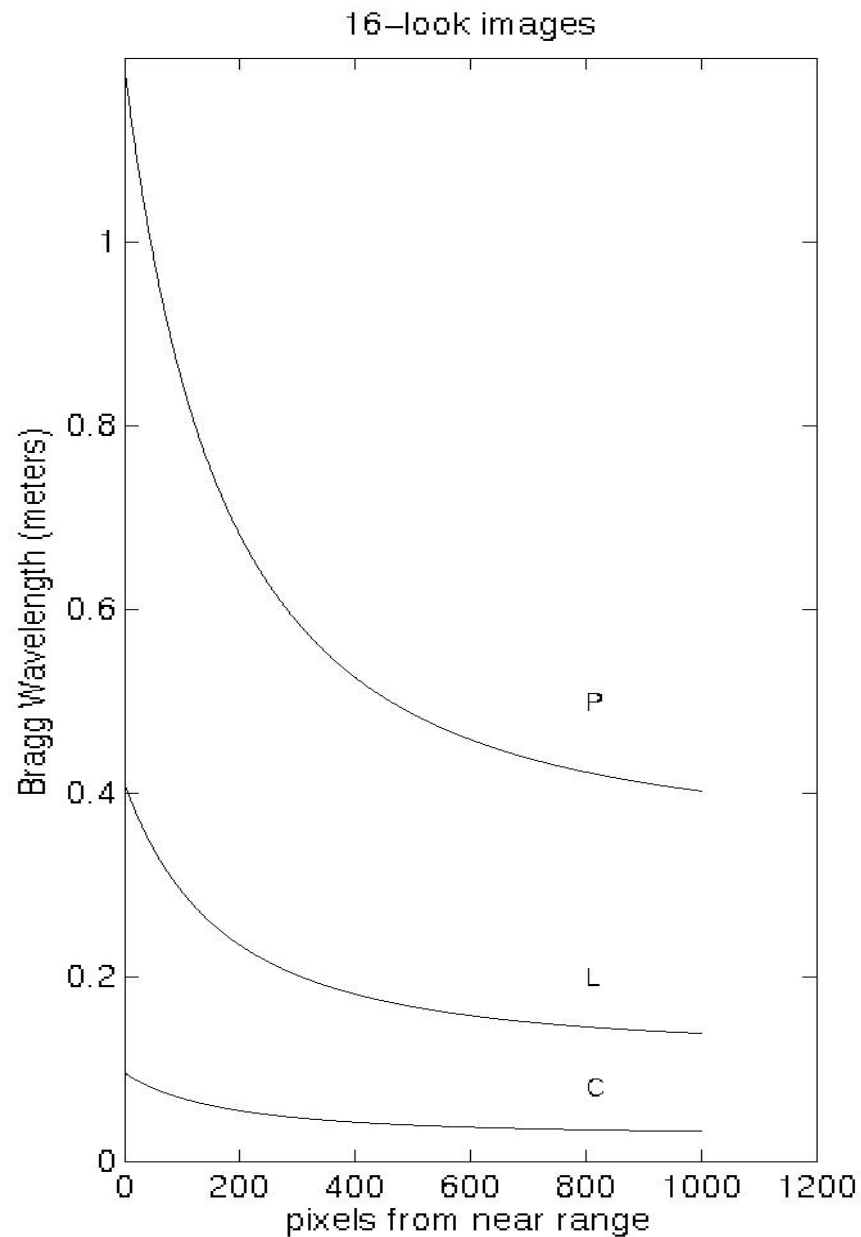
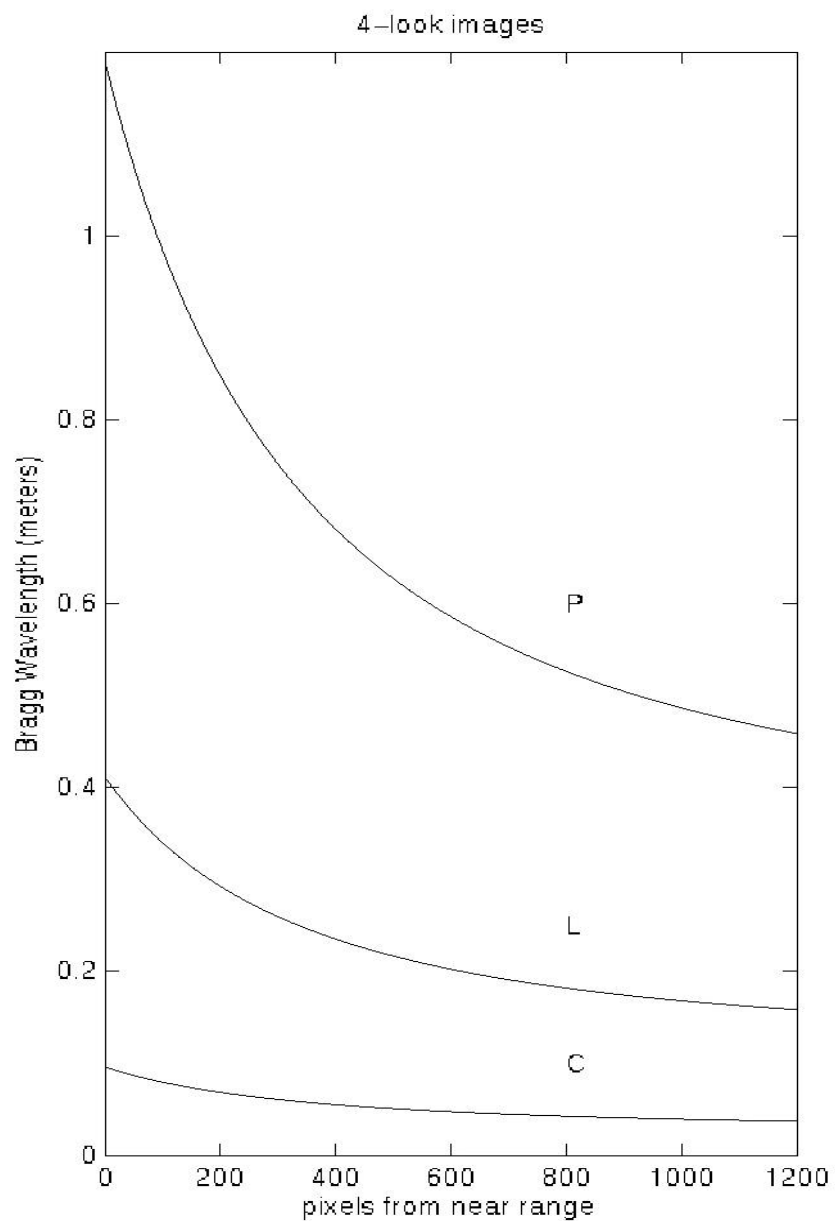
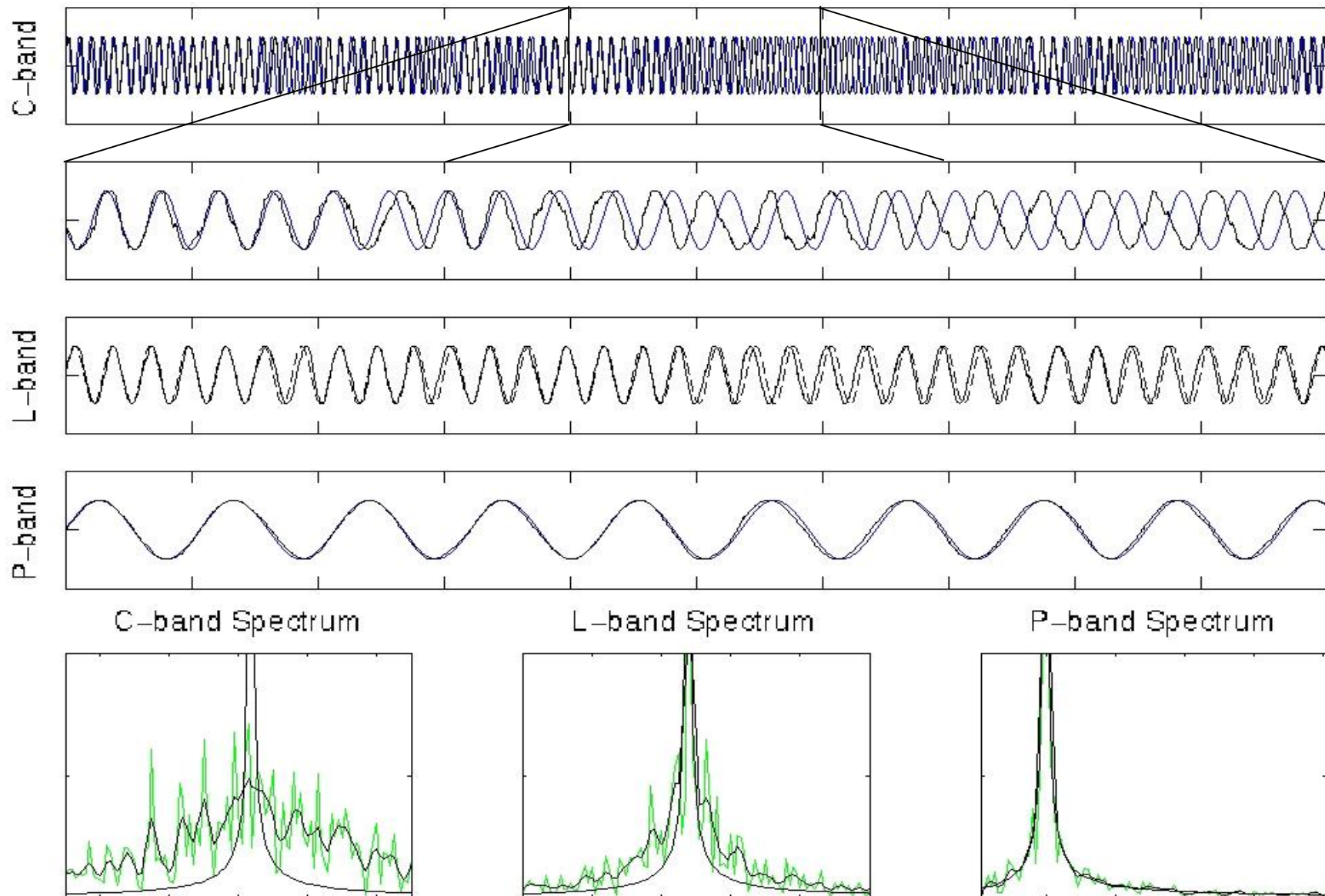
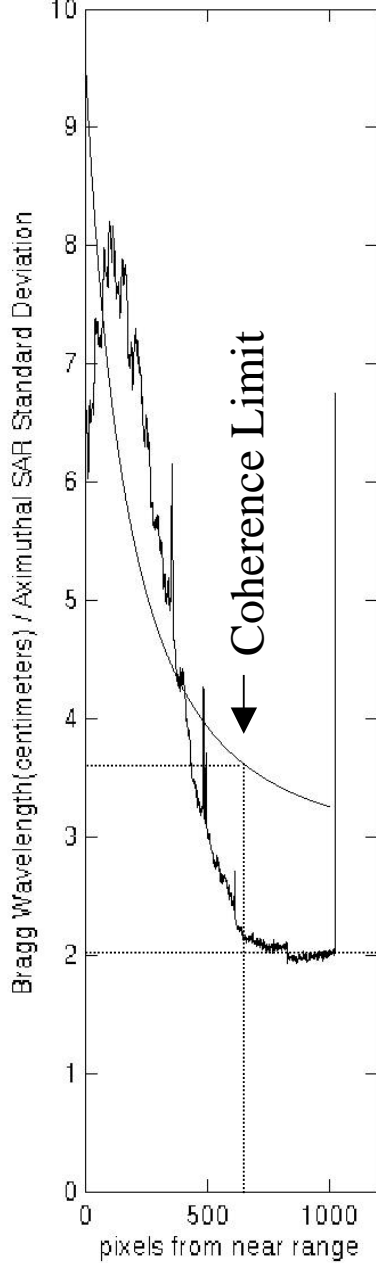
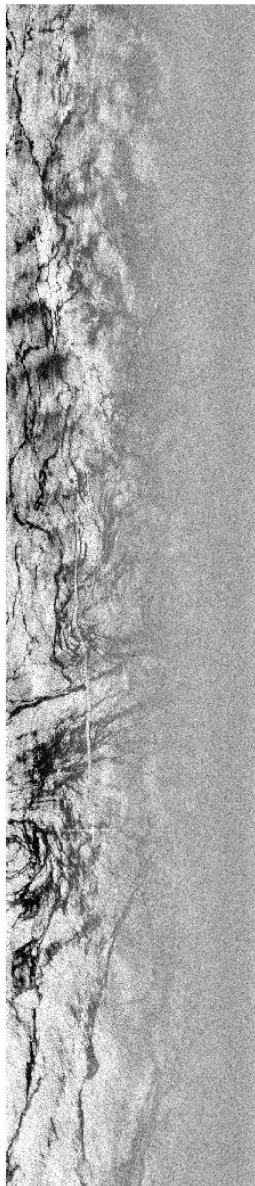
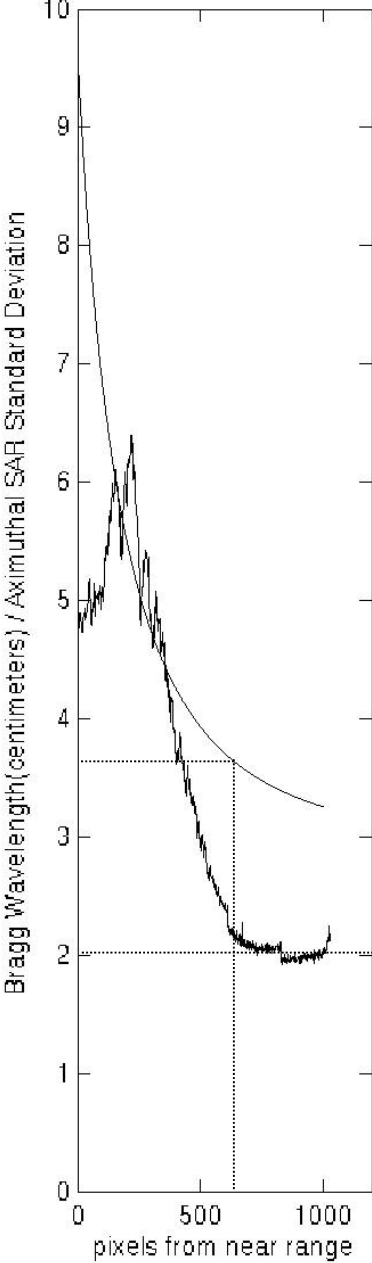
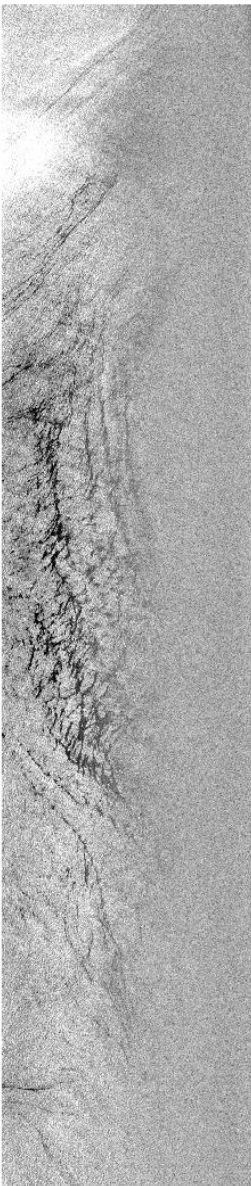


Illustration of the Effect of a Random Perturbation on Phase Coherence



AIRSAR C-band Bragg Wave Incoherence at Shallow Incidence Angles

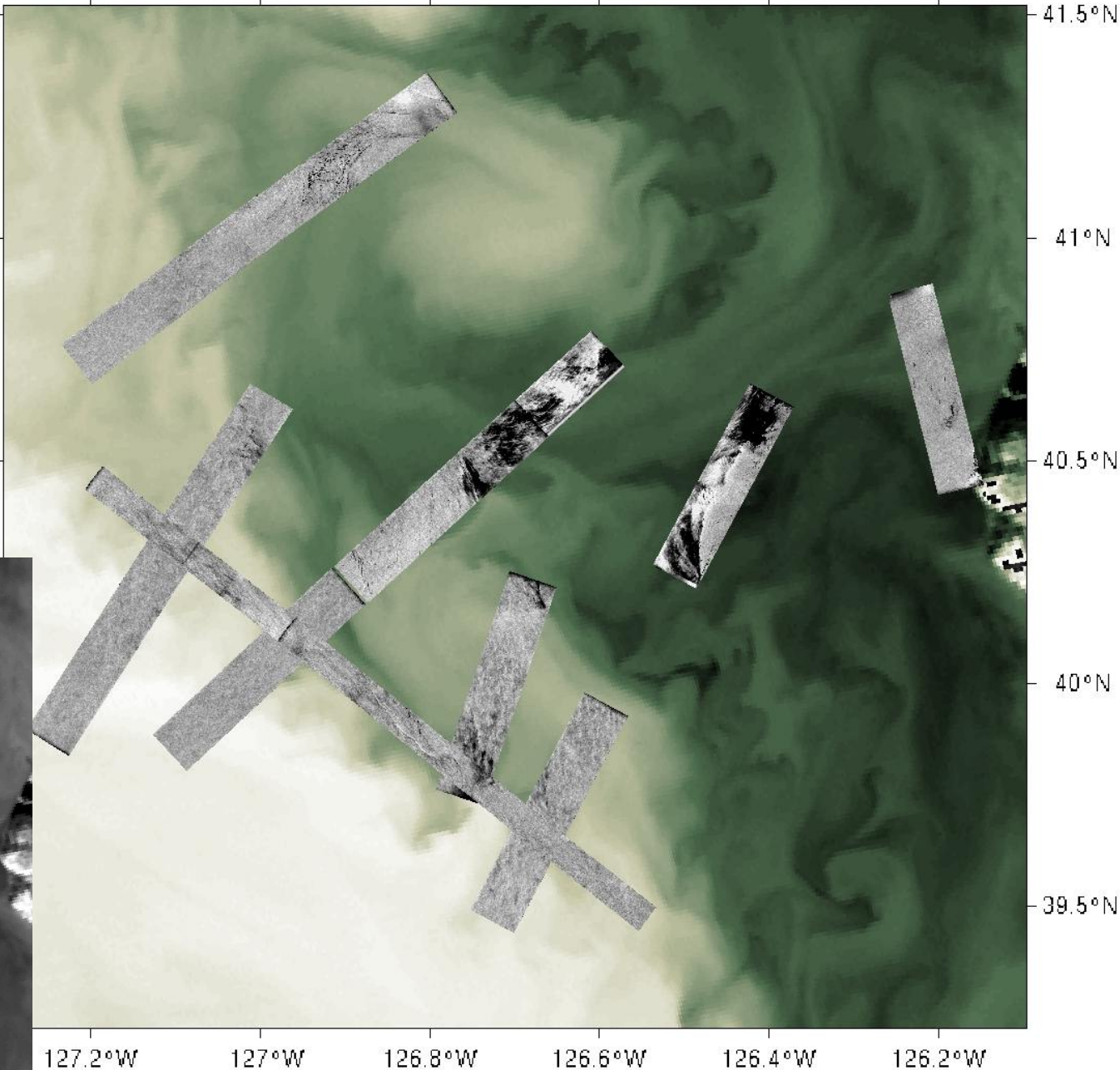


Corresponding
Bragg
Wavelength

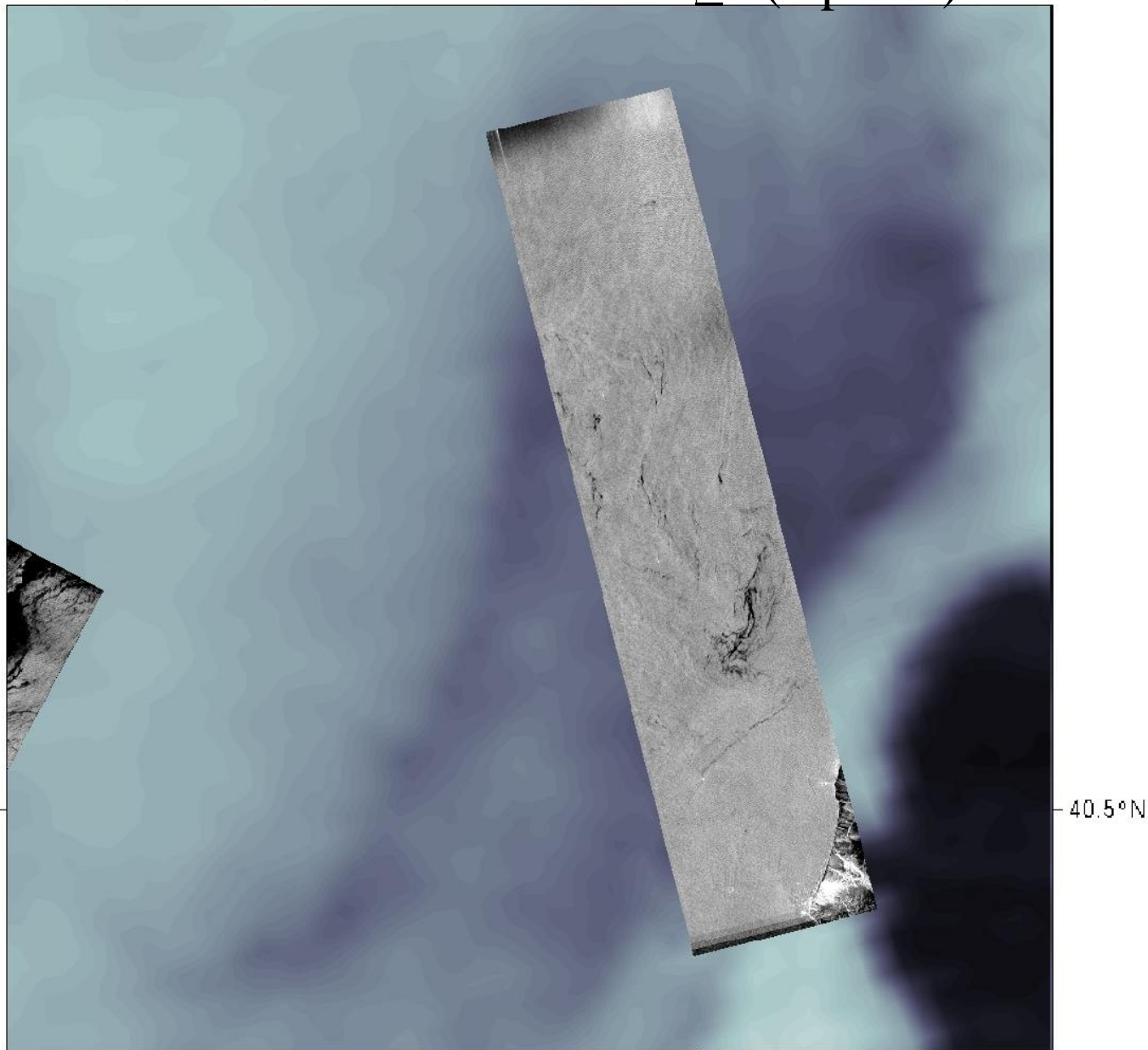
Noise Floor

AVHRR ch_4 / SAR L-band

Approximate Temperature (°C)



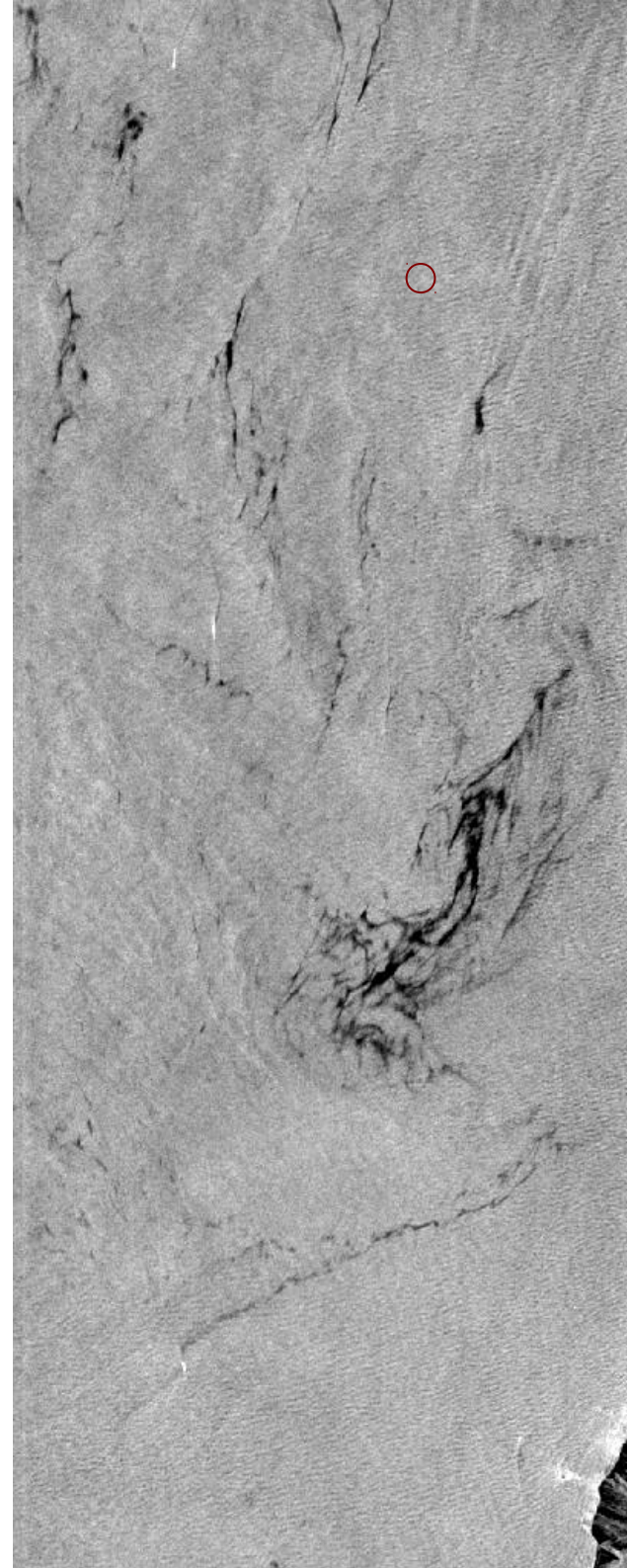
09/08/89 21:07 AVHRR ch_1 (Optical)



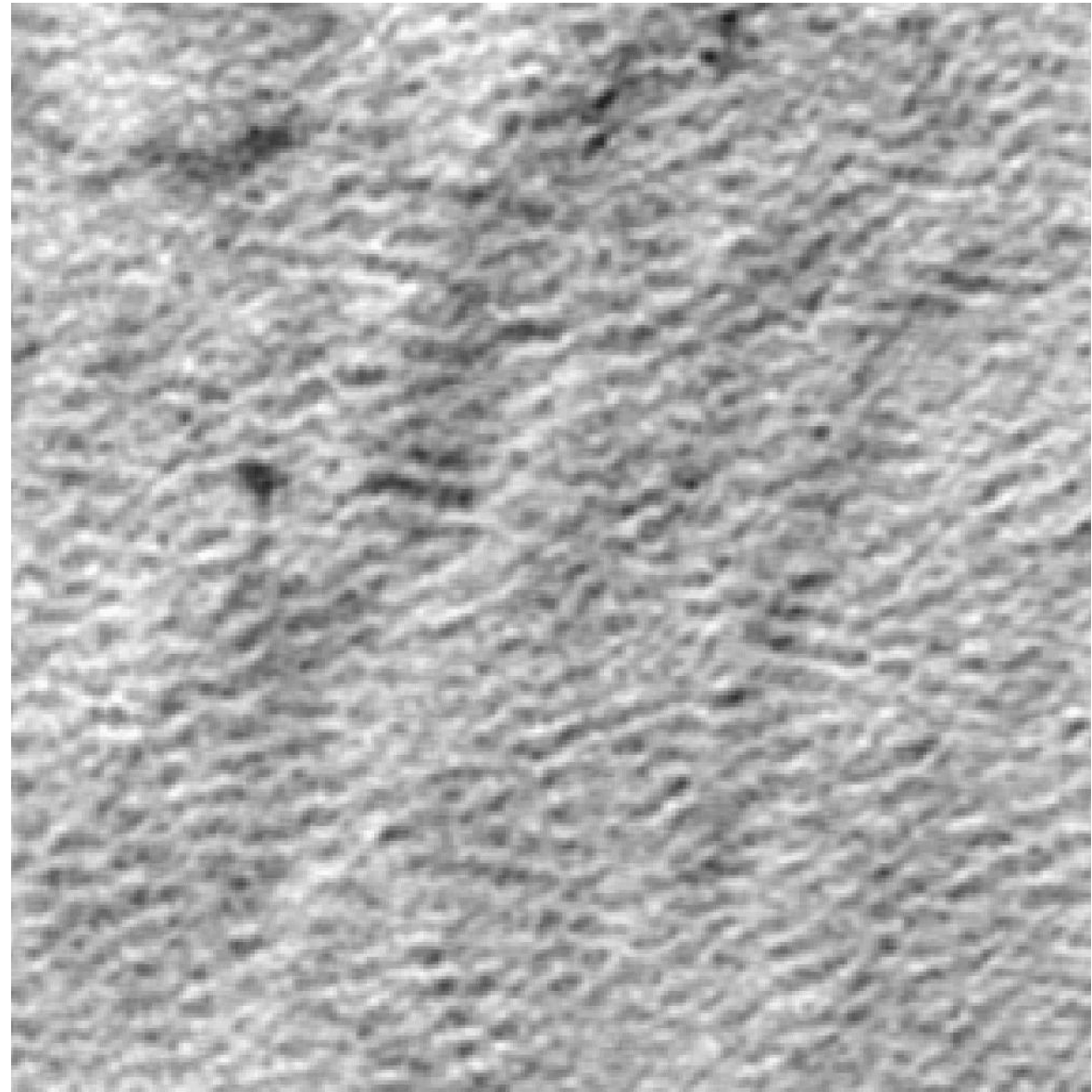
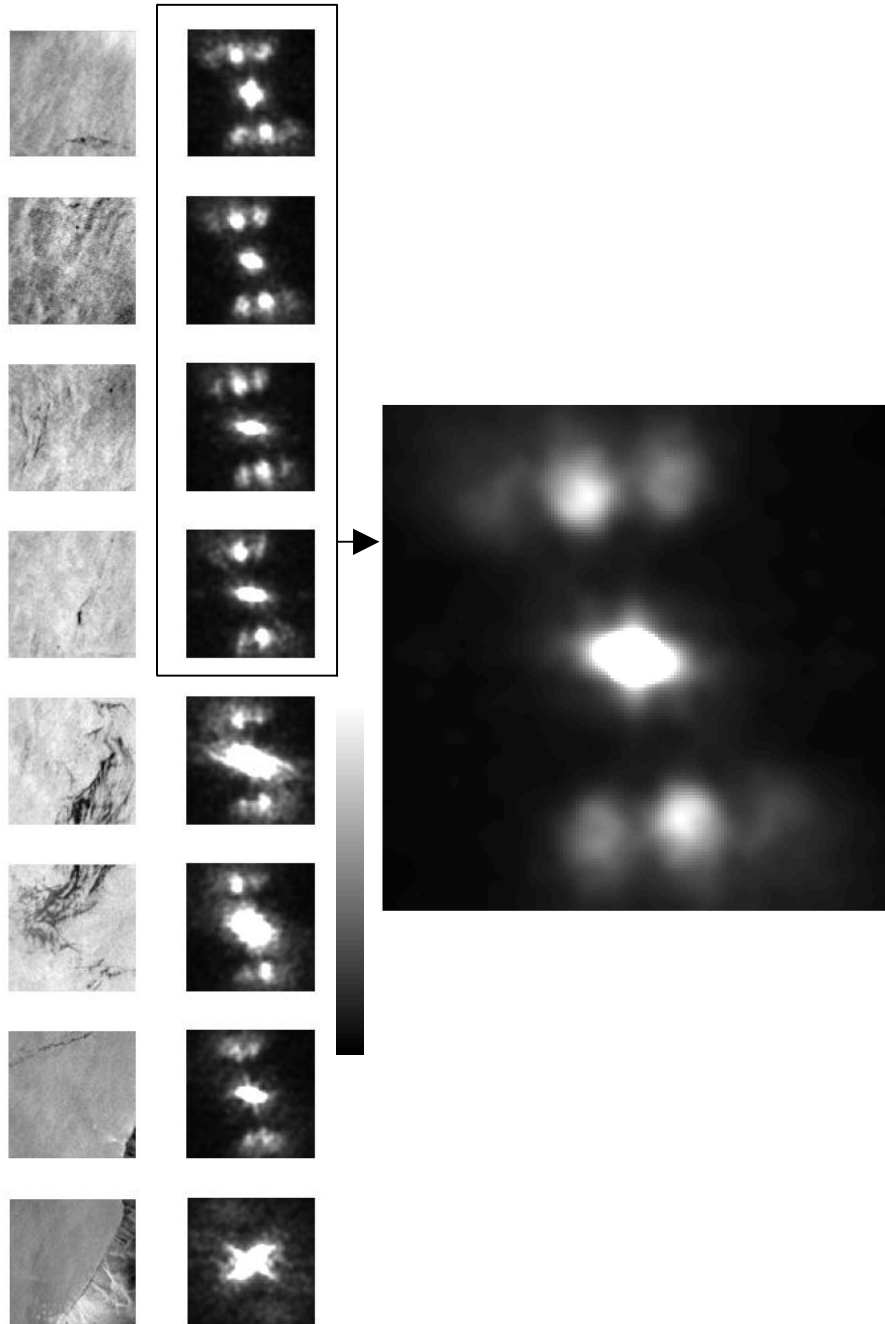
124.5°W

40.5°N

$\lambda \sim 250$
m

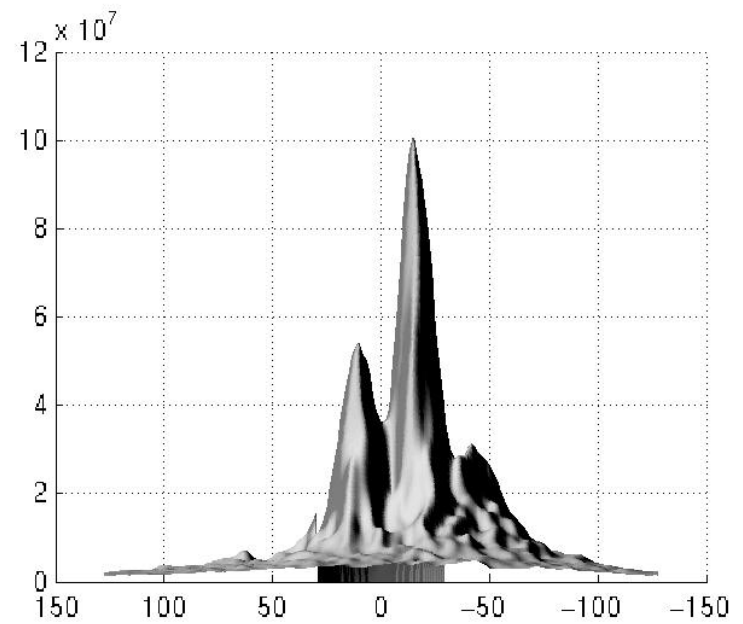
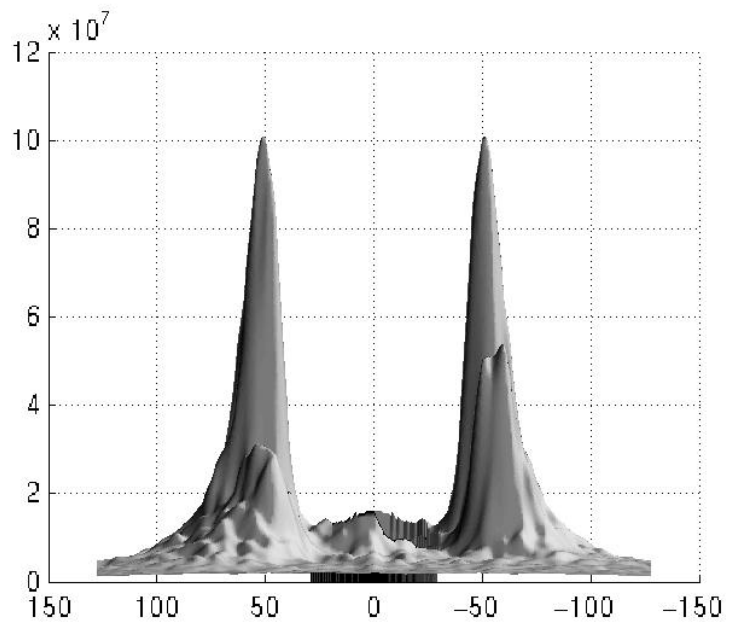
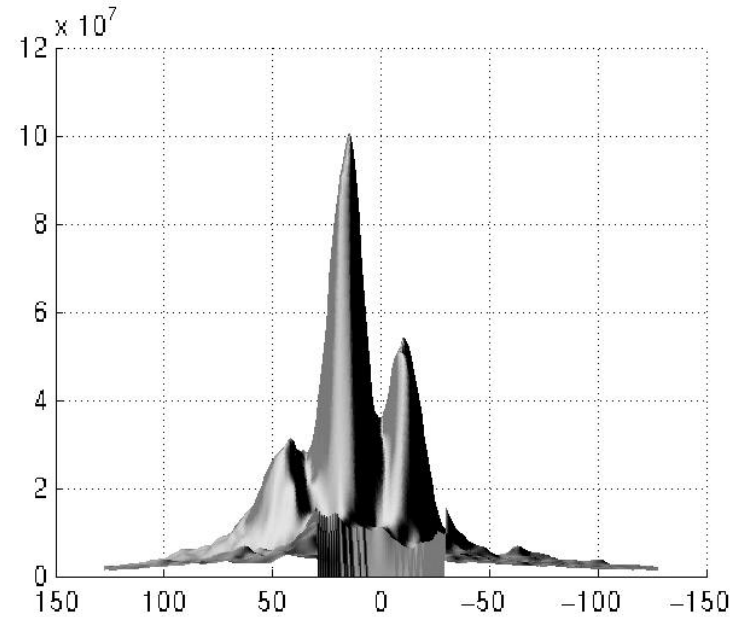
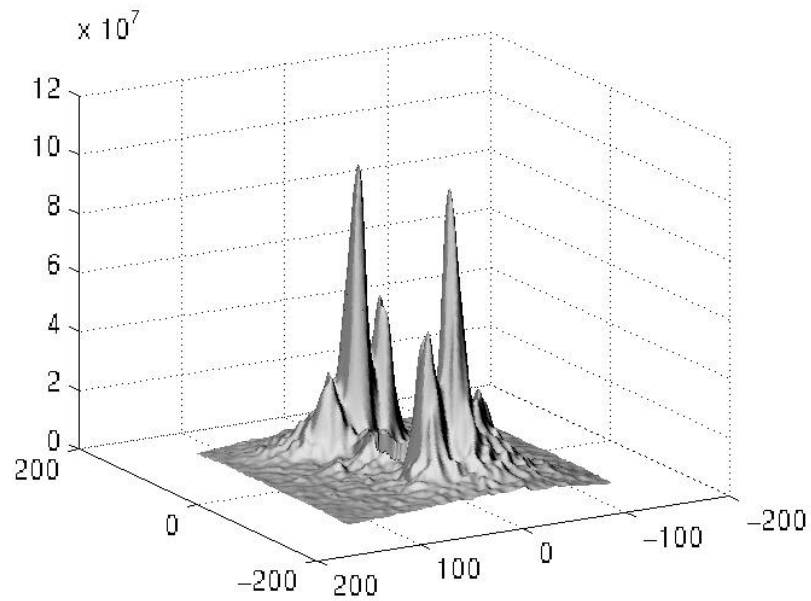


SAR Derived Swell Spectra



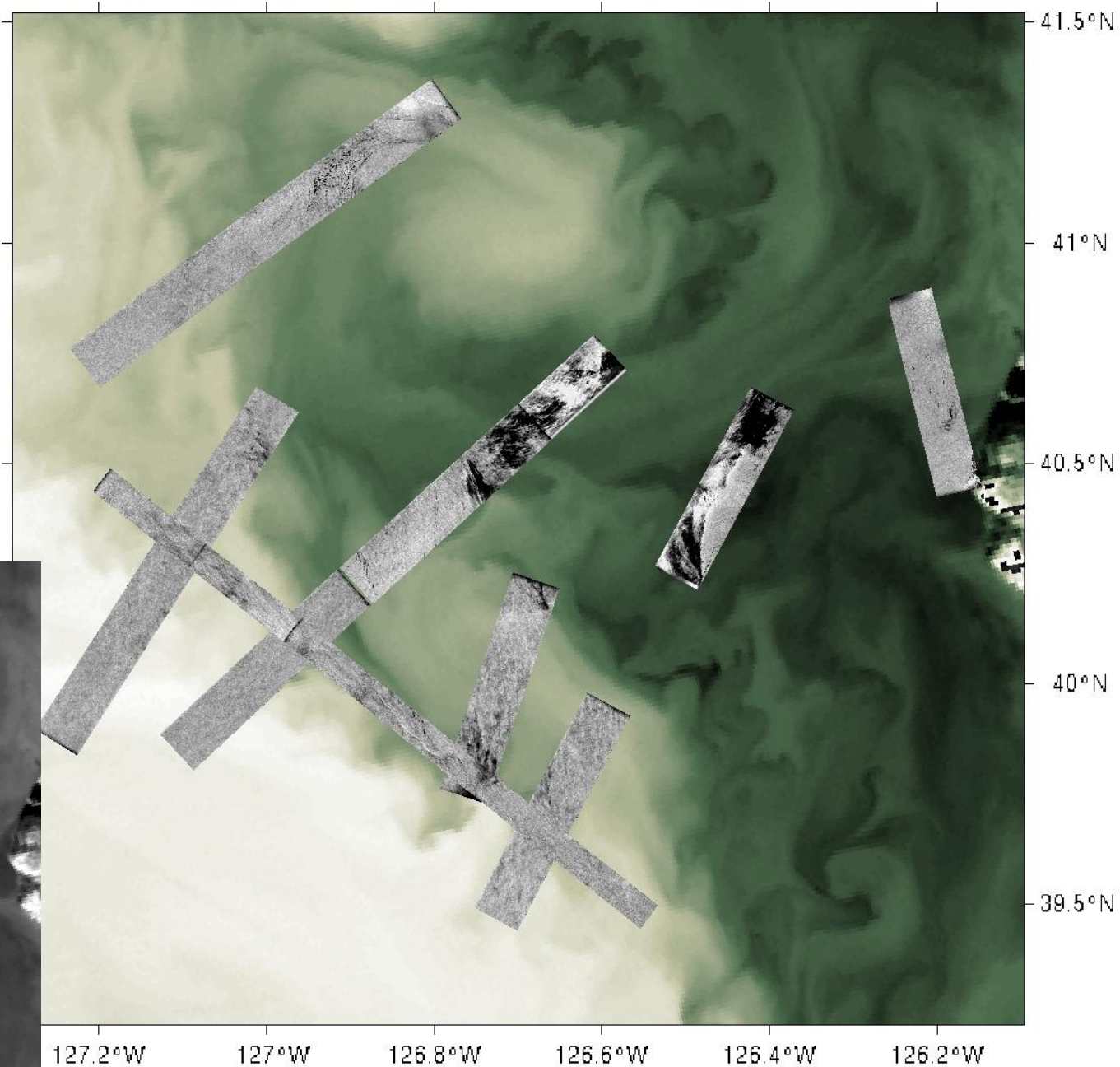
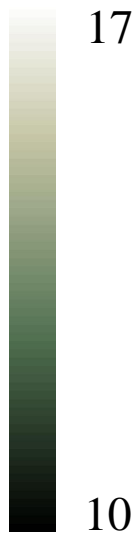
$\lambda \sim 120$
m

SAR Derived Swell Spectra

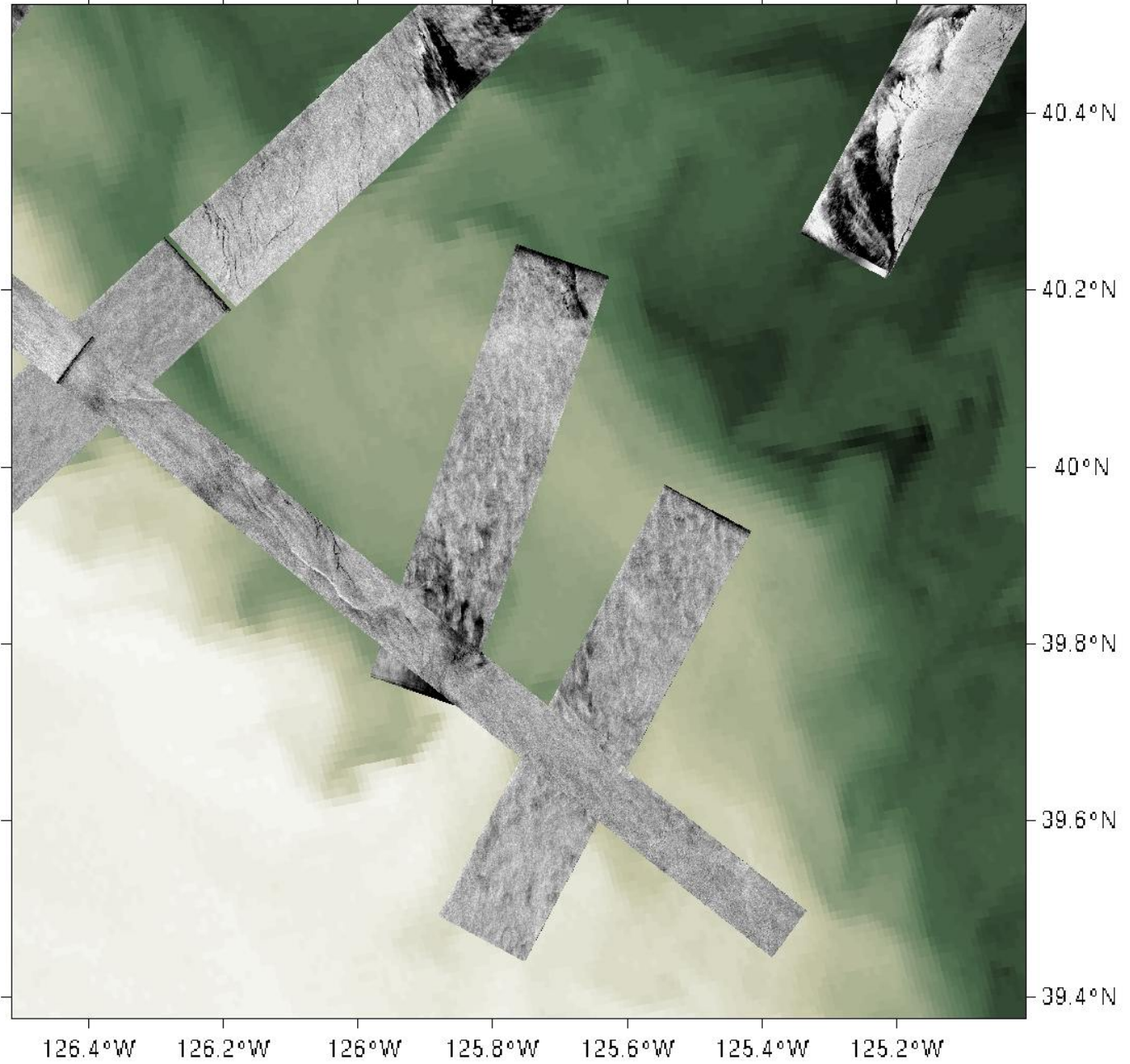
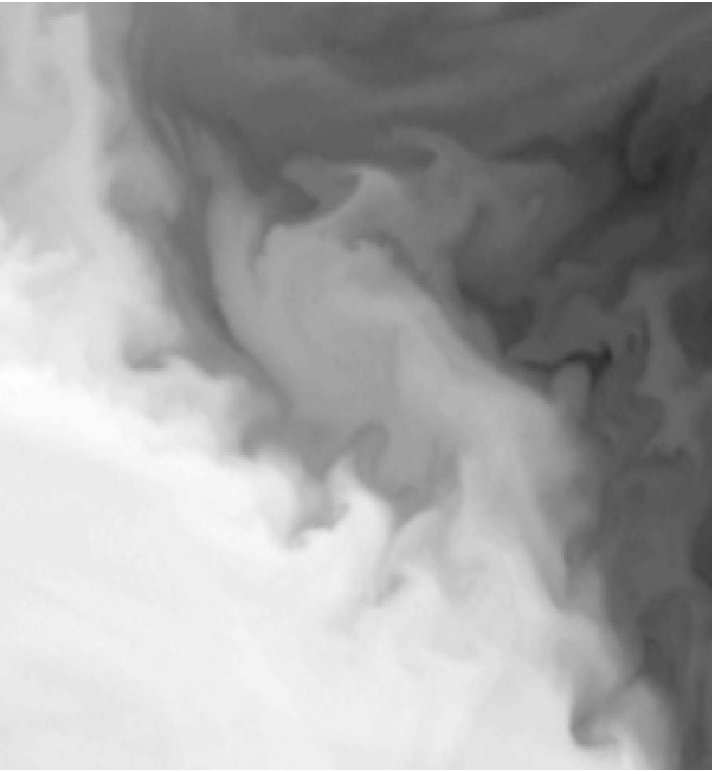


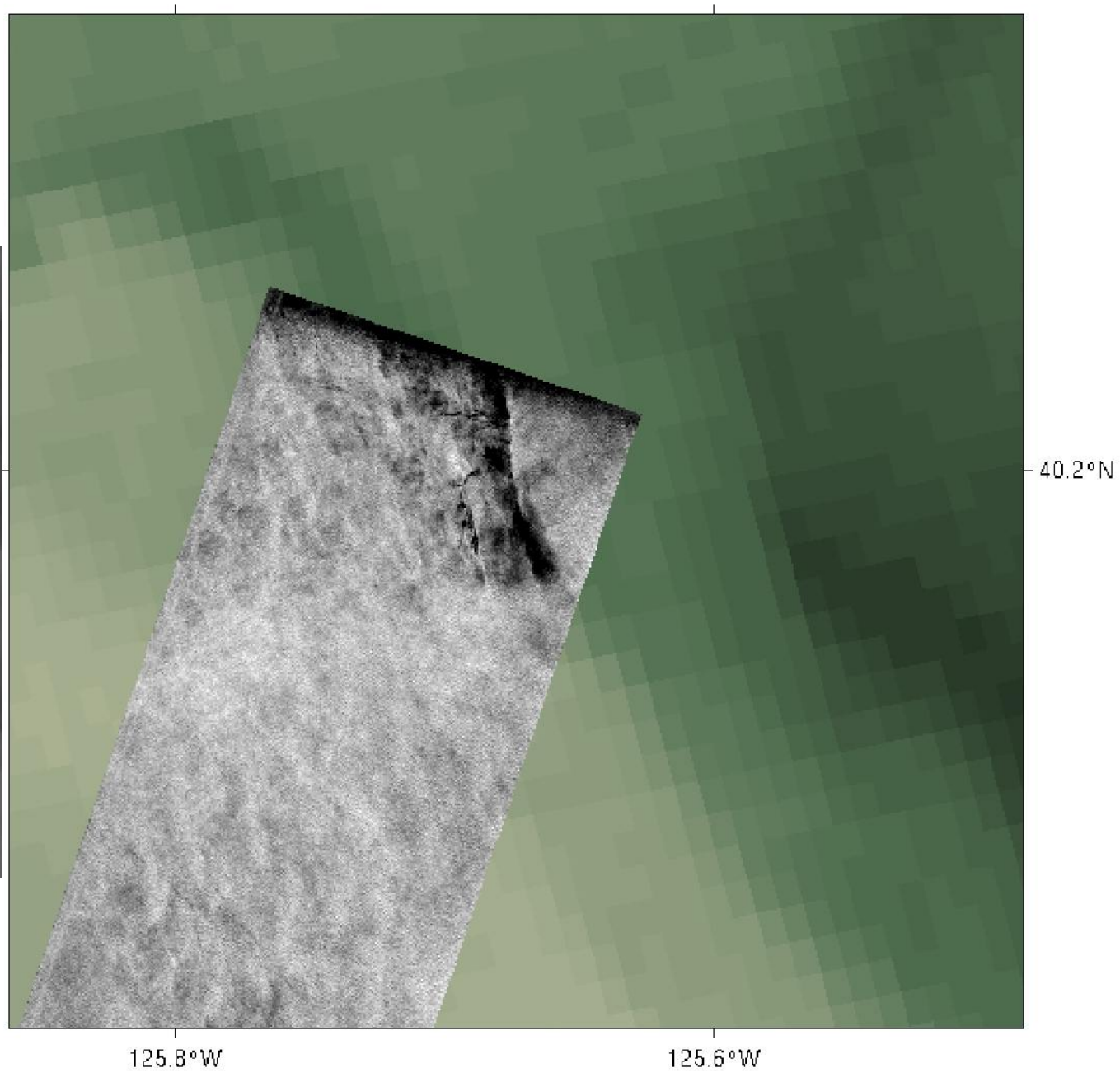
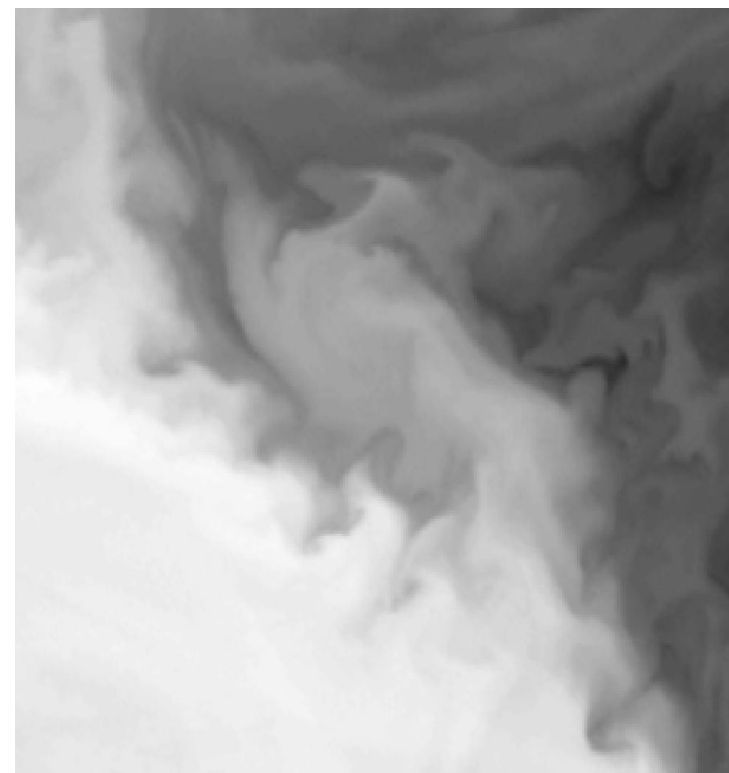
AVHRR ch_4 / SAR L-band

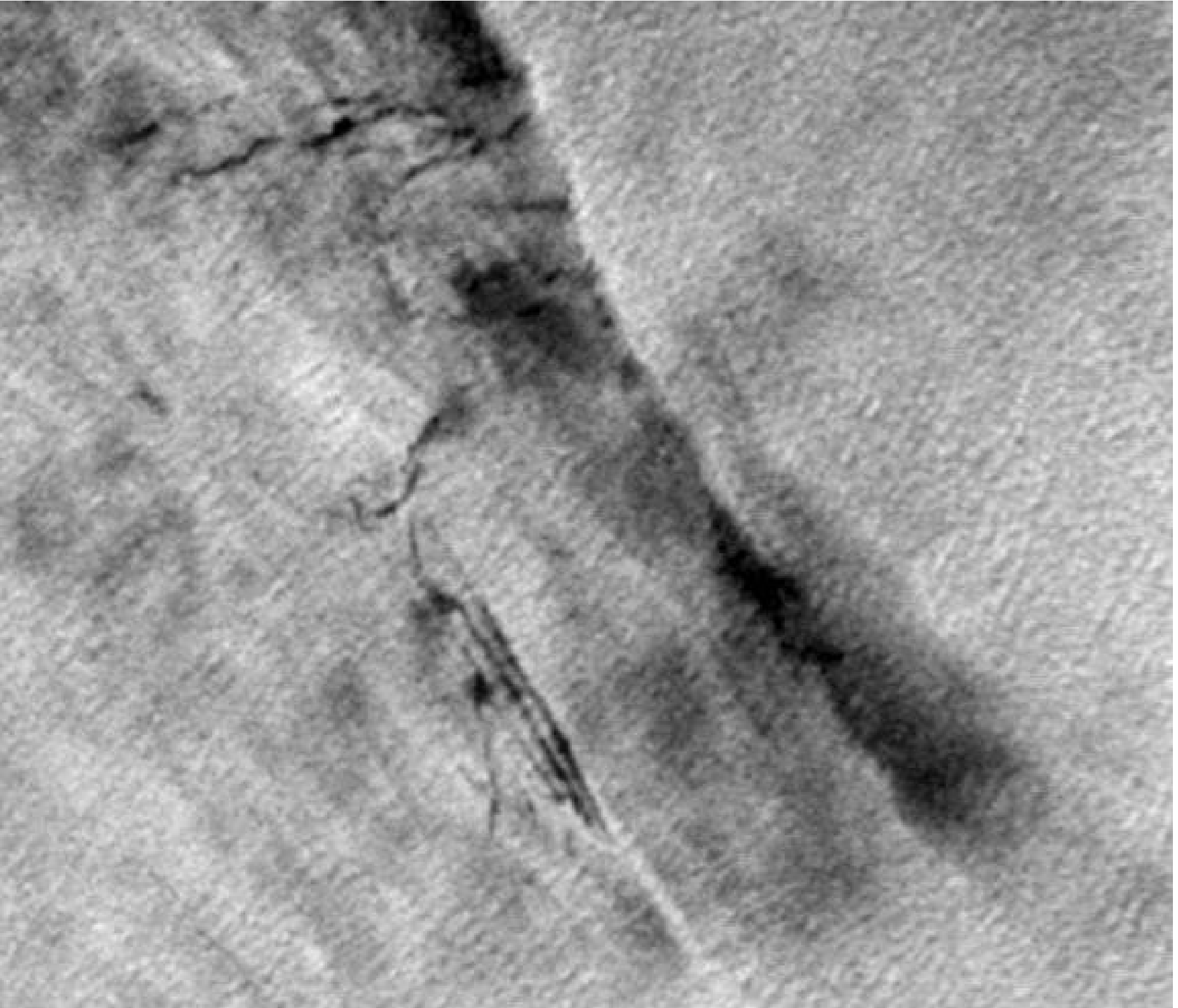
Approximate Temperature (°C)



Cyclone



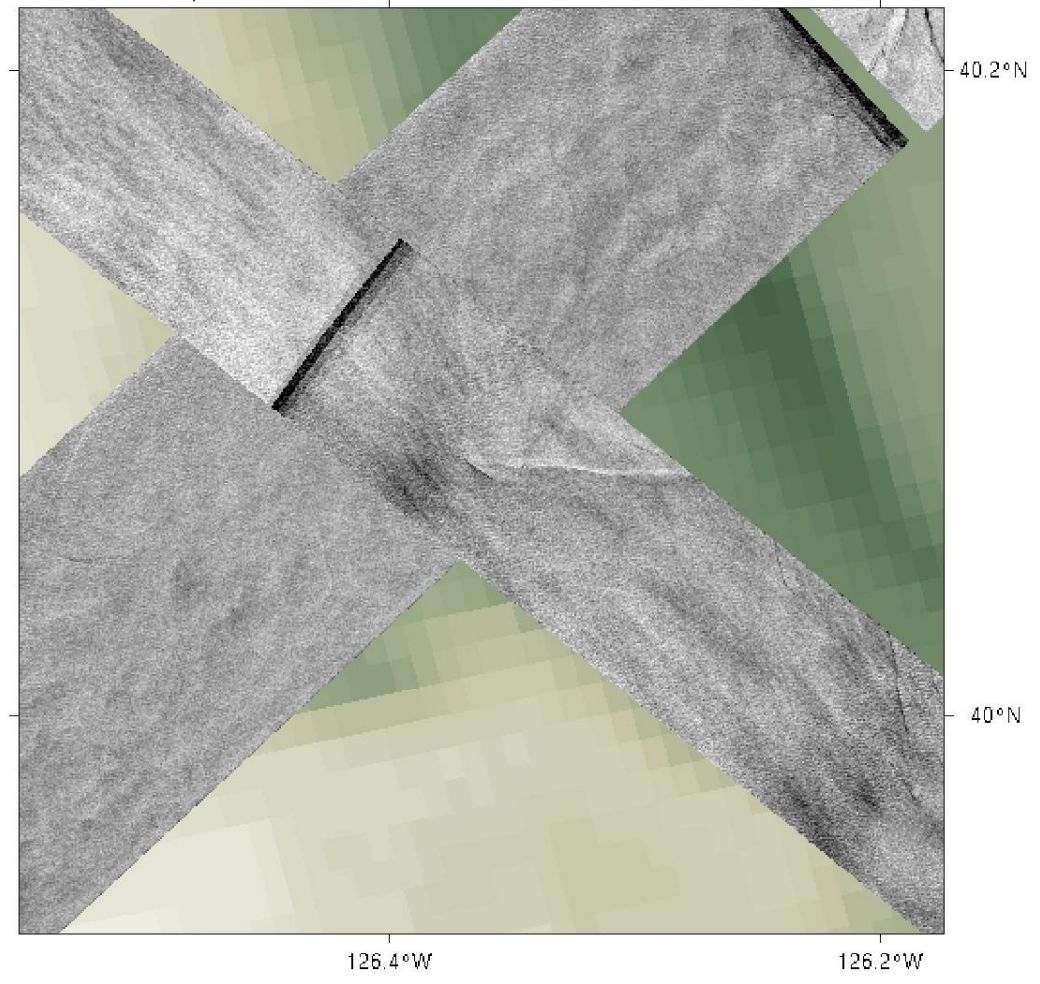
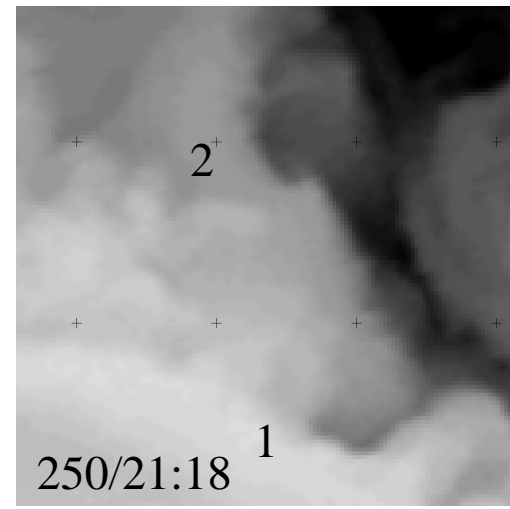
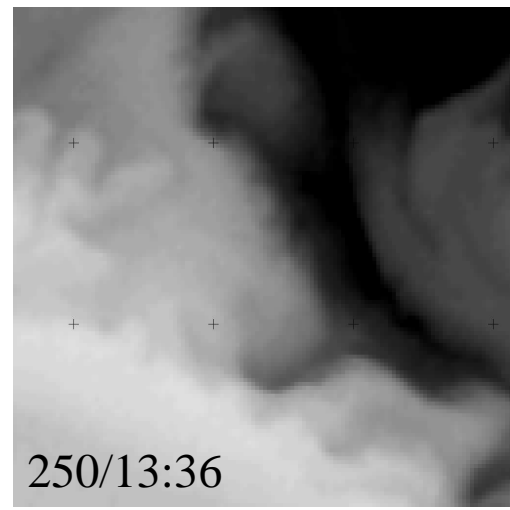
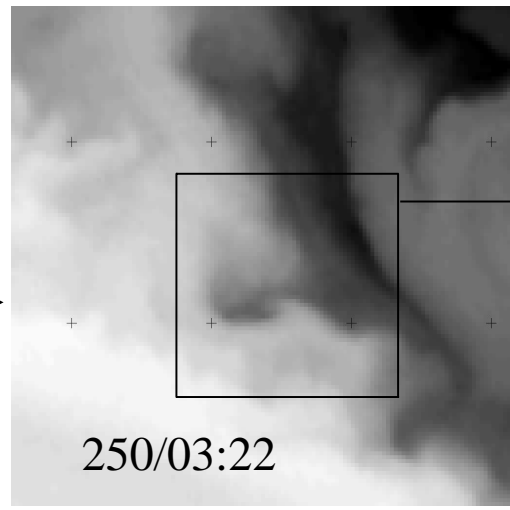
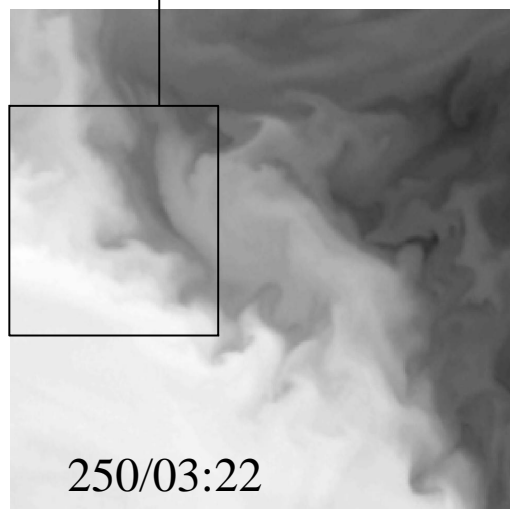




$\lambda \sim 120$

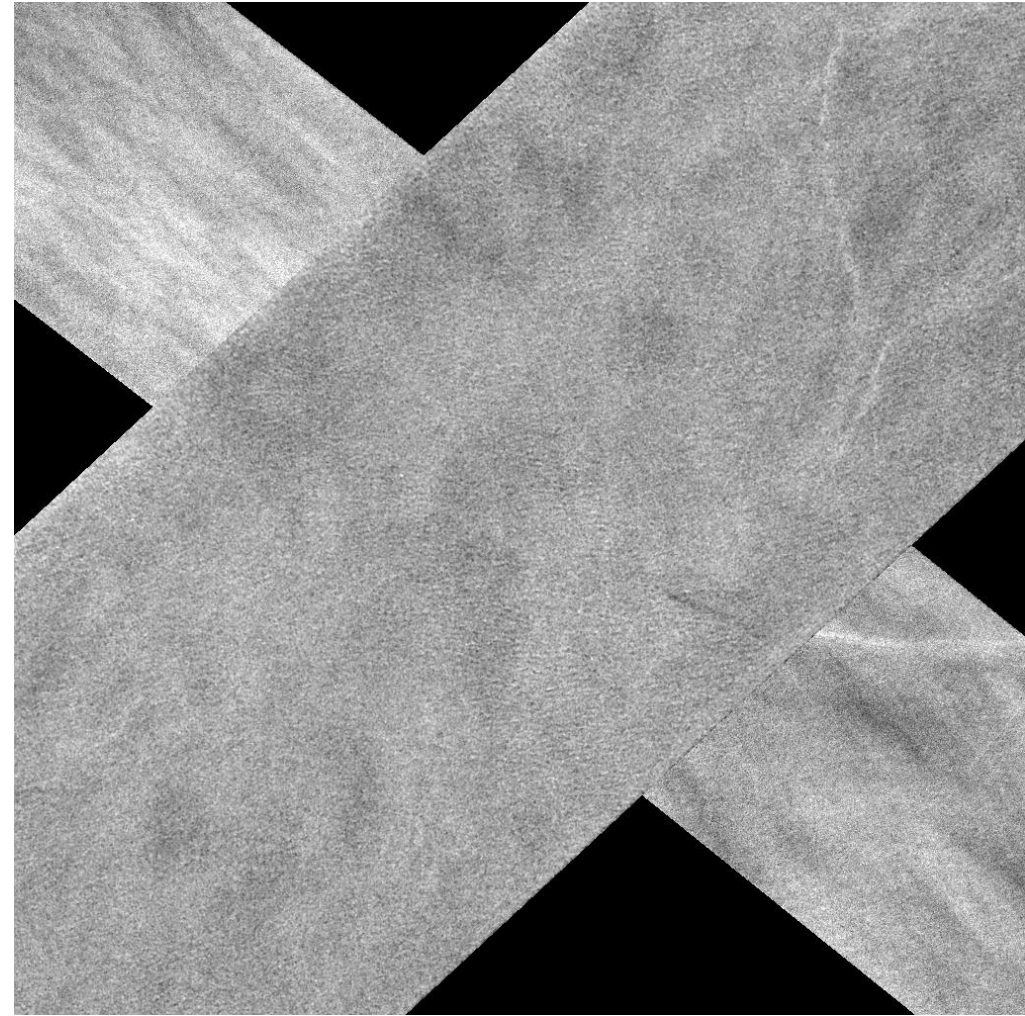
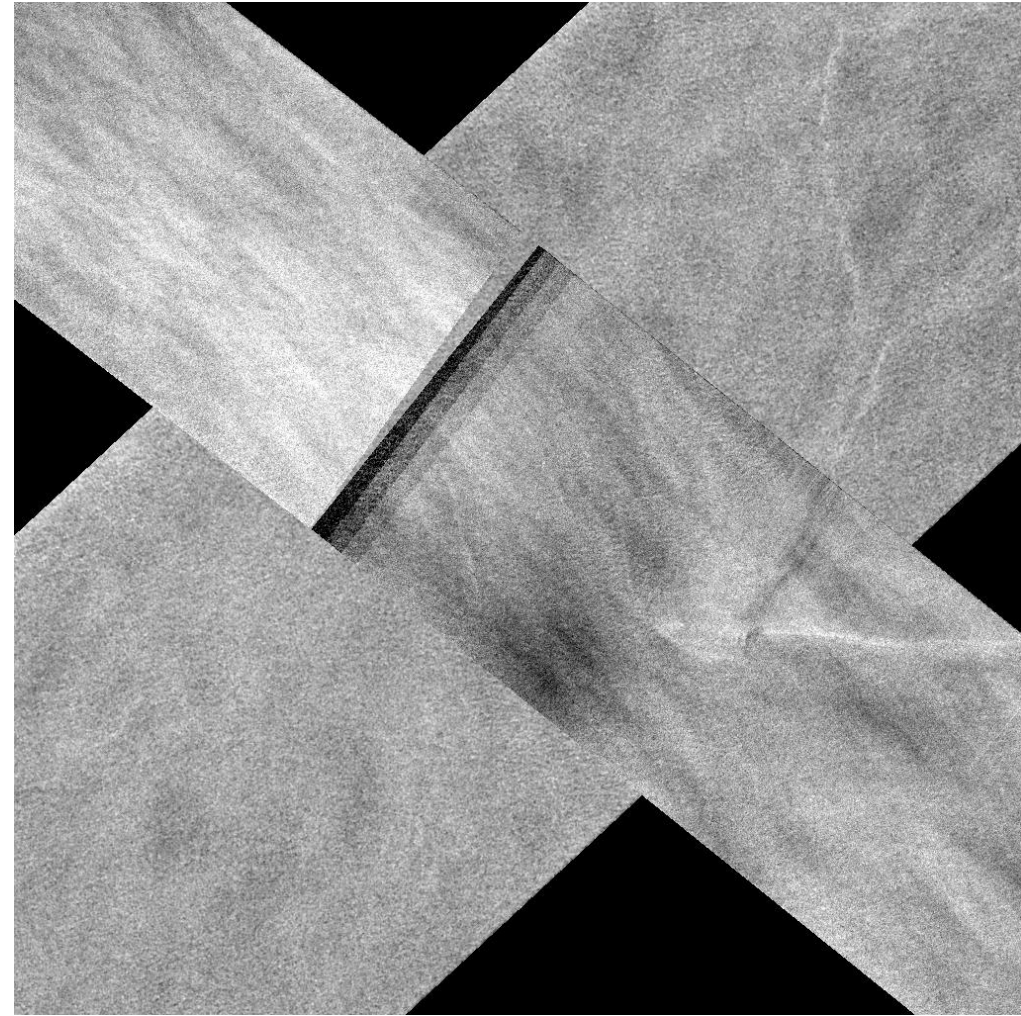
m

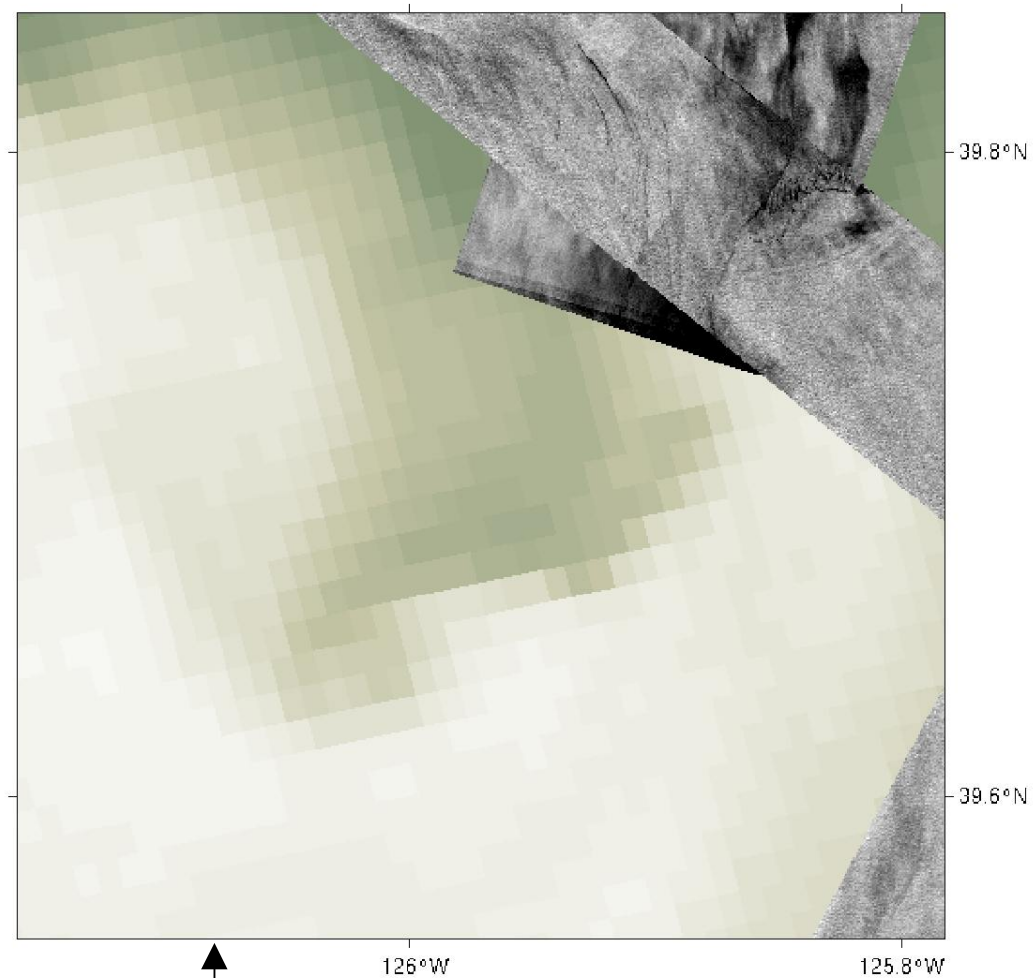
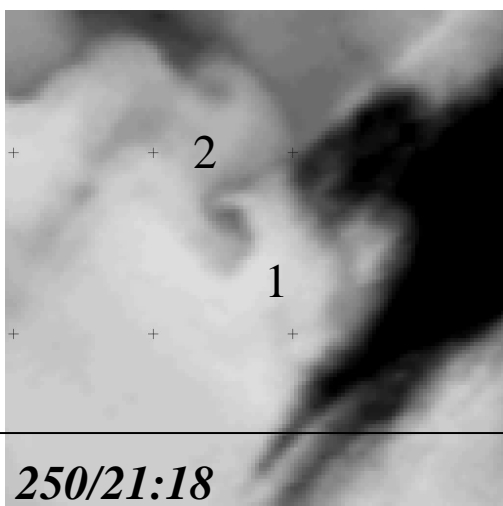
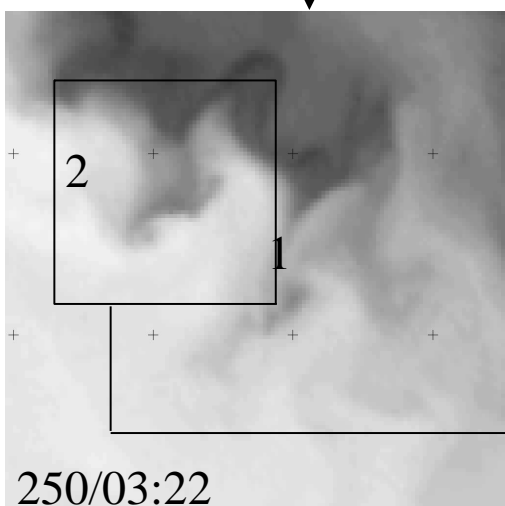
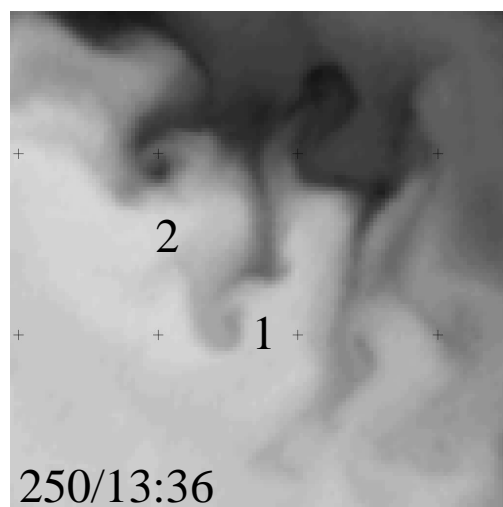
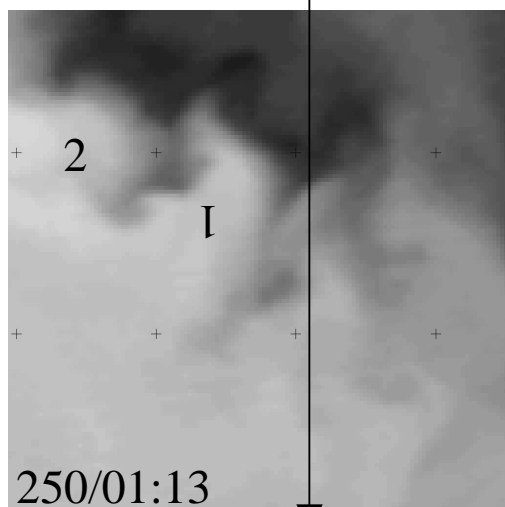
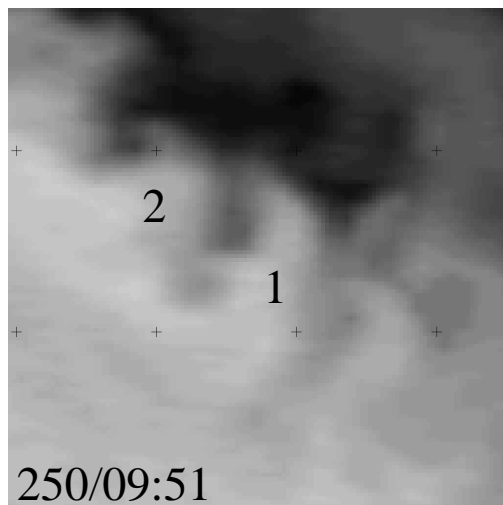
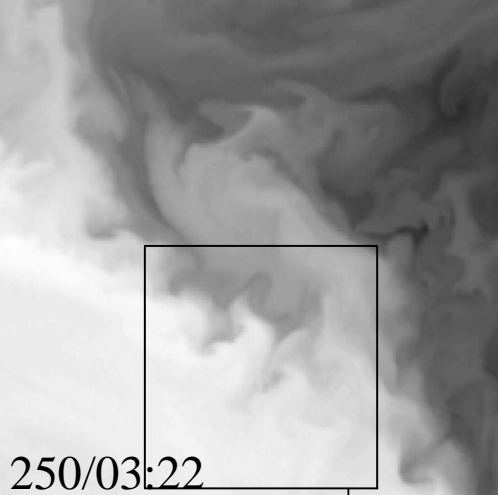
~ 10km/10hr --> ~ 1 km/hr

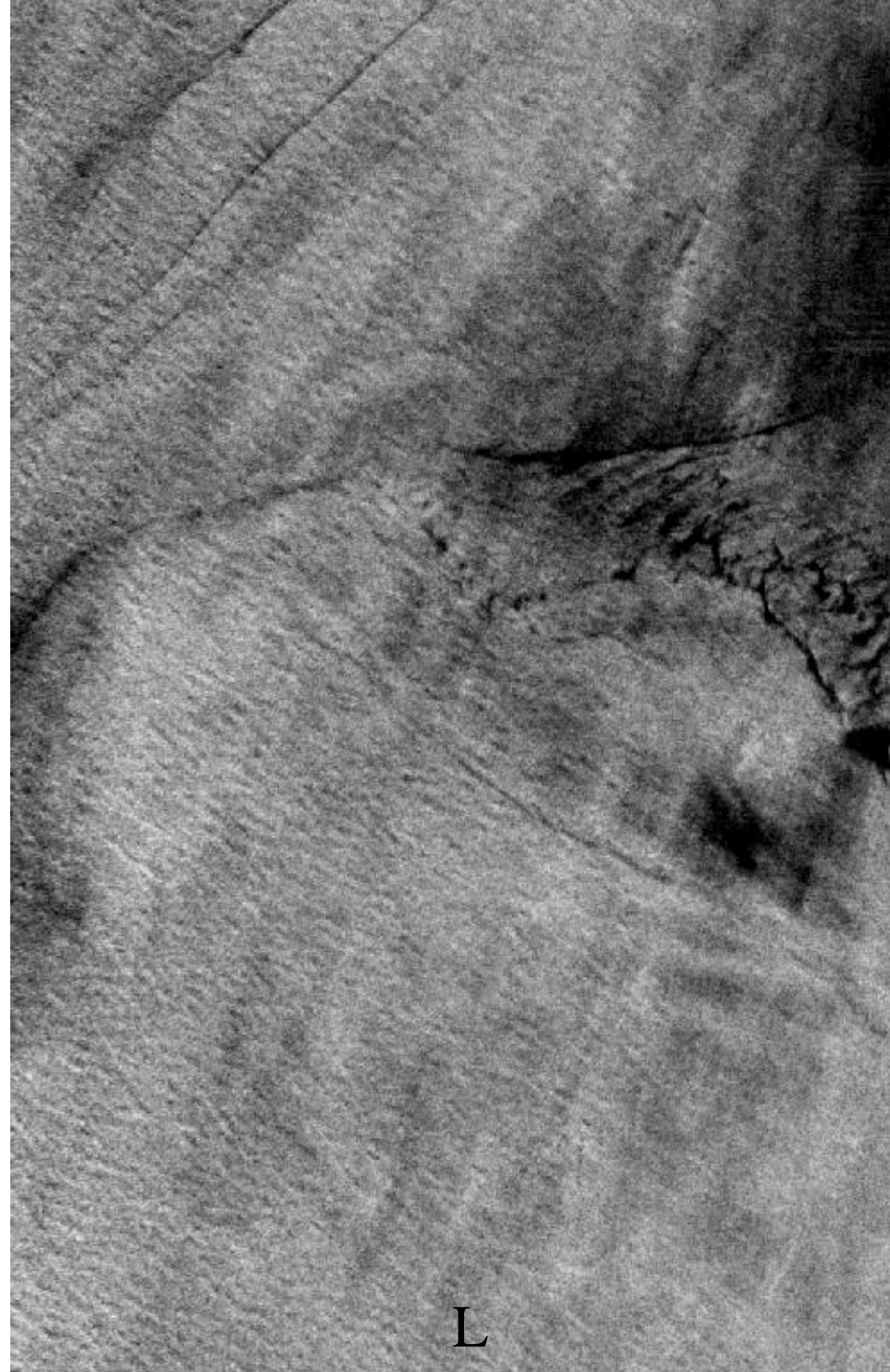
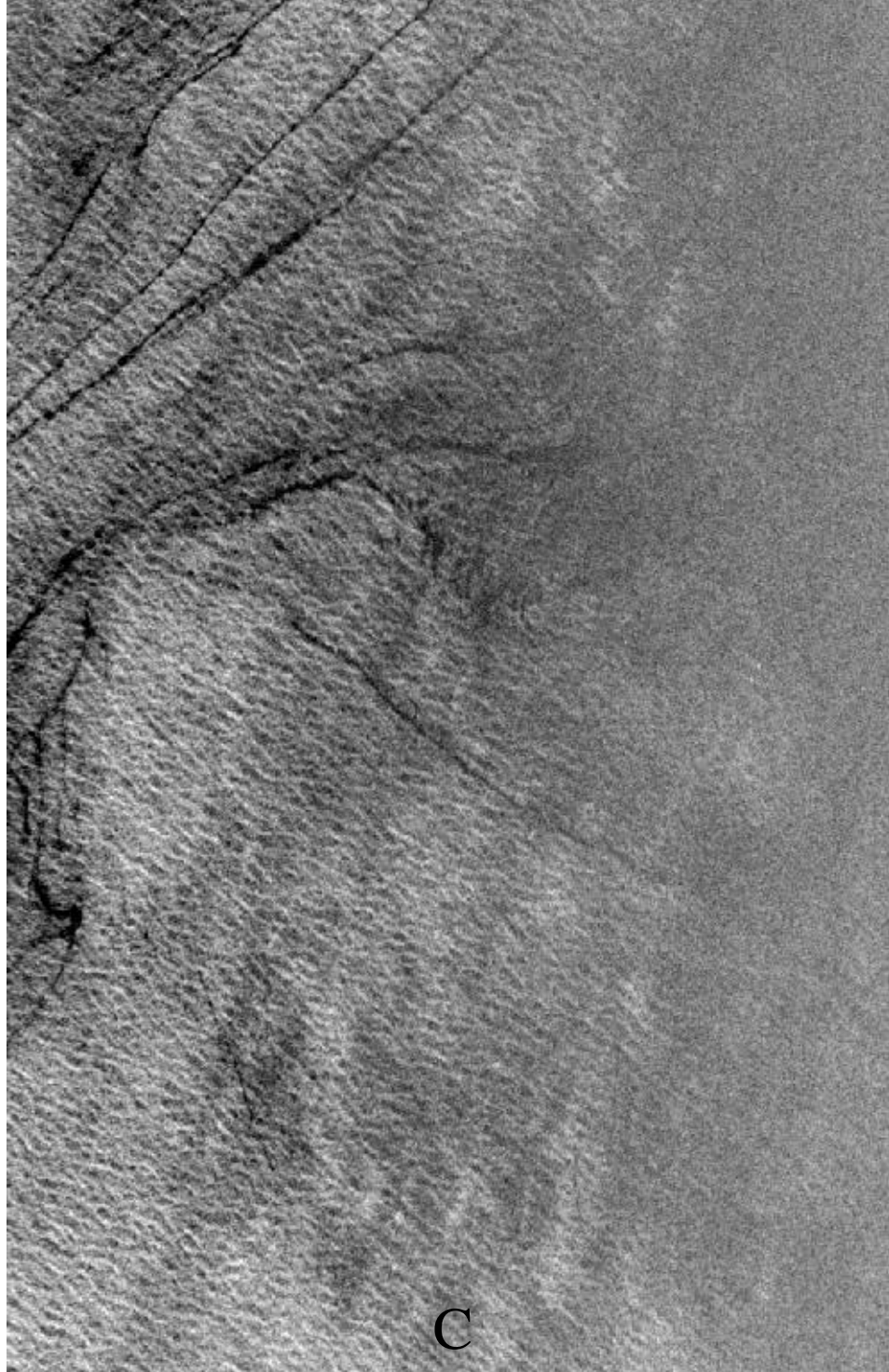




SAR P-band Crossing

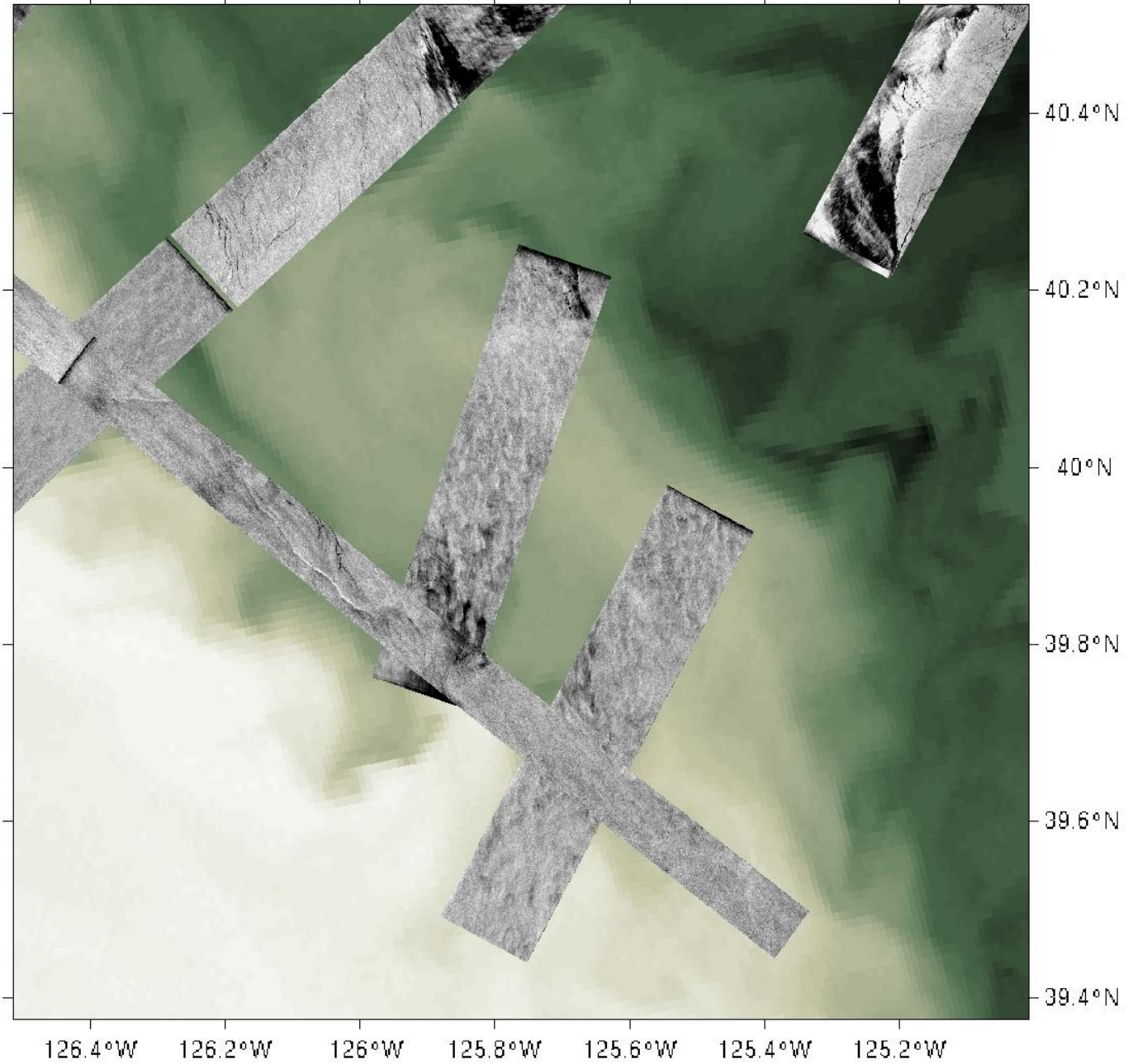
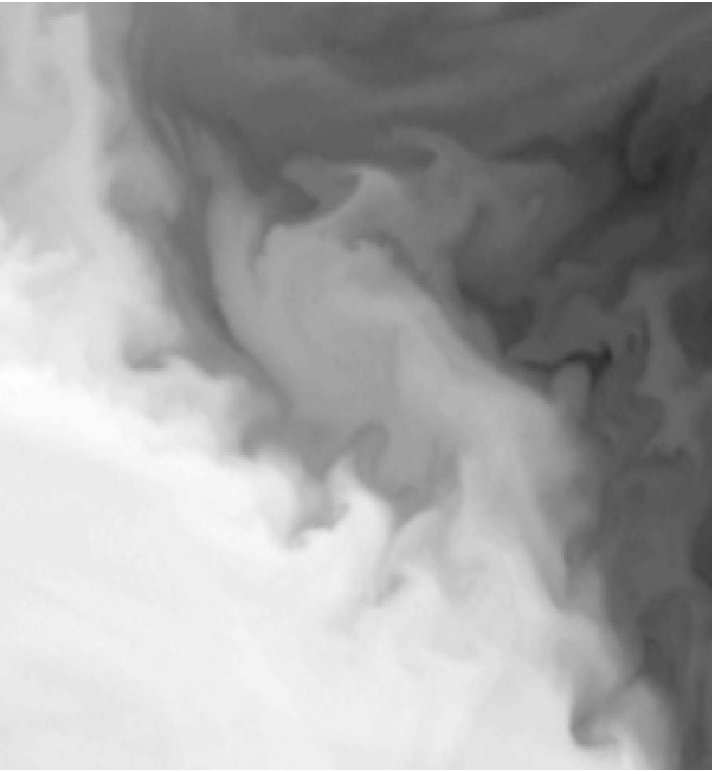


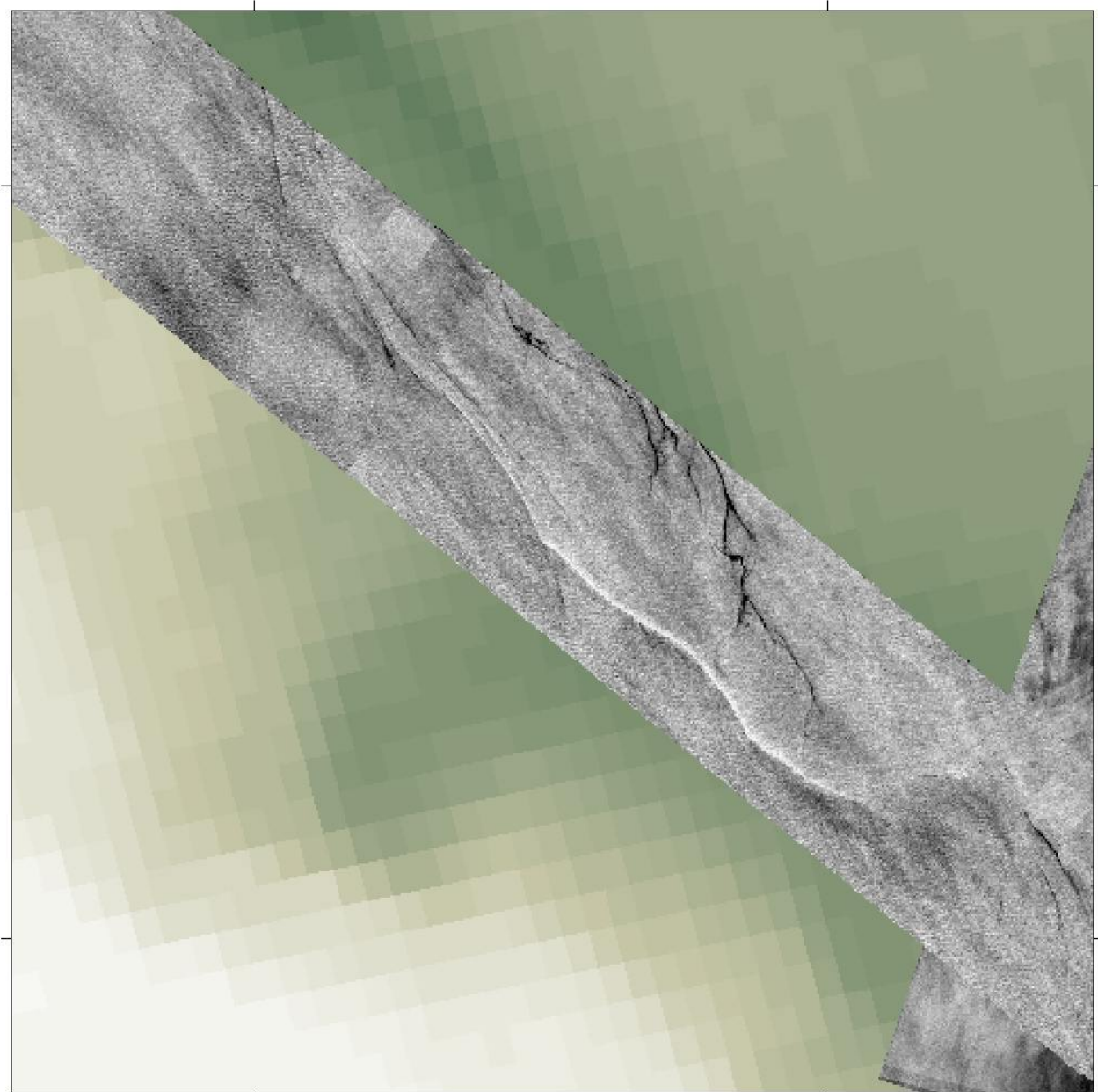
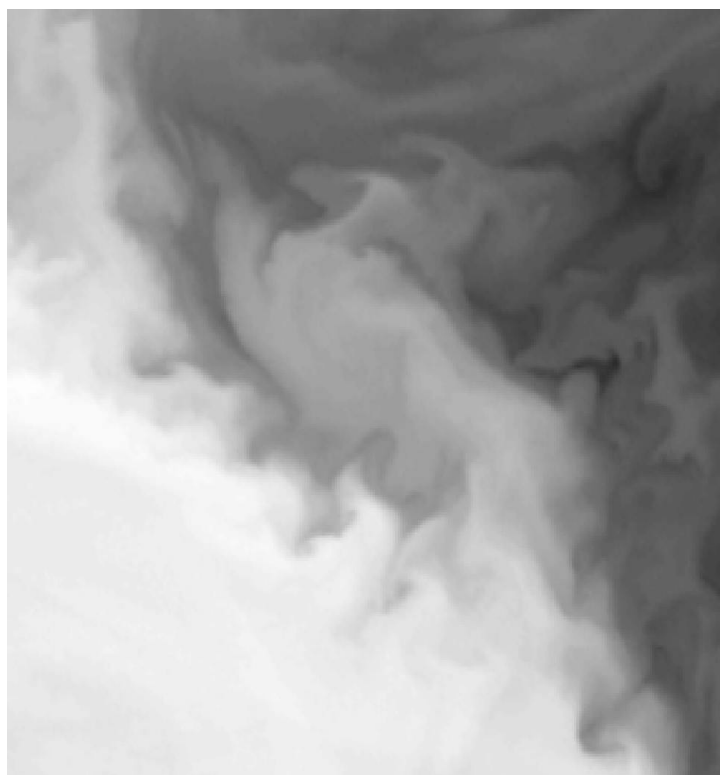




$\lambda \sim 220$

Cyclone



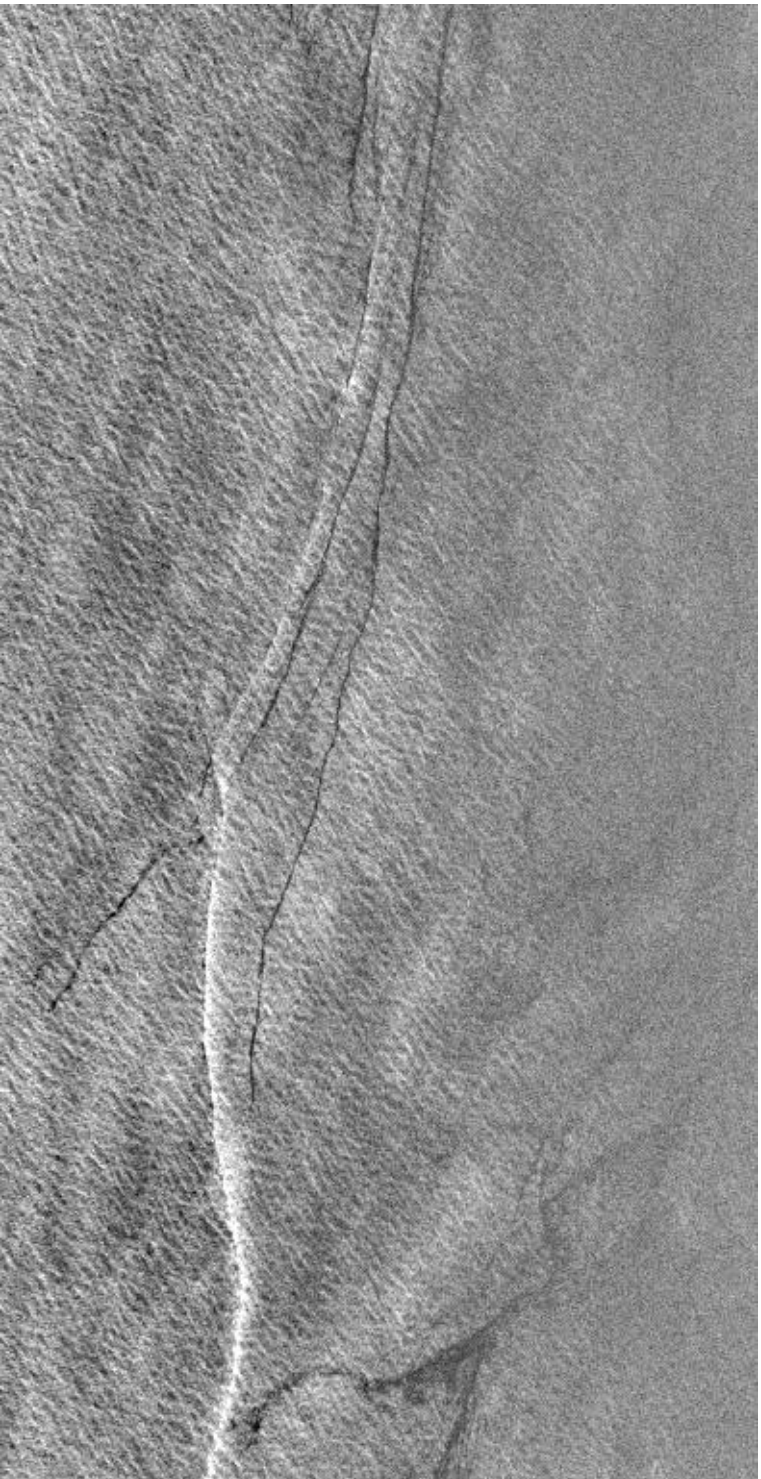
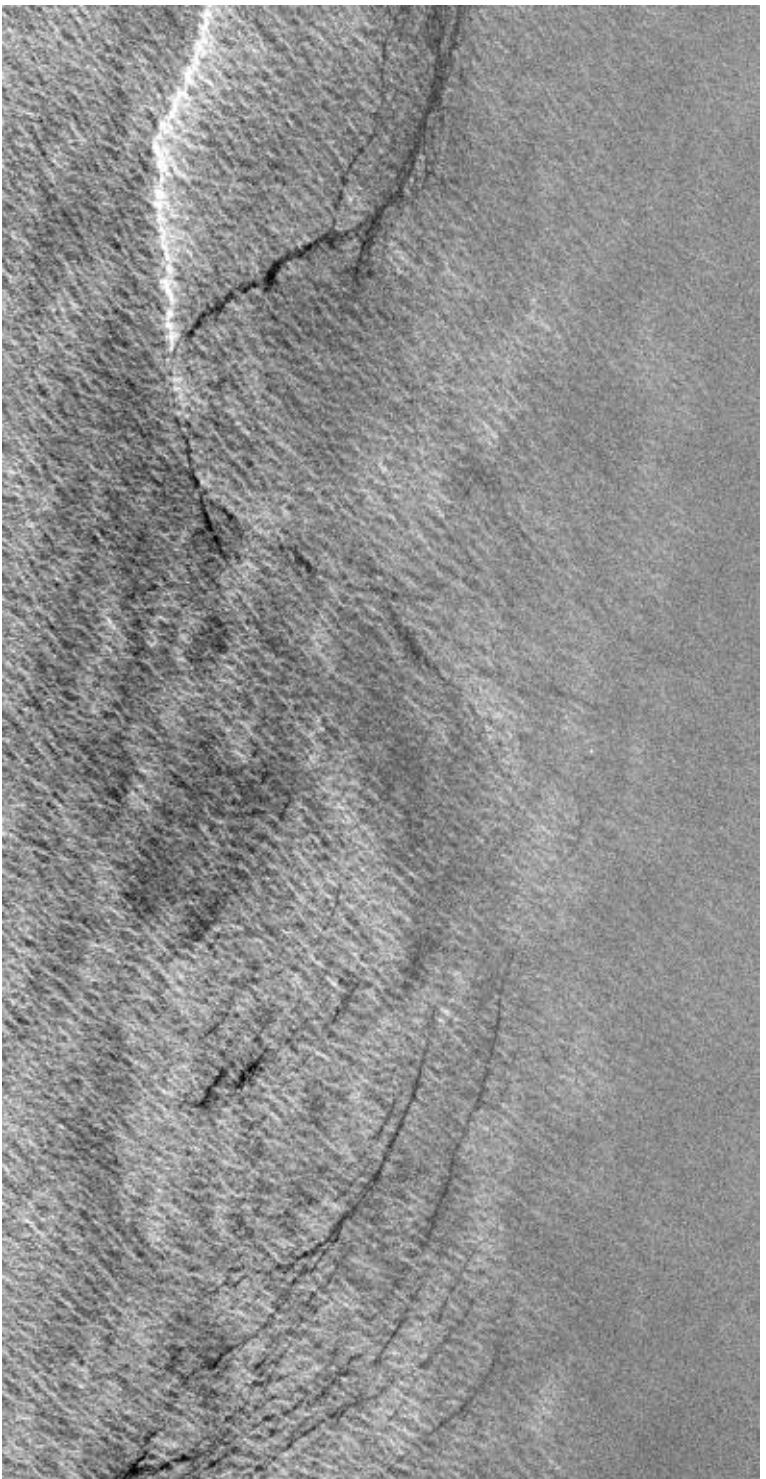


40°N

39.8°N

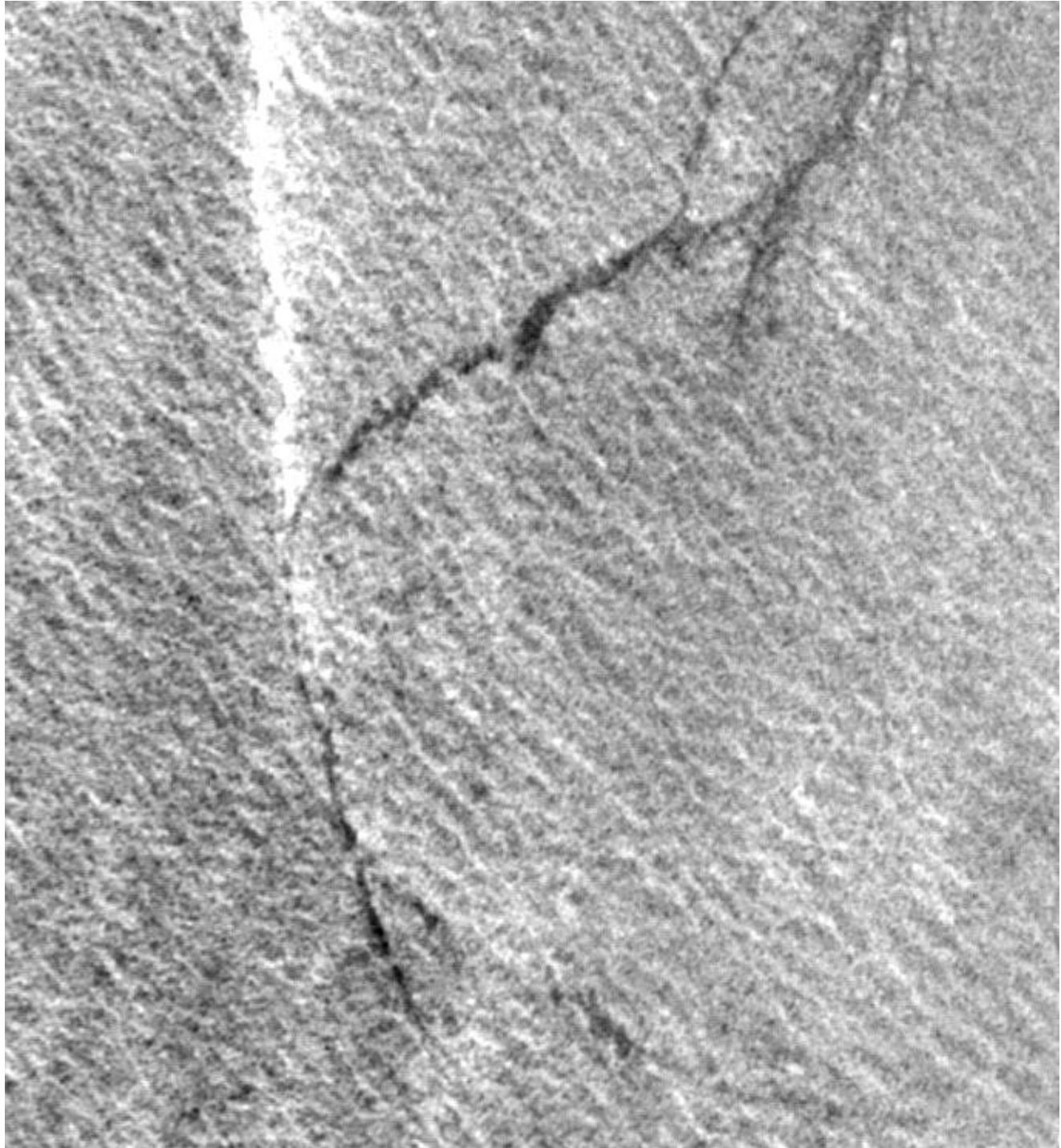
126.2°W

126°W



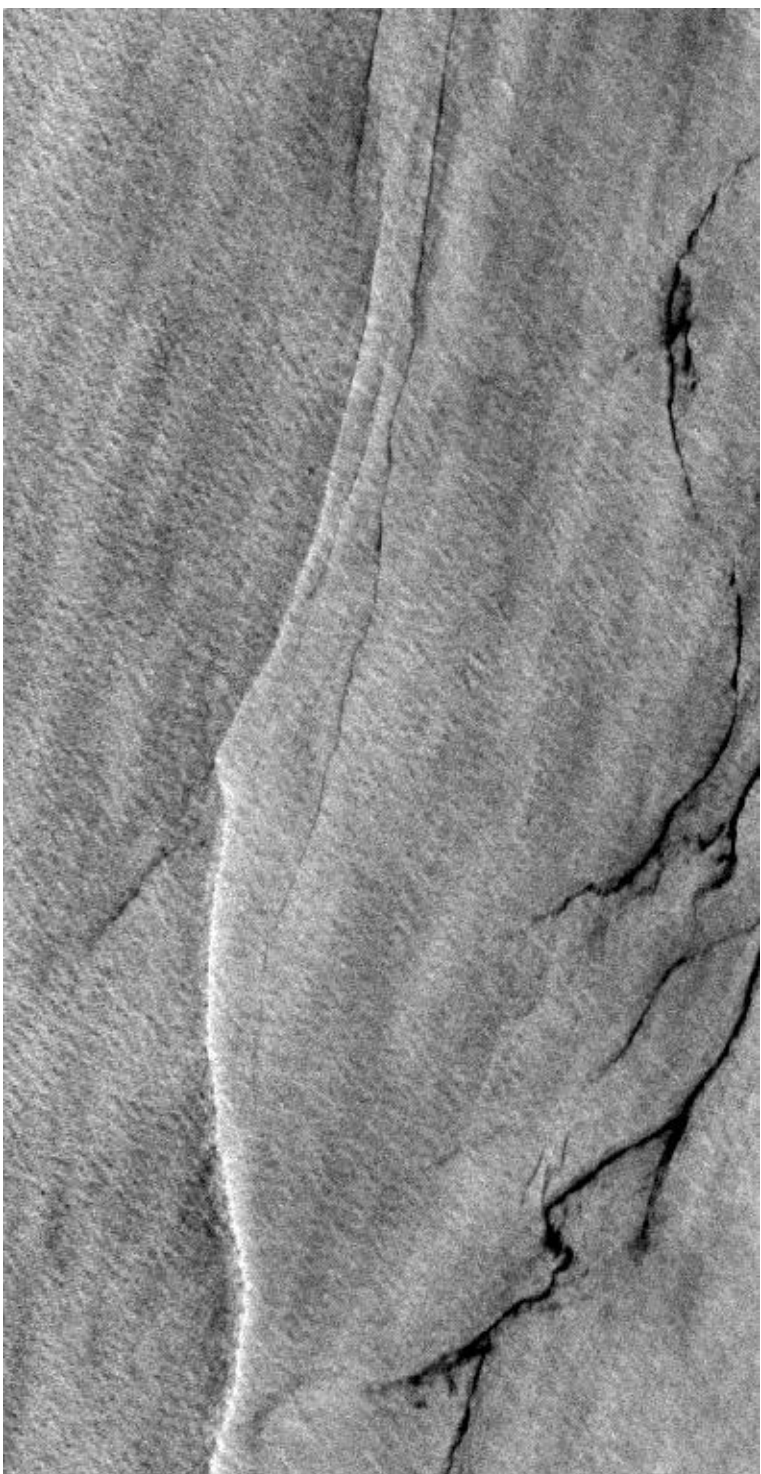
C-band



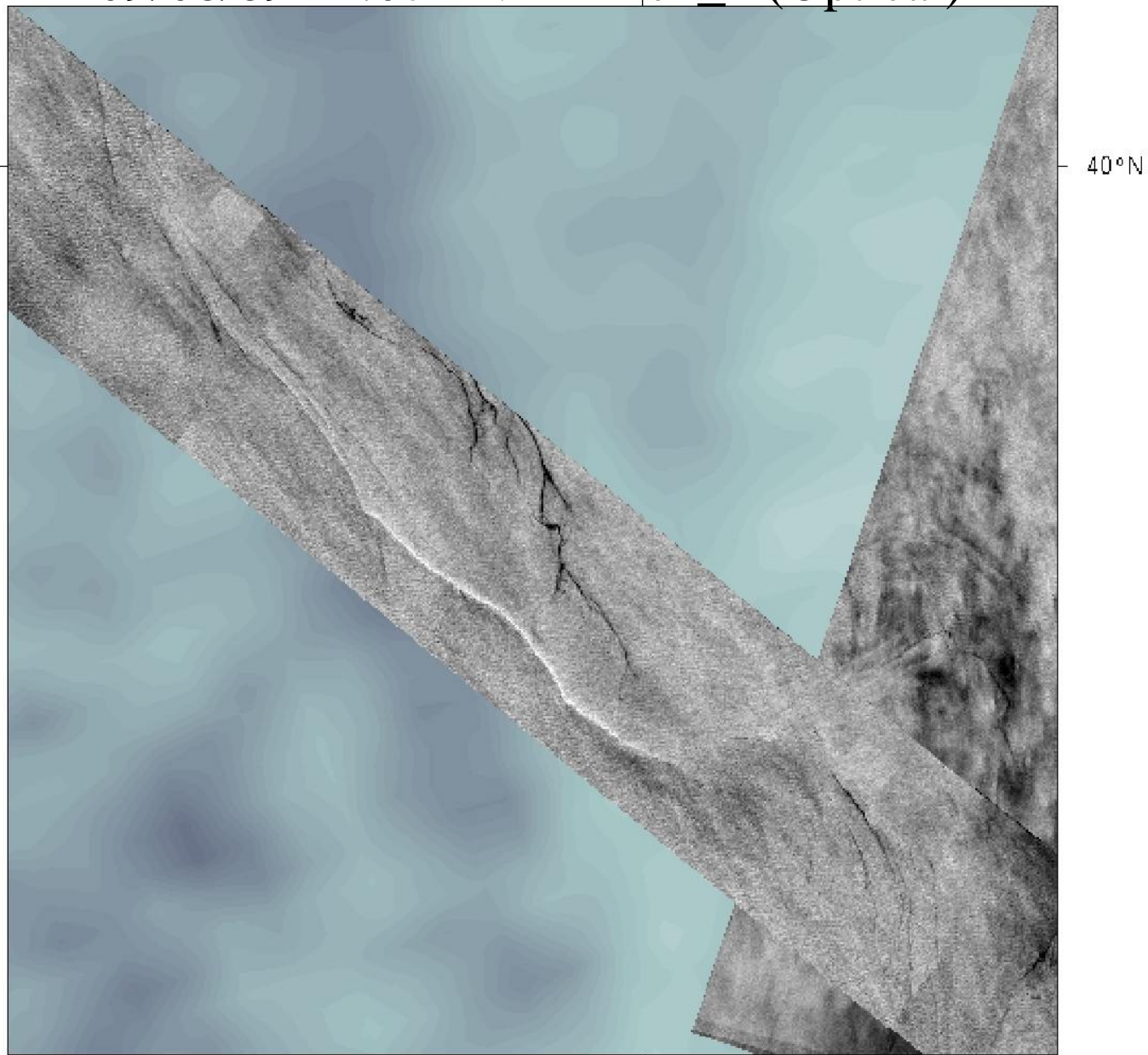




L-band

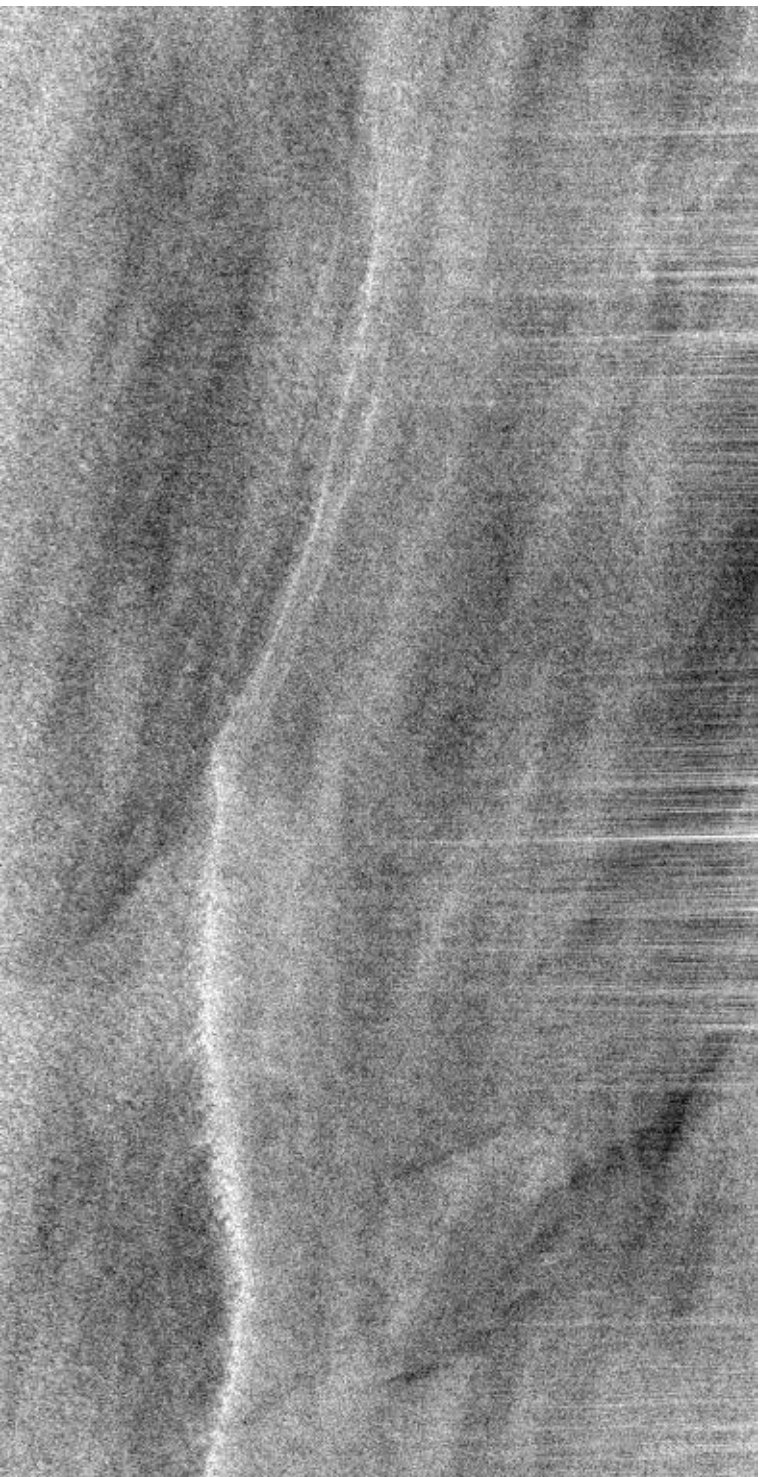
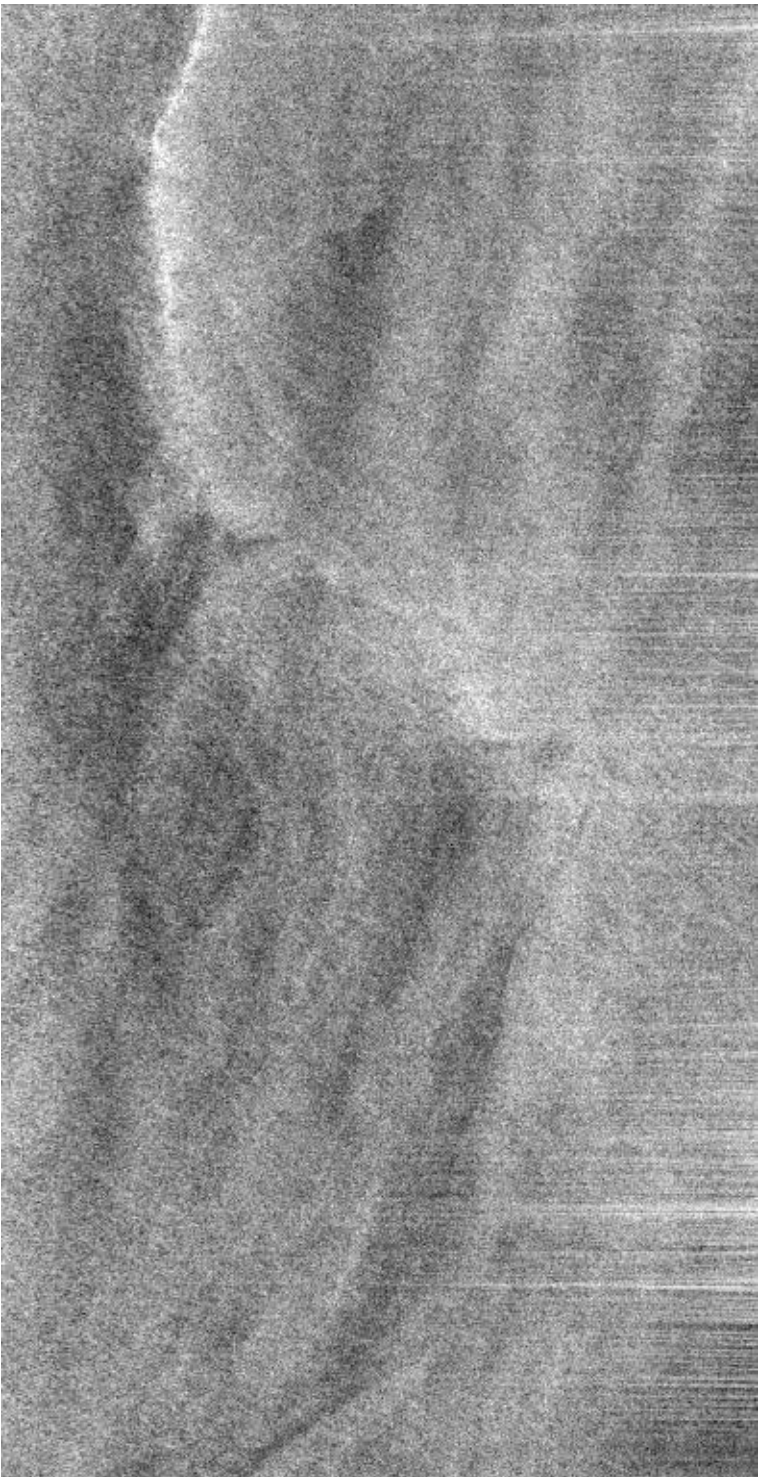


09/08/89 21:07 AVHRR_ch_1 (Optical)



40°N

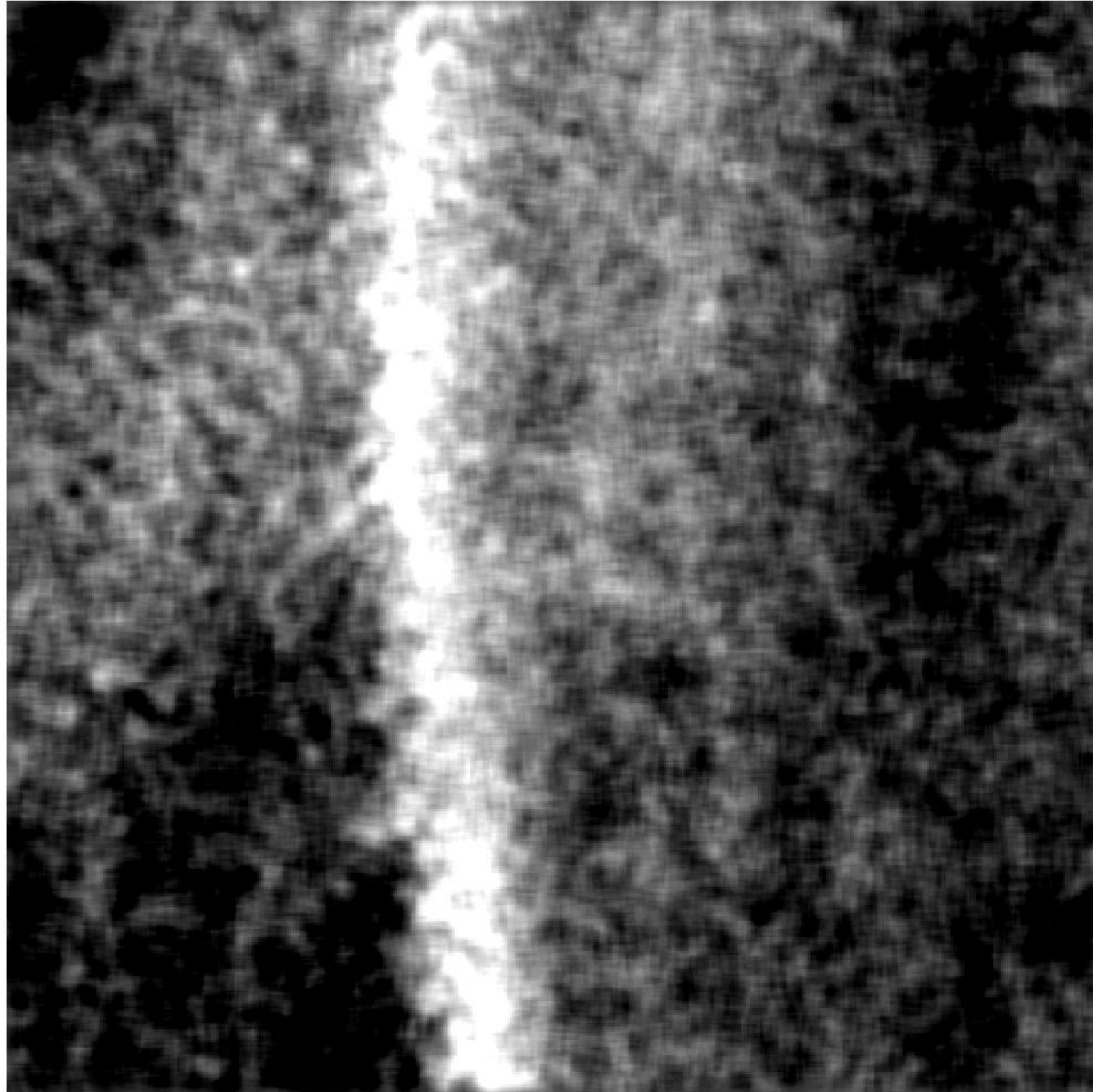
126°W



P-band



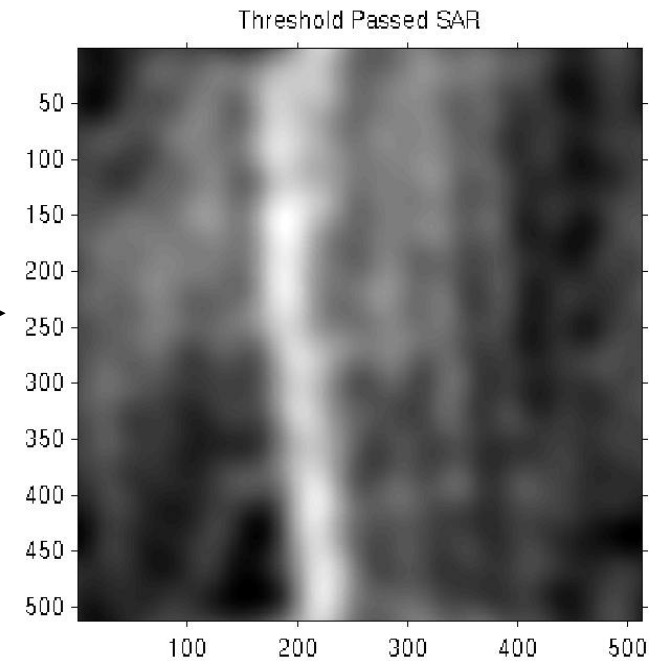
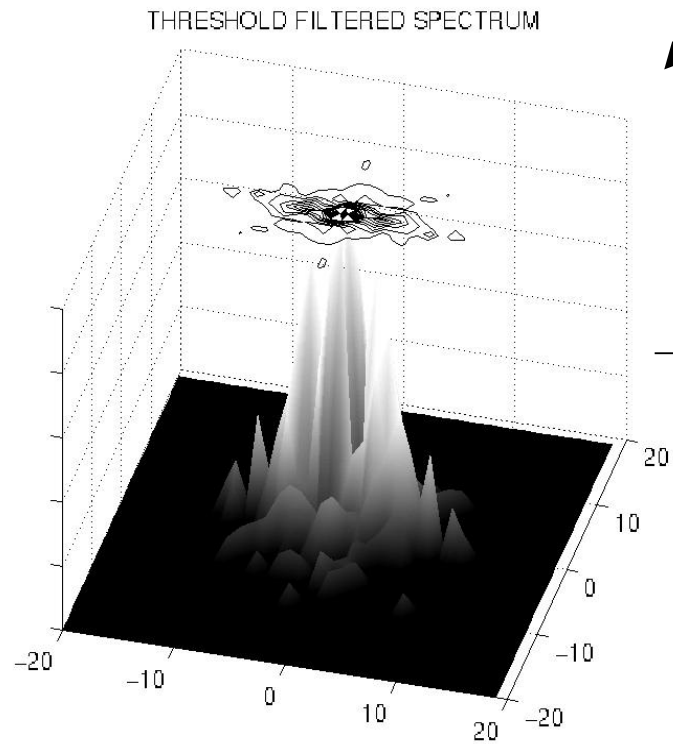
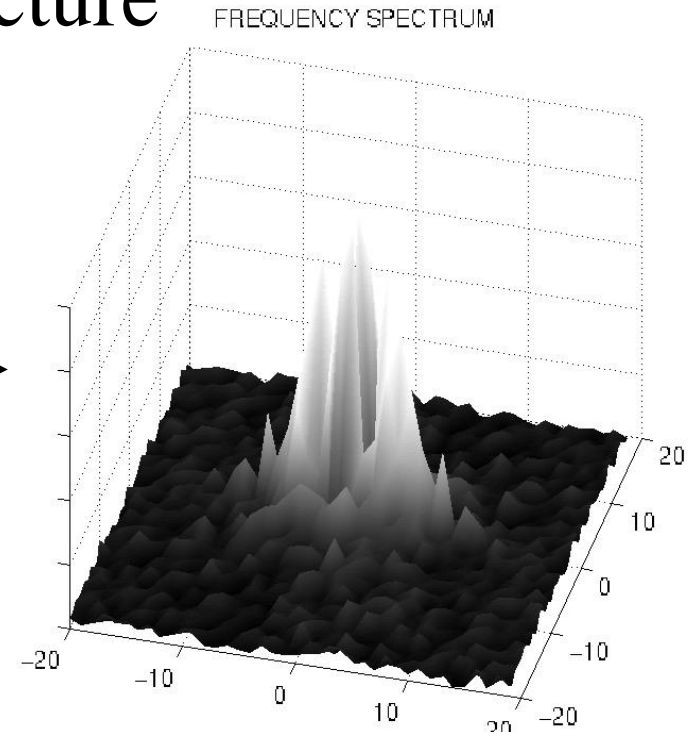
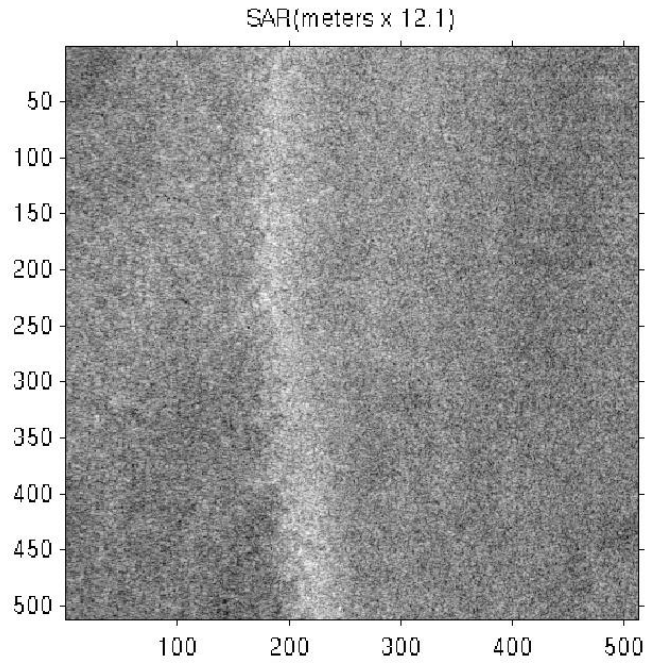
(9x9 Boxcar Mean)



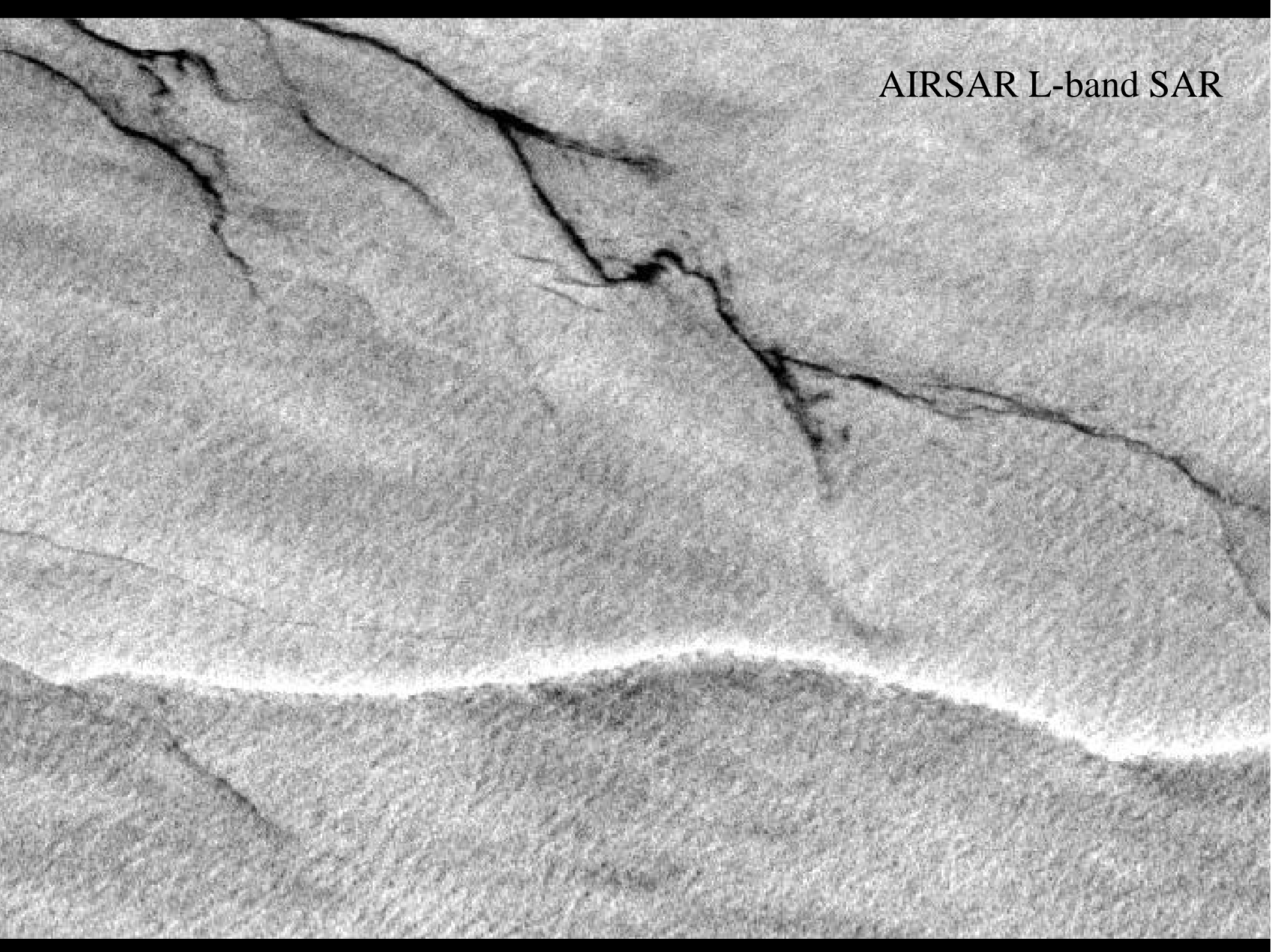
$\lambda \sim 300$

m

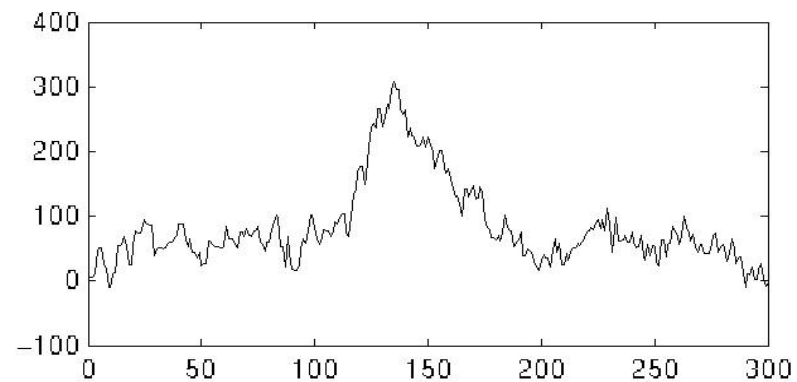
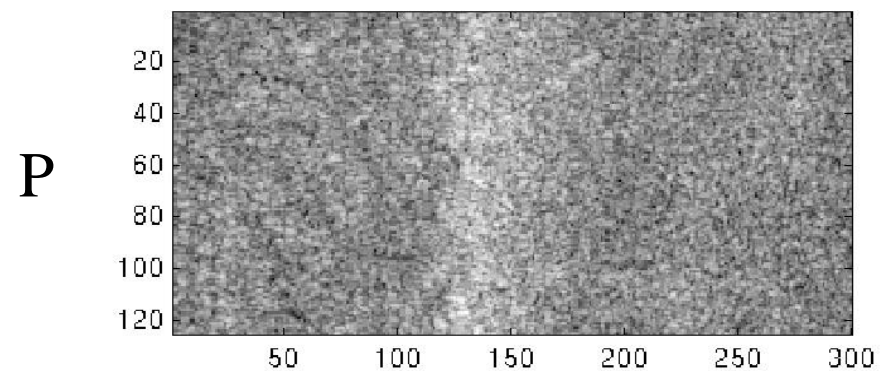
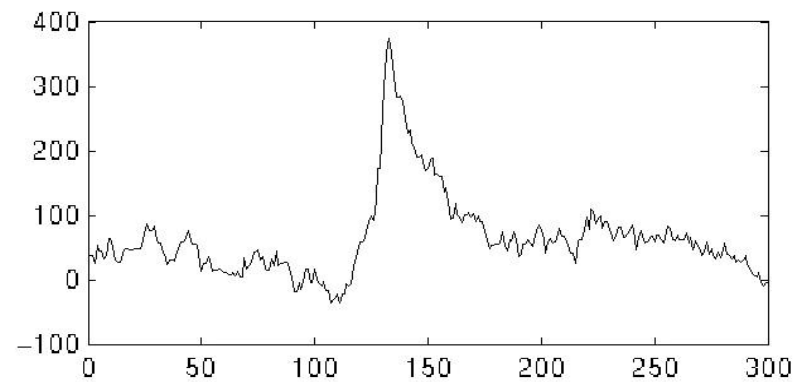
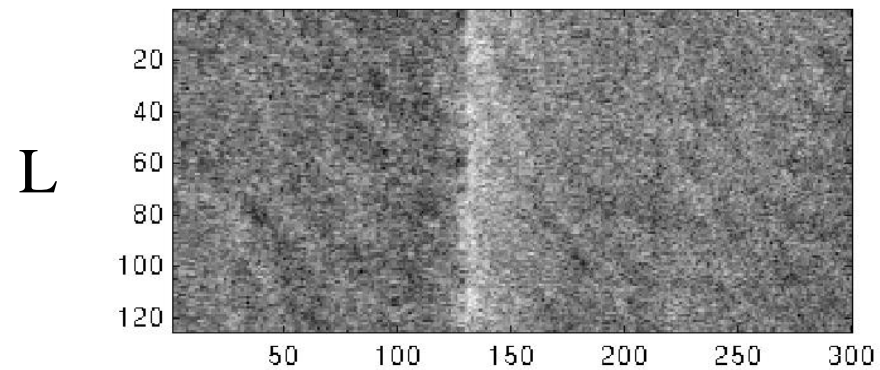
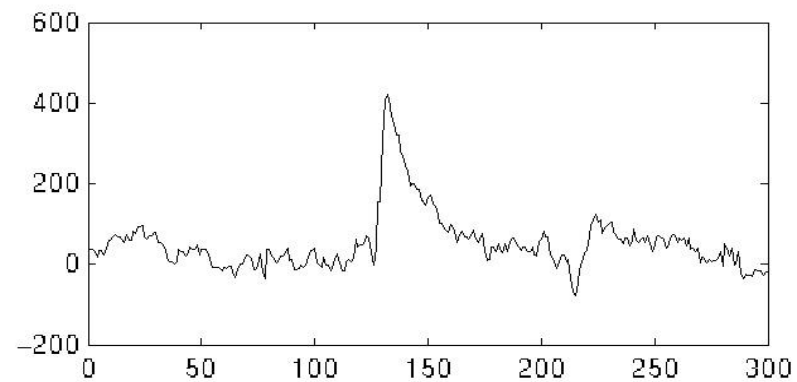
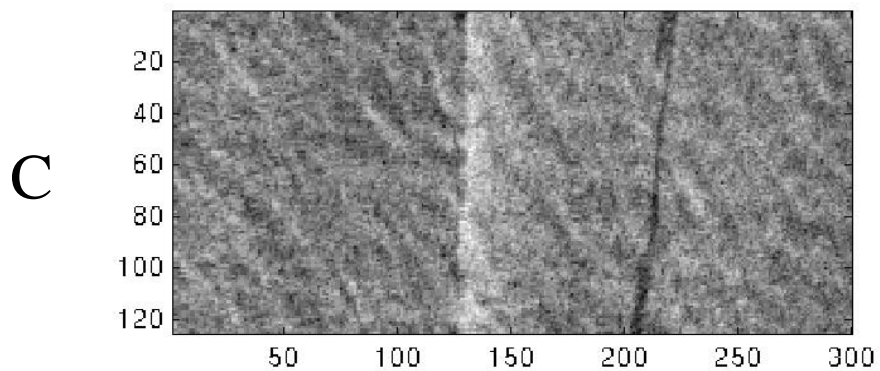
Jet Associated Periodic Structure



AIRSAR L-band SAR



SAR Profile Across Azimuthal Front



Wave Modulation Theory of Longuet-Higgins and Stewart

The change in phase velocity, wave number, angle, and amplitude are given by:

$$c/c_0 = 1/[1 - (v/c_0)\sin\theta_0]$$

$$k/k_0 = [1 - (v/c_0)\sin\theta_0]^2$$

$$\sin\theta = \sin\theta_0/[1 - (v/c_0)\sin\theta_0]^2$$

which hold for

$$v/c_0 \leq [1 - (\sin\theta_0)^{1/2}]/\sin\theta_0$$

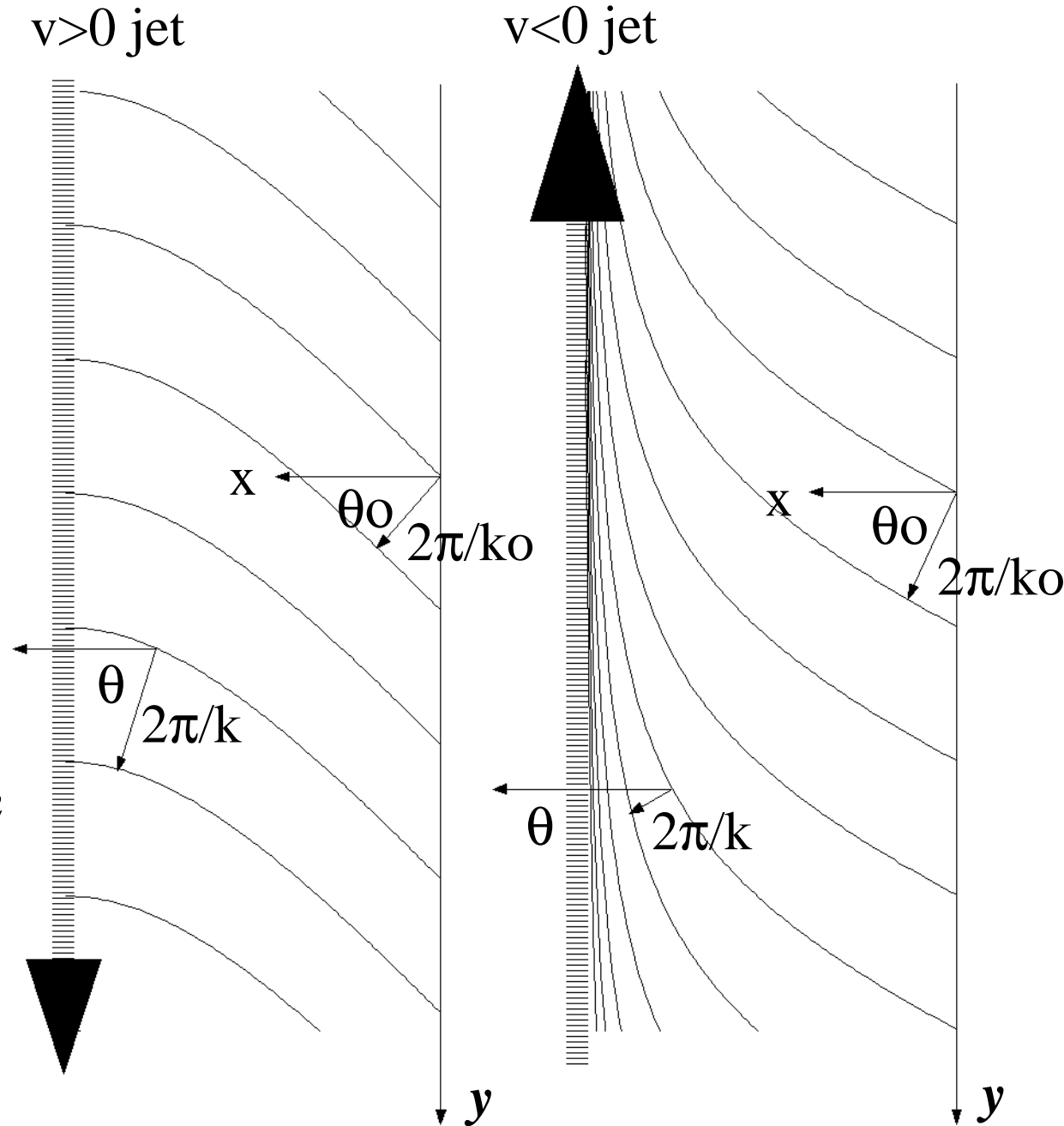
and

$$a/a_0 = (E/E_0)^{1/2} = (\sin 2\theta_0/\sin 2\theta)^{1/2}$$

For

$$v/c_0 > [1 - (\sin\theta_0)^{1/2}]/\sin\theta_0$$

total reflection occurs

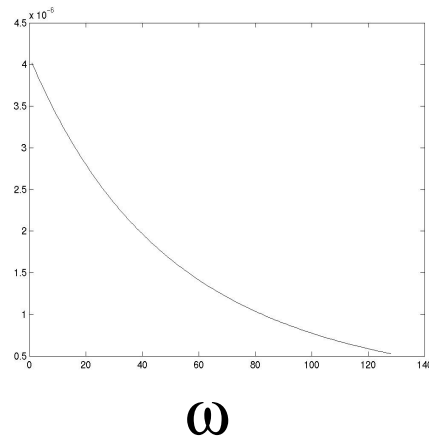


Wave Field Used in the Numerical Simulation

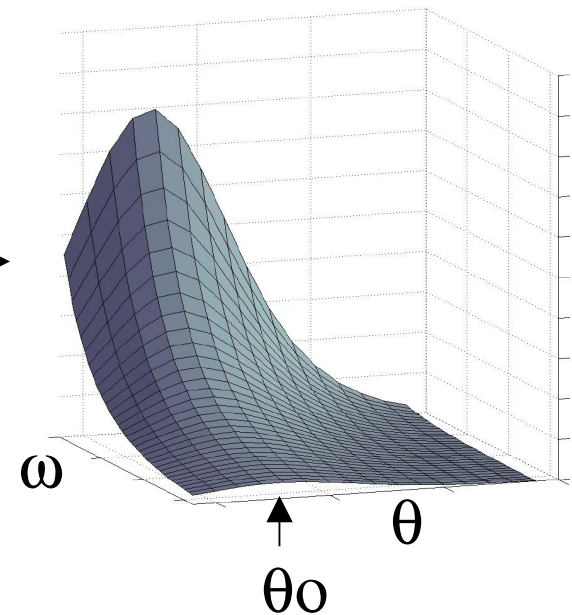
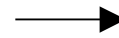
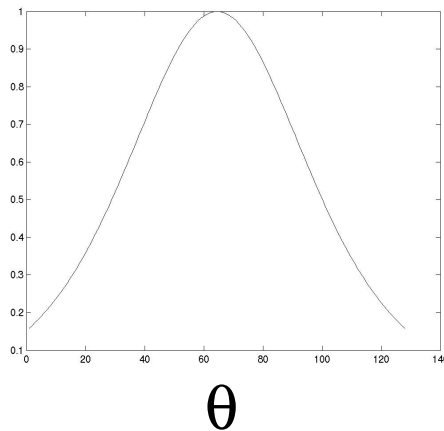
(Pierson-Moskowitz Spectrum) \times (sech² angular distribution)

$$F_0 \sim \omega^{-5} e^{- (5/4)(\omega/\omega_p)^{-4}} \times \text{sech}^2(\theta - \theta_0)$$

where $\omega_p = 0.13\pi g/u_{10} \sim 0.6$ hz



\times



Model Assumptions:

Velocity bunching effects are negligible:

In this case this means net surface convergence across the front is small compared to semigeostrophic jet velocity.

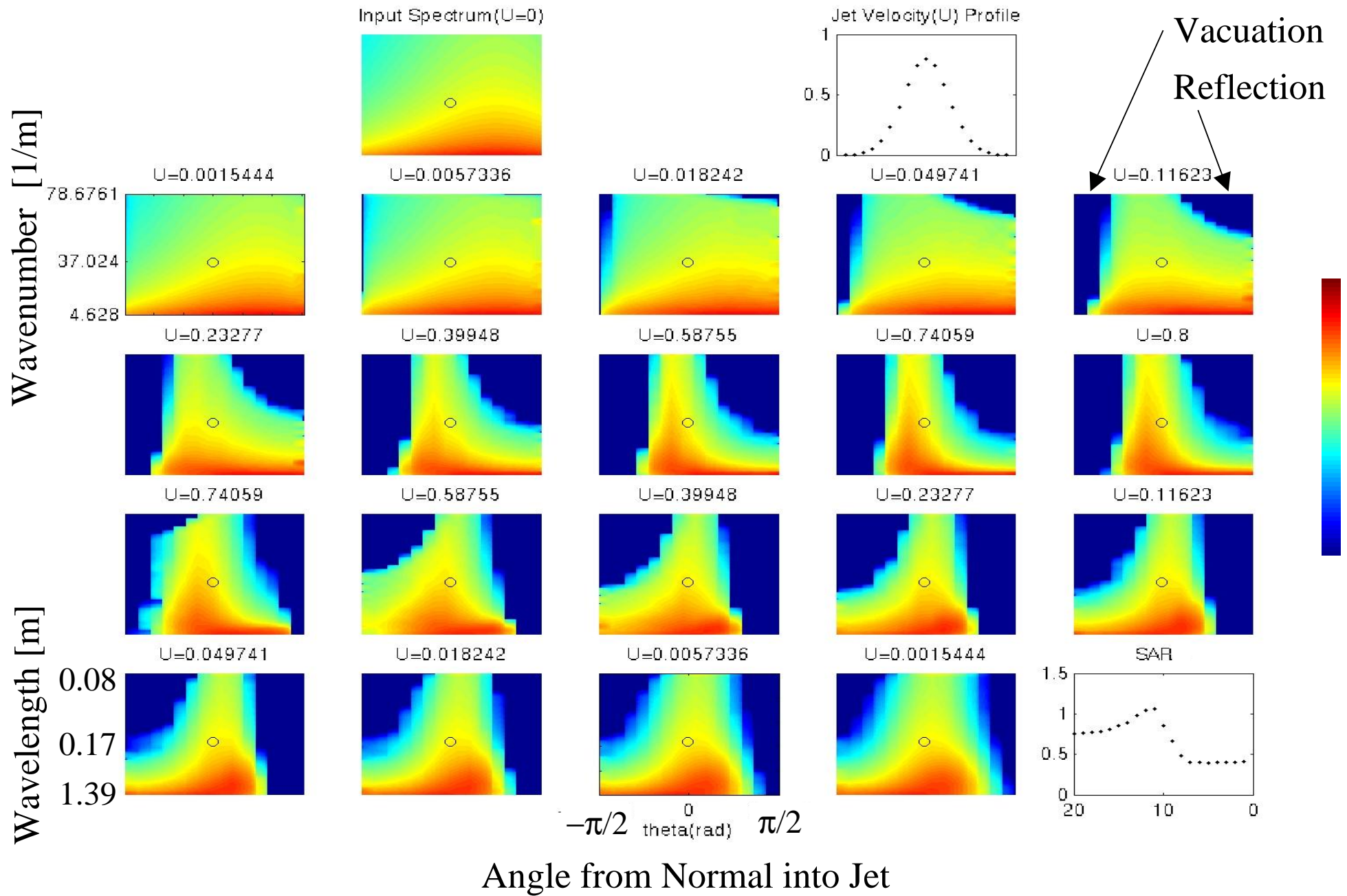
First order Bragg scattering is dominant:

Scattering from waves an integer multiple of the first order Bragg wavelengths contribute substantially less to the normalized radar cross section than scattering from the smallest Bragg wavelength.

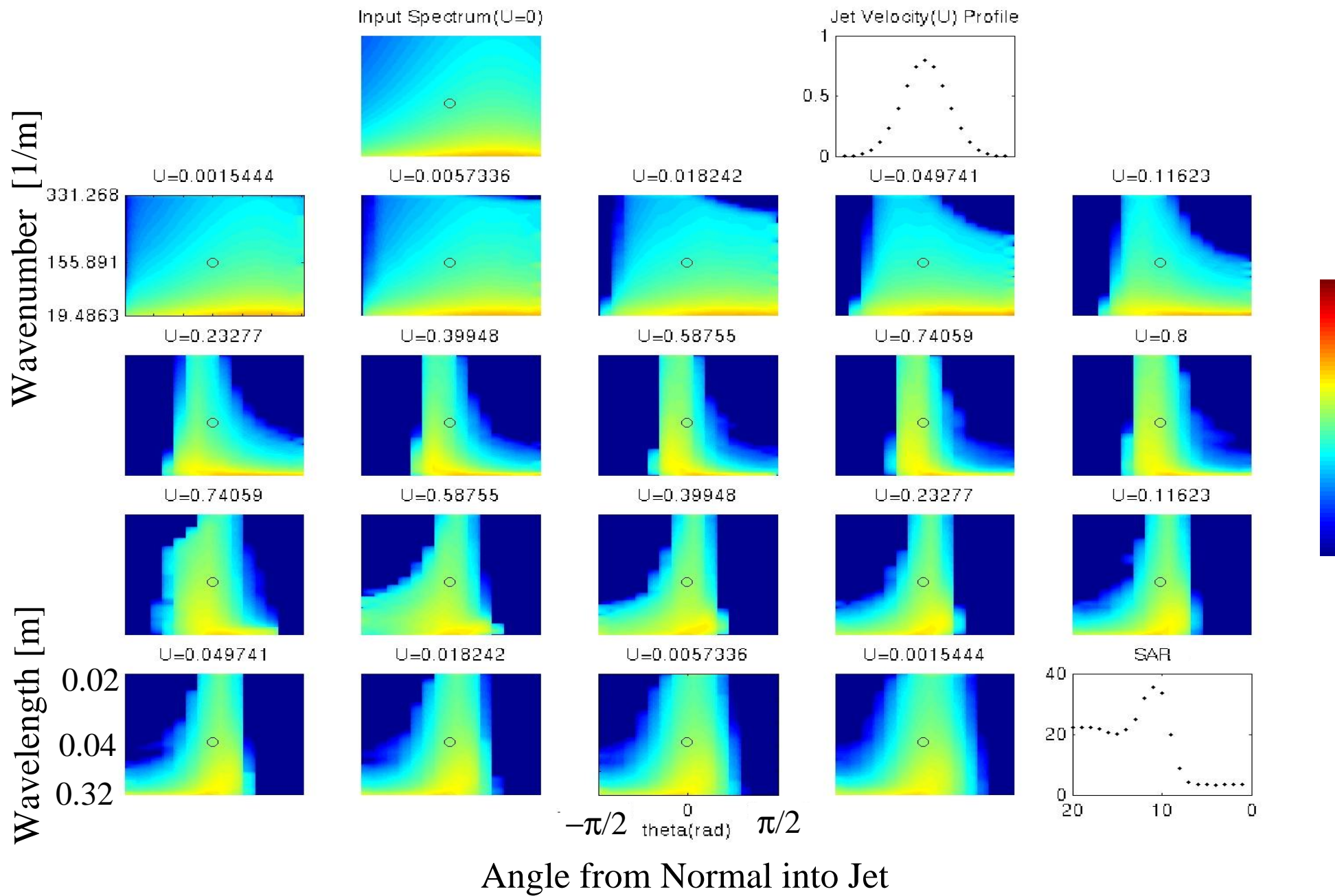
All reflection at critical shear is incoherent:

This implies a negligible first order Bragg return from reflected components of the wave field.

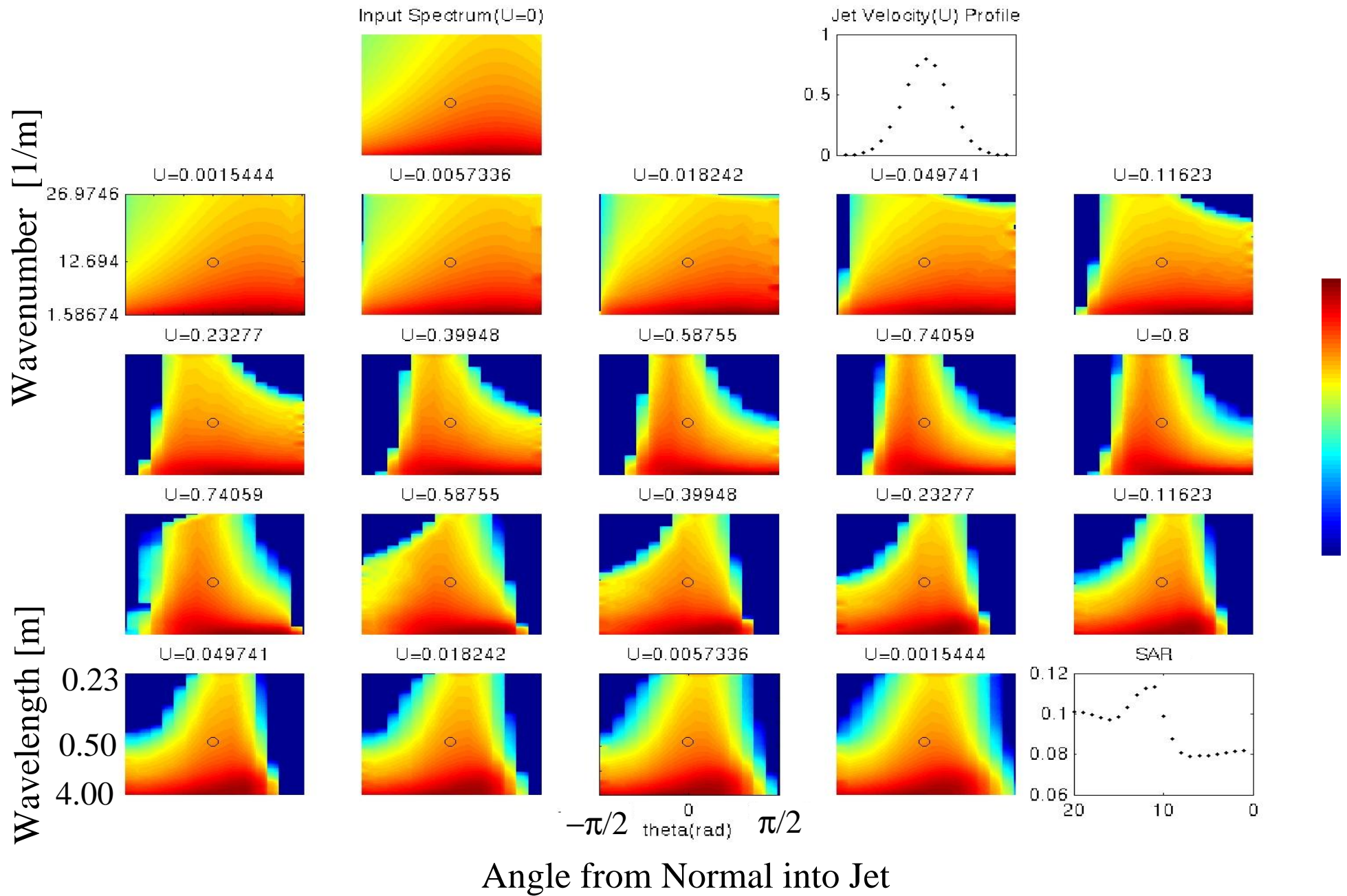
Model results for L-band AIRSAR Profile of Southeastward Azimuthal Gaussian Jet



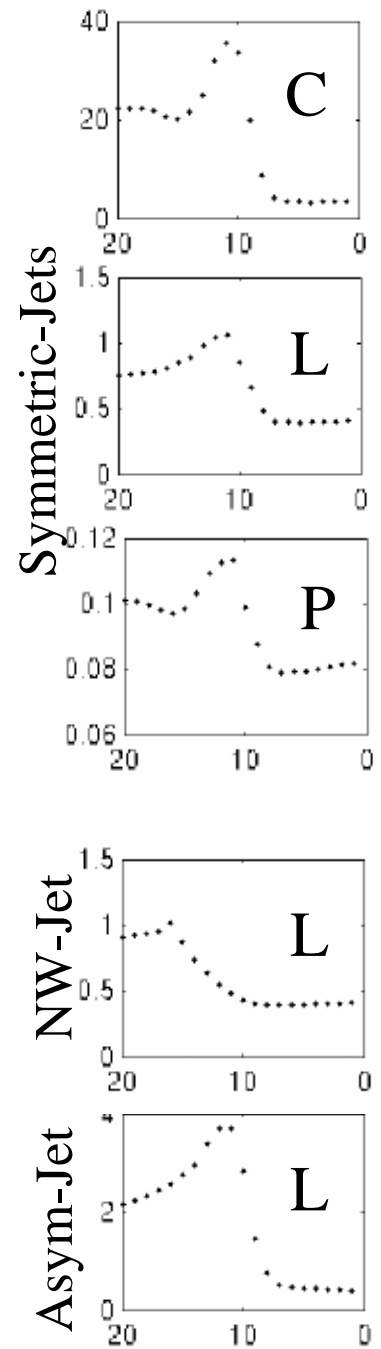
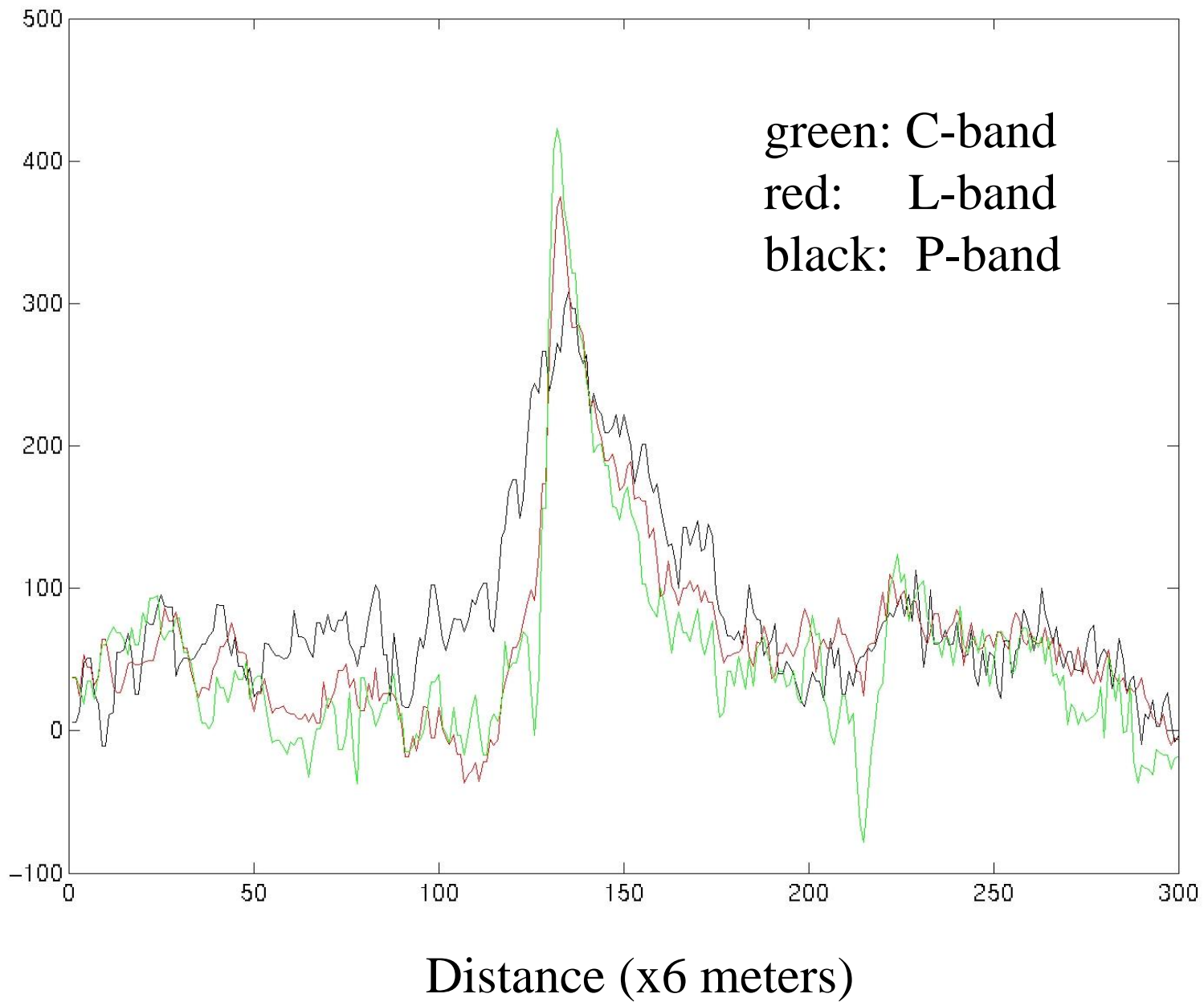
Model results for C-band AIRSAR Profile of Southeastward Azimuthal Gaussian Jet



Model results for P-band AIRSAR Profile of Southeastward Azimuthal Gaussian Jet



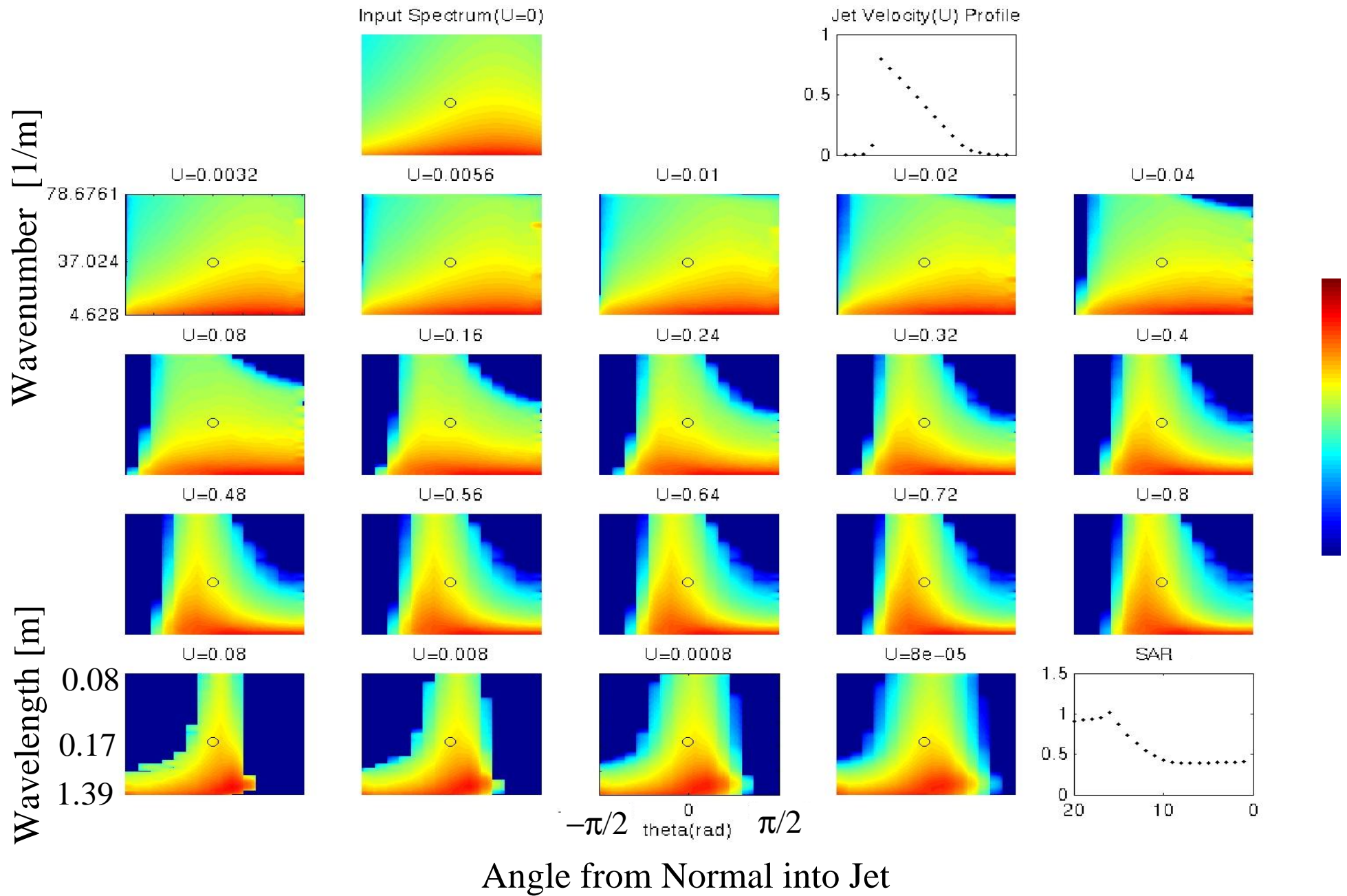
SAR Backscatter Profile Across Azimuthal Front



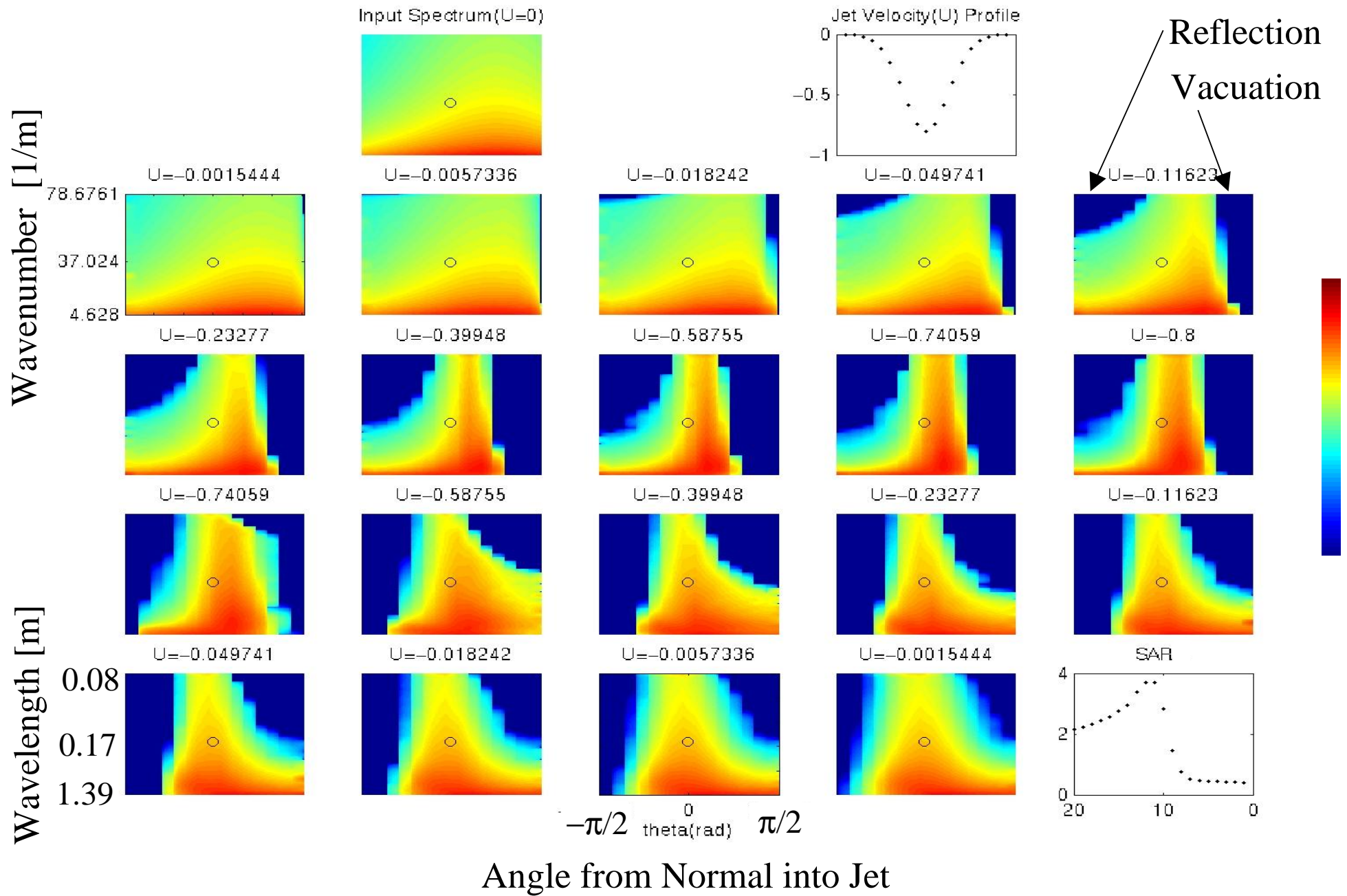
Conclusions

- Ocean wave coherence at the spatial scale of the AIRSAR C-band spatial resolution approaches zero just below 4 cm wavelength.
- SAR imaged internal waves in this stratified upwelling environment are strongly front associated.
- Comparison of "simplest" model results with SAR data suggest wave breaking at a semi-geostrophic front for wavelengths of 7 cm and 25 cm, and no breaking, but rather turbulence induced damping (due to the breaking of smaller waves), for wavelengths of 77 cm.

Model results for L-band AIRSAR Profile of Southeastward Azimuthal Asymmetric Jet



Model results for L-band AIRSAR Profile of Northwestward Azimuthal Gaussian Jet



ERS-1 SAR Jul/Aug 1992

